

INFORMATION TO USERS

The most advanced technology has been used to photograph and reproduce this manuscript from the microfilm master. UMI films the text directly from the original or copy submitted. Thus, some thesis and dissertation copies are in typewriter face, while others may be from any type of computer printer.

The quality of this reproduction is dependent upon the quality of the copy submitted. Broken or indistinct print, colored or poor quality illustrations and photographs, print bleedthrough, substandard margins, and improper alignment can adversely affect reproduction.

In the unlikely event that the author did not send UMI a complete manuscript and there are missing pages, these will be noted. Also, if unauthorized copyright material had to be removed, a note will indicate the deletion.

Oversize materials (e.g., maps, drawings, charts) are reproduced by sectioning the original, beginning at the upper left-hand corner and continuing from left to right in equal sections with small overlaps. Each original is also photographed in one exposure and is included in reduced form at the back of the book. These are also available as one exposure on a standard 35mm slide or as a 17" x 23" black and white photographic print for an additional charge.

Photographs included in the original manuscript have been reproduced xerographically in this copy. Higher quality 6" x 9" black and white photographic prints are available for any photographs or illustrations appearing in this copy for an additional charge. Contact UMI directly to order.

U·M·I

**University Microfilms International
A Bell & Howell Information Company
300 North Zeeb Road, Ann Arbor, MI 48106-1346 USA
313/761-4700 800/521-0600**

Order Number 9009765

**Polymerization of tetrahydro-1-(4-hydroxy-3-(2-hydroxyethoxy))
phenyl thiophenium hydroxide inner salt**

O'Callaghan, Michael P., Ph.D.

City University of New York, 1989

Copyright ©1989 by O'Callaghan, Michael P. All rights reserved.

U·M·I
300 N. Zeeb Rd.
Ann Arbor, MI 48106

POLYMERIZATION OF
TETRAHYDRO-1-(4-HYDROXY-3-(2-HYDROXYETHOXY))
PHENYL THIOPHENIUM HYDROXIDE INNER SALT

A

By:

Michael P. O'Callaghan

A dissertation submitted to the Graduate Faculty in
Chemistry in partial fulfillment of the requirements for
the degree of Doctor of Philosophy, The City University
of New York.

1989

COPYRIGHT BY
MICHAEL P. O'CALLAGHAN
1989

This manuscript has been read and accepted for the Graduate Faculty in Chemistry in satisfaction for the dissertation requirement for the degree of Doctor of Philosophy.

5/23/89

date

George Odian

Chairman of Examining Committee

5/30/89

date

A. M. Rosen

Executive Officer

George Odian

Howard Haubenstein

Arthur Woodward

Dr. G. ODIAN

Dr. H. HAUBENSTOCK

Dr. A. WOODWARD

Supervisory committee

The City University of New York

Abstract

POLYMERIZATION OF
TETRAHYDRO-1-(4-HYDROXY-3-(2-HYDROXYETHOXY)
PHENYL THIOPHENIUM HYDROXIDE INNER SALT

By: Michael P. O'Callaghan

Adviser: Professor George Odian

The polymerization of tetrahydro -1-(4-hydroxy -3-(2-hydroxyethoxy) phenyl thiophenium hydroxide inner salt (hydroxyethoxy zwitterion) has been investigated in bulk and solution (DMSO-d₆) at 50-140 °C. The hydroxyethoxy zwitterion has been shown to polymerize without added initiator by a zwitterion mechanism as well as through a cationic mechanism in the presence of trifluoroacetic acid. Analysis of reaction by-products and end group analysis of polymer, utilizing ¹H and ¹³C NMR spectroscopy with reference to low molecular weight model compounds, showed evidence of termination due to cyclization, and destruction of the tetrahydrothiophenium ring forming polymer molecules terminated by phenolic groups on one end and either vinyl or alcoholic groups at the other end. Polymerization in the presence of added nucleophiles and electrophiles in solution affected the mechanism of the polymerization as evidenced by a change in product

distribution observed by ^1H NMR spectroscopy. The kinetics of the initiated and thermal polymerization of the hydroxyethoxy zwitterion in solution are consistent with initiation being rate determining for the thermal polymerization and faster initiation with the trifluoroacetate salt of the hydroxyethoxy zwitterion formed when trifluoroacetic acid is added as a cationic catalyst. The kinetics observed are consistent with a chain mechanism, monomer apparently much less prone to react with itself than with an intermediate formed either by slow self reaction of monomer in the case of the zwitterion polymerization, or reaction of monomer with initiator. Analysis of relative molecular weight versus extent of reaction for bulk polymerized samples was also consistent with a chain type of mechanism as high molecular weight material formed early in the course of the reaction. Number average molecular weights, relative to poly(styrene) of up to 94,100 ($M_w=290,500$) were achieved.

ACKNOWLEDGEMENT

I would like to express my sincere gratitude to Dr. George Odian for his help and friendship over the last four years.

I thank Dr. Peter Mazella for his early encouragement and Dr. Aurthur Woodward and Dr. Howard Haubensstock for their many helpful and essential suggestions. I am most appreciative of the many useful conversations with Dr. Pathiraja (Guna) Gunatillake, as well as other graduate students, post doctoral associates and faculty. I also acknowledge the early work done by Dr. C. K. Chien and other workers that provided valuable clues in the direction of work to follow. Thanks is also due to Dr. Gunatillake for fractionating several reaction mixtures using preparative HPLC and reproducing several experiments.

Without the help of my family this work could not have been accomplished. To my wife Carole who went to work to feed us; to Christine who cheerfully put up with domestic upheaval and hard economic times; and to Megan, Michael and Alex who made this period our very happiest by being with us; God bless you all.

I gratefully acknowledge financial support of this work by grants from the Dow Chemical Co, National Science Foundation (DMR-8105865) and the City University of New

York (PSC-CUNY 10-13140, 11-13350, 12-13685) as well as teaching appointments from the College of Staten Island.

CONTENTS

	Page
ABSTRACT	iv
CONTENTS	viii
LIST OF FIGURES	xi
LIST OF TABLES	xiv
1.0 INTRODUCTION	1
2.0 BACKGROUND	4
2.1 NUCLEOPHILIC/ELECTROPHILIC MONOMER PAIRS	4
2.2 NONIONIC ADDUCTS CAPABLE OF ZWITTERION FORMATION	7
2.3 STABLE SULPHONIUM ZWITTERIONS	9
3.0 EXPERIMENTAL	19
3.1 MATERIALS	19
3.2 SYNTHESIS AND PURIFICATION OF MONOMER ..	19
3.3 POLYMERIZATION METHODS	20
3.3.1 Bulk Polymerization ...	20
3.3.2 Solution Polymerization	22
3.4 SPECTROSCOPIC ANALYSIS	23
3.5 DIRECT NMR ANALYSIS OF POLYMERIZATION REACTION MIXTURES	24
3.5.1 Monitoring Sample Temperature	24
3.5.2 Quantitation of Reaction Mixtures	25
3.5.3 Control of Spectra Accumulation	30
3.6 CHROMATOGRAPHIC ANALYSIS	35
3.6.1 Gel Permeation Chromatography	35
3.6.2 High Performance Liquid Chromatography.	35
3.7 THERMAL ANALYSIS	36
3.8 PREPARATION OF MODEL COMPOUNDS	37
4.0 RESULTS AND DISCUSSION	41
4.1 CHARACTERIZATION OF MONOMER	41
4.1.1 Proton NMR Spectrum	41
4.1.2 Infrared Spectra	44
4.1.3 ¹³ C NMR Spectrum	48
4.1.4 Thermal Analysis	50
4.2 POLYMER CHARACTERIZATION	53
4.2.1 Proton NMR Spectrum	53
4.2.2 ¹³ C NMR Spectrum	62
4.3 PRODUCT DISTRIBUTION OF THE POLYMERIZATION	63

4.3.1 Bulk Polymerization	64
4.3.2 Solution polymerization	68
4.4 ANALYSIS OF REACTION BY-PRODUCTS	72
4.4.1 Characterization of Cyclic Dimer	72
4.4.1.1 Proton NMR Spectrum	73
4.4.1.2 Infrared Spectrum	76
4.4.1.3 ¹³ C NMR Spectrum	81
4.4.2 Characterization of Higher Cyclics ..	81
4.4.3 Calculation of Product Distribution by ¹ H NMR Spectroscopy and GPC	87
4.5 CHARACTERIZATION OF COMPOUNDS MODELING POLYMER END GROUPS	90
4.5.1 The Phenolic Diol	91
4.5.2 The Vinyl Phenol	96
4.6 EXAMINATION OF POLYMER END GROUPS	96
4.6.1 Evidence From ¹ H NMR Spectroscopy	101
4.6.2 Evidence From ¹³ C NMR Spectroscopy ...	104
4.6.3 Evidence of Unidentified End Group ...	104
4.7 ADDITIVE STUDIES	109
4.7.1 Bulk Polymerization	109
4.7.2 Solution Polymerization	112
4.8 PRODUCT DISTRIBUTION OF INITIATED POLYMERIZATION	116
4.8.1 Relative Reactivity of HEZI Carboxylates	119
4.8.2 Effect of Initiator On Cyclic Content .	125
4.8.3 Effect of Initiator On Molecular Weight of Linear Product	131
4.8.4 Effect of Initiator On Solution Polymerization Kinetics	131
4.9 KINETICS OF BULK POLYMERIZATION	144
4.9.1 Molecular Weight Versus Extent of Reaction	146
4.9.2 Treatment of Kinetic Data	149
4.9.3 Kinetics of Monomer Dehydration	152
4.9.4 Kinetics of Polymerization	153
4.9.5 Correlation Between Rates of Dehydration and Polymerization	153
4.10 SOLUTION POLYMERIZATION KINETICS	159
4.10.1 Mechanism	159
4.10.2 Thermal Polymerization	163
4.10.2.1 Reaction Orders	163
4.10.2.2 Derivation of Rate Equations	185
4.10.2.3 Modeling of the Thermal Polymerization	187
4.10.2.4 Effect of Temperature	189
4.10.3 Initiated Solution Polymerization ...	191
4.10.3.1 Determination of Reaction Orders	191
4.10.3.2 Derivation of Rate Equations	196
4.10.3.3 Modeling the Initiated Polymerization	202

5.0	CONCLUSIONS	205
-----	-------------------	-----

APPENDICES

A1	TREATMENT OF KINETIC DATA	209
----	---------------------------------	-----

A2	DERIVATION OF KINETIC EXPRESSIONS	216
----	---	-----

A2.1	PROPOSED MECHANISM	216
------	--------------------------	-----

A2.2	UNINITIATED POLYMERIZATION	219
------	----------------------------------	-----

A2.3	INITIATED POLYMERIZATION	226
------	--------------------------------	-----

REFERENCES	230
------------------	-----

LIST OF FIGURES

Figure		Page
1	Synthetic Methods Used To Prepare Cyclic Sulphonium Phenoxides	10
2	Temperature Calibration of The NMR Sample Compartment	26
3	¹ H NMR Spectra Showing the Aromatic Region of Linear Polymer, Cyclic Dimer and Monomer ...	28
4	¹ H NMR Spectrum of Solution Polymerization Mixture	32
5	¹ H NMR Spectrum of the Hydroxyethoxy Zwitterion	42
6	Infrared Spectrum of the Hydroxyethoxy Zwitterion	45
7	¹³ C NMR spectrum of the Hydroxyethoxy Zwitterion	48
8	Thermogram Showing Water loss of the Hydroxyethoxy Zwitterion	51
9	¹³ C NMR spectrum of Poly(hydroxyethoxy zwitterion)	55
10	¹ H NMR Spectrum of Poly(hydroxyethoxy zwitterion)	57
10a	¹ H NMR Spectrum of Poly(hydroxyethoxy zwitterion) Expanded to Show End Group Signals	59
11	¹ H NMR Spectrum of a Bulk Polymerization Mixture	66
12	¹ H NMR Spectrum of Cyclic Dimer	74
13	Infrared Spectrum of Poly(hydroxyethoxy zwitterion)	77
14	Infrared Spectrum of Cyclic Dimer	79

15	^{13}C NMR spectrum of Cyclic Dimer	82
16	HPLC Chromatogram of a Solution Polymerization Reaction Mixture	84
17	GPC of Initiated Solution Polymerization Reaction Mixture	88
18	^{13}C NMR spectrum of 2-Hydroxyethoxy-4- (4-hydroxy butanthio) phenol	92
19	^1H NMR Spectrum of 2-Hydroxyethoxy-4- (4-hydroxy butanthio) phenol	94
20	^1H NMR Spectrum of 2-Hydroxyethoxy-4- (4-butenylthio) phenol	97
21	^{13}C NMR spectrum of 2-Hydroxyethoxy-4- (4-butenylthio) phenol	99
22	Overlay of Polymer Spectra Before and After Bromination	102
23	Infrared Spectrum of Tetrahydro 1-[4 hydroxy 3-(2-hydroxyethoxy) phenyl] thiophenium acetate	121
24	Infrared Spectrum of Tetrahydro 1-[4 hydroxy 3-(2-hydroxyethoxy) phenyl] thiophenium acetate After Melting	123
25	Infrared Spectrum of Tetrahydro 1-[4 hydroxy 3-(2-hydroxyethoxy) phenyl] thiophenium trifluoroacetate	126
26	Infrared Spectrum of Tetrahydro 1-[4 hydroxy 3-(2-hydroxyethoxy) phenyl] thiophenium trifluoroacetate After Melting	128
27	Second Order Monomer Loss in Uninitiated Solution Polymerization	136
28	First Order Monomer Loss in Initiated Solution Polymerization	138
29	Comparison of Initiated and Uninitiated Reaction Rates	140
30	Apparent First Order Rate constants of Initiated Polymerization as a Function of Initial Initiator Concentration	142

31	Product Molecular Weight of Bulk Polymerization as a Function of Extent of Reaction	147
32	Conversion Versus Time Plots For the Bulk Polymerization of the Hydroxyethoxy Zwitterion	150
33	Arrhenius Plots for Bulk Polymerization and Dehydration	156
34	Calculated and Experimental Values For Monomer Loss $M_0 = 0.208$ moles/L	165
35	Calculated and Experimental Values For Monomer Loss $M_0 = 0.101$ moles/L	167
36	Calculated and Experimental Values For Monomer Loss $M_0 = 0.0404$ moles/L	169
37	Calculated and Experimental Values For Cyclic Formation $M_0 = 0.203$ moles/L	171
38	Calculated and Experimental Values For Cyclic Formation $M_0 = 0.101$ moles/L	173
39	Calculated and Experimental Values For Cyclic Formation $M_0 = 0.0404$ moles/L	175
40	Order of Reaction of Monomer Loss; Uninitiated Polymerization; Fractional Life Method	177
41	Orders of Reaction; Uninitiated Polymerization Initial Rate Method	180
42	Order of Reaction of Cyclic Dimer Formation; Uninitiated Polymerization; Fractional Life Method	183
43	Order of Reaction; Initiated Polymerization Initial Rate Method	194
44	Order of Reaction; Initiated Polymerization Fractional Life Method	197
45	Calculated and Experimental Values For Monomer Loss; Initiated Polymerizations	203

LIST OF TABLES

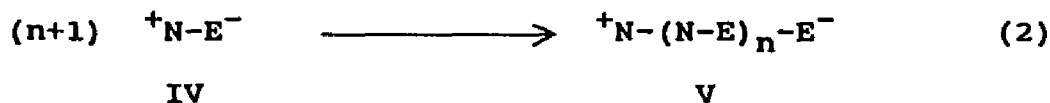
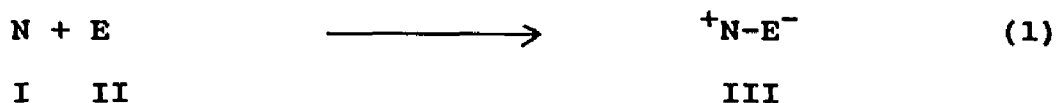
Table	Page
1	STRUCTURES OF REPORTED CYCLIC SULPHONIUM PHENOXIDES 13
2	PRODUCT DISTRIBUTIONS PRODUCED BY THE BULK POLYMERIZATION OF CYCLIC SULPHONIUM PHENOXIDES 15
3	NMR ASSIGNMENTS OF ARYL PROTONS USED FOR POLYMERIZATION MIXTURE QUANTITATION 31
4	MICROPROGRAM USED TO ACQUIRE KINETIC DATA .. 34
5	¹³ C NMR SPECTRAL ASSIGNMENTS 54
6	EFFECT OF REACTION TEMPERATURE ON THE MOLECULAR WEIGHT OF BULK POLYMERIZED SAMPLES. 68
7	EFFECT OF INITIAL MONOMER CONCENTRATION ON PRODUCT DISTRIBUTION IN FINAL REACTION MIXTURE 70
8	THE EFFECT OF TEMPERATURE ON PRODUCT DISTRIBUTION 71
9	BULK POLYMERIZATION IN THE PRESENCE OF ADDED SODIUM METHOXIDE111
10	BULK POLYMERIZATION IN THE PRESENCE OF ADDED TFA SALT.....113
11	SCREENING OF ADDITIVES IN SOLUTION POLYMERIZATION114
12	EFFECT OF INITIATOR LOADING ON THE PRODUCT DISTRIBUTION OF SOLUTION POLYMERIZATION132
13	EFFECT OF INITIAL MONOMER LOADING ON THE PRODUCT DISTRIBUTION OF INITIATED SOLUTION POLYMERIZATION133
14	EFFECT OF INITIATOR LOADING ON PRODUCT MOLECULAR WEIGHT IN INITIATED SOLUTION POLYMERIZATIONS.134
15	EFFECT OF TEMPERATURE ON THE RATE OF MONOMER DEHYDRATION154
16	EFFECT OF TEMPERATURE ON THE RATE OF BULK POLYMERIZATION155

17	CORRELATION OF RATES OF POLYMERIZATION AND DEHYDRATION OF THE HYDROXYETHOXY ZWITTERION	155
18	SUMMARY OF ORDER OF REACTION EXPERIMENTS - UNCATYLYZED SOLUTION POLYMERIZATION	182
19	EFFECT OF TEMPERATURE ON RATE OF UNINITIATED SOLUTION POLYMERIZATION	190
20	ORDER OF REACTION SUMMARY - INITIATED POLYMERIZATION	193

1.0 INTRODUCTION

The zwitterionic polymerization of many different pairs of nucleophilic (N) and electrophilic (E) monomers have been described (1-6). Appropriate pairs of nucleophilic and electrophilic monomers, for example, 2-methyl 2-oxazoline and acrylic acid (7,8), polymerize spontaneously to form low molecular weight alternating copolymers.

The generally accepted mechanism involves reaction of the nucleophilic and electrophilic comonomers to form a genetic zwitterion specie which is self reactive.

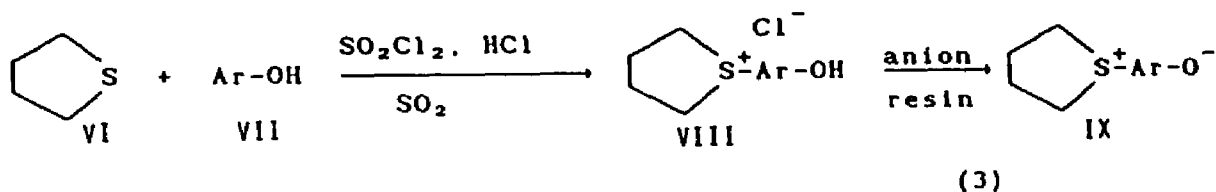


Unfortunately, the genetic and macro zwitterion species, III and V, are often capable of reacting with monomers and other materials present in the reaction mixture in large excess to cause termination, severely limiting the molecular weight attained.

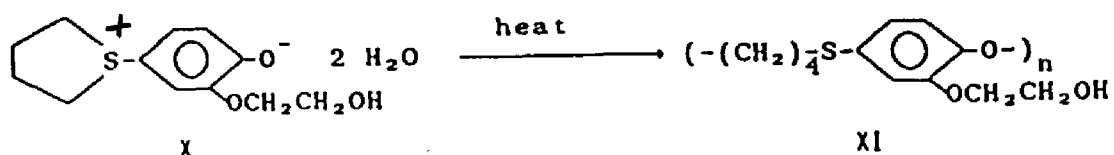
A successful approach to the problem of achieving

higher molecular weight product was implemented by Hatch and Schmidt and their co-workers (9-13). Their systems differ from other zwitterion polymerizations in that the genetic zwitterion is sufficiently stable to be isolated from starting materials and thus be polymerized in systems of much higher zwitterion concentration.

The zwitterions of this type are conveniently formed by reaction of tetrahydrothiophene with a hydroxy arly compound.



We have investigated the polymerization of tetrahydro-1-(4-hydroxy-3-(2-hydroxyethoxy) phenyl thiophenium hydroxide inner salt, X, to poly [oxytetramethylenethio (2-[2-hydroxyethoxy]) -1,4- phenylene], XI. X is referred to in the remainder of this work as hydroxyethoxy zwitterion or monomer and XI referred to as poly hydroxyethoxy zwitterion or polymer.



(4)

The goal of the research undertaken was to elucidate the mechanism of the polymerization of the hydroxy ethoxy zwitterion with respect to initiation, propagation and termination processes. Three approaches were used to this end.

a) Polymer end group analysis was used to identify the termination processes responsible for limiting product molecular weight.

b) Analysis of product/ by-product distribution was employed to assess the importance of by-product formation in the polymerization and additives capable of perturbing the product distribution were sought and studied in more detail to uncover factors determining the course of the reaction.

c) Polymerization kinetics were studied to propose a mechanism in accord with all of the experimental evidence.

2.0 BACKGROUND.

Three types of spontaneous polymerizations may be distinguished which are believed to proceed by way of a macrozwitterion propagating intermediate. A discussion of these approaches is useful to place the current work in context before presenting a detailed discussion of the experimental results.

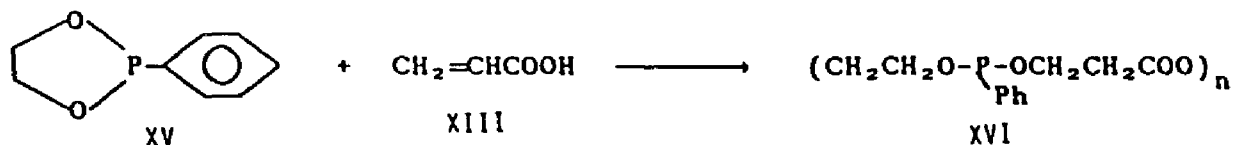
2.1 Nucleophilic/ Electrophilic Monomer Pairs.

The scope of this type of zwitterion polymerization as a synthetic tool to yield interesting polymer structures containing a variety of functional groups as a part of the polymer chain or pendant to the backbone can be seen when considering some of the systems which have been studied.

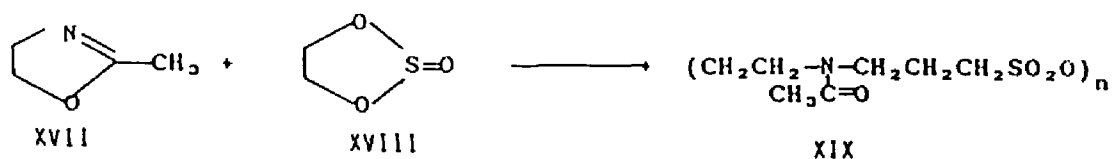
(5). 2-oxazoline and β -propiolactone or acrylic acid.



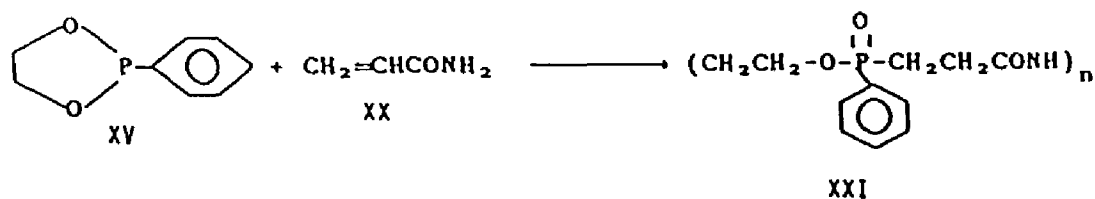
(6) . Ethylene phenylphosphonite and acrylic acid.



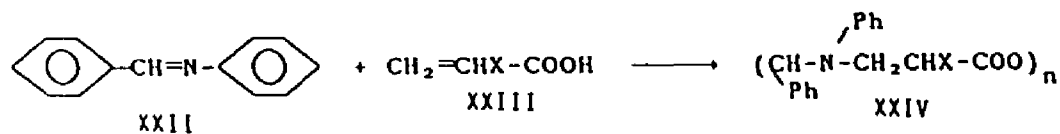
(7). 2-Methyl-2-oxazoline and 3-hydroxy-1-propane sulfonic acid sultone.



(8). Ethylene phenylphosphonite and acrylamide.



(9). N-Benzylideneaniline and α chloroacrylic acid.



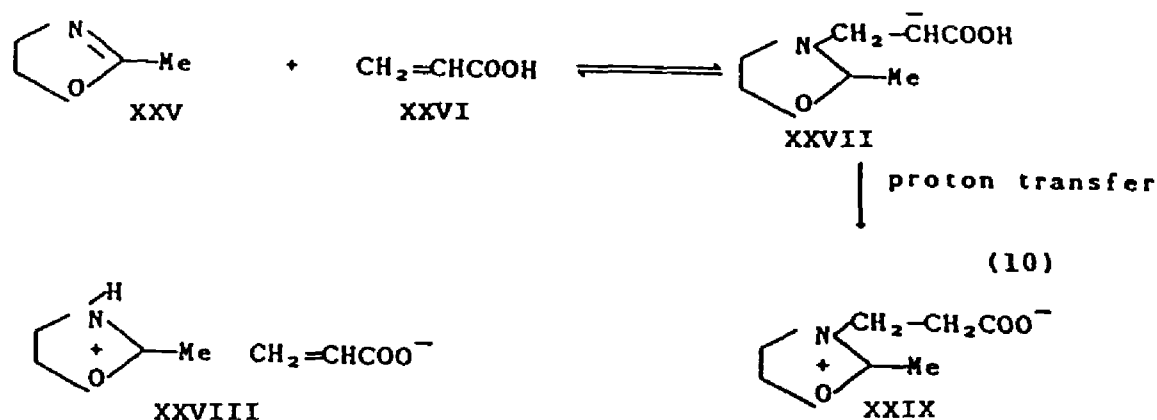
The approach of reacting nucleophilic and electrophilic pairs of monomers leads without exception to low molecular weight products, the largest reported value found being $M_n = 19,000$ (14).

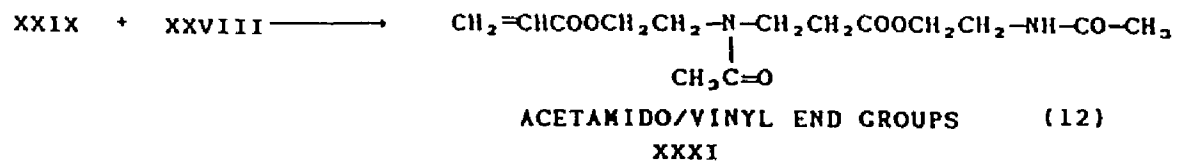
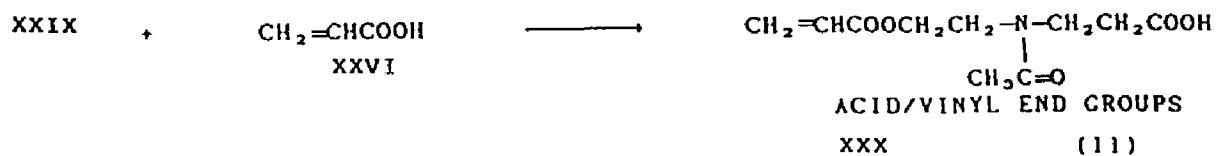
Detailed studies have been carried out on the spontaneous polymerization of 2 methyl 2- oxazoline and acrylic acid (7,8).

The oxazoline nitrogen is alkylated by acrylic acid forming the genetic zwitterion, XXIX, after a proton transfer step. XXIX can then combine with propagating species of various sizes producing chain extension.

It has been determined that this comonomer system contains the seeds of its own destruction, as the zwitterion propagating specie, XXIX, can react with acrylic acid or the oxazolinium acrylate, XXVIII, that builds up causing termination processes to be favored over chain growth.

The product is found to consist of low molecular weight molecules of various sizes terminated with vinyl, and either acid or acetamido groups (Equation 11 and 12).





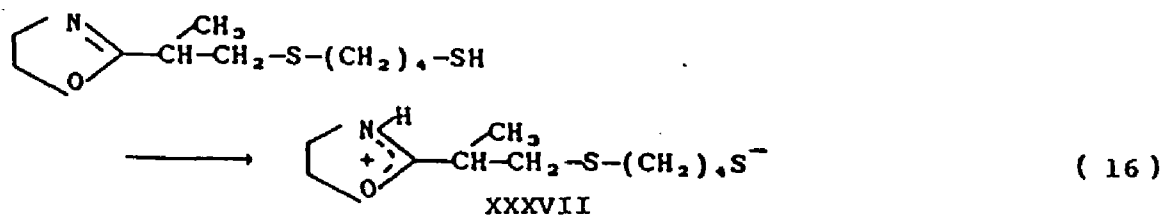
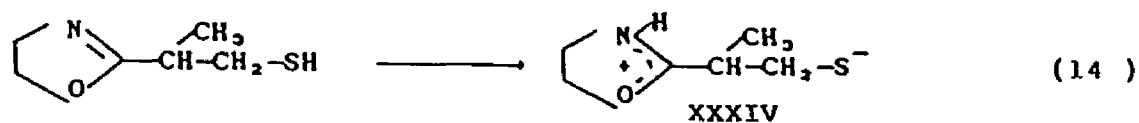
The above reactions were deduced by analysis of polymer end groups of samples using NMR spectroscopy. The samples were purified using preparative HPLC. Analysis of polymer hydrolysis products supported the assignment of end groups obtained spectroscopically.

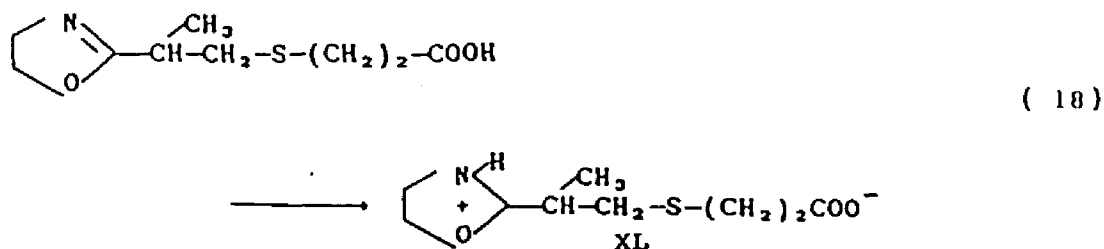
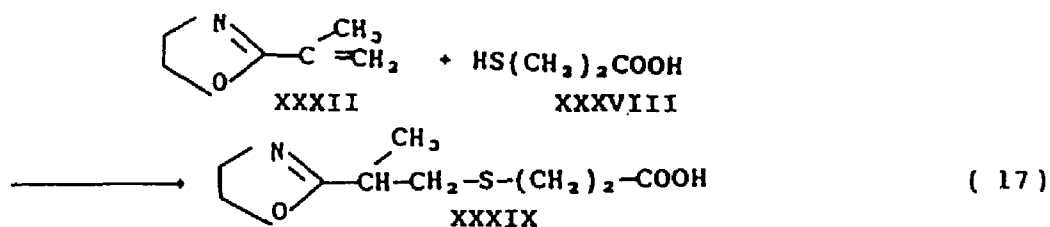
2.2 Nonionic Adducts Capable of Zwitterion Formation.

Another approach being pursued to achieve high molecular weight product is the isolation of neutral adducts capable

of forming zwitterion species capable of propagation. By isolating and purifying an adduct from impurities due to excess reactants and by-products, a stoichiometric balance is imposed upon the subsequent polymerization of the adduct and excess reactants are unavailable to take part in termination reactions.

Examples of this type are the polymerization of adducts of 2-isopropenyl-2-oxazoline and hydrogen sulfide, 1,2-ethanedithiol and mercapto propionic acid (15-18).





This approach has met with success as the product molecular weight achieved using these materials are higher than than materials produced using the nucleophilic/electrophilic comonomer pair approach, number average molecular weights of 49,000 being reported for the 2-isopropenyl-2-oxazoline/1,2 ethanedithiol adduct (17).

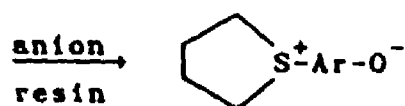
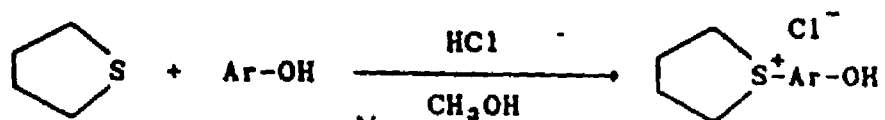
2.3 Stable Sulphonium Zwitterion.

Stable sulphonium zwitterions have been used successfully in attempting to achieve higher molecular weight products through macrozwitterion polymerization. Studies using this approach are convenient as the starting materials themselves are zwitterionic in nature and less ambiguity as to the nature of the propagating specie exists.

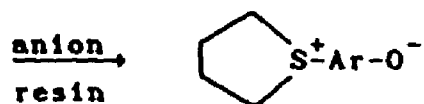
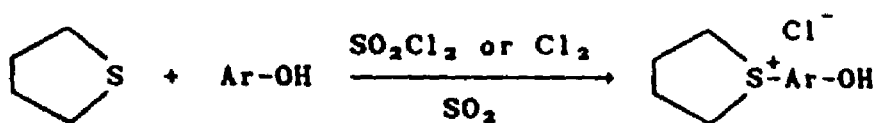
Three synthetic methods have been reported for the preparation of cyclic sulphonium phenoxides. They are outlined in Figure 1. All three methods prepare cyclic sulphonium phenol halides as a key intermediate. The

Figure 1. Synthetic methods used to prepare cyclic sulphonium phenoxides.

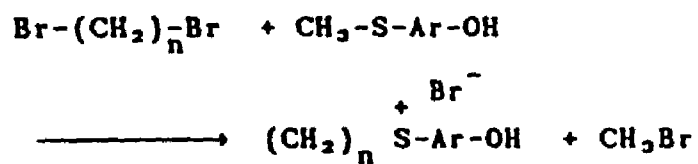
Method I



Method II



Method III

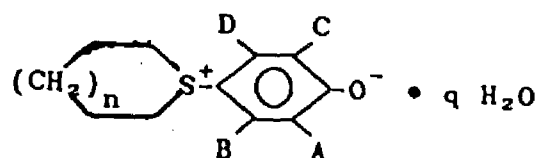




sulphonium halide is then treated with an anion exchange resin in its hydroxide form to produce the final zwitterion. Methods one and two are specific for cyclic sulphonium phenoxides possessing a five membered ring. In method one, chlorotetrahydrothiophenium chloride is produced. Electrophilic substitution of the phenolic substrate then occurs to form the cyclic sulphonium phenol halide.

Method three, the nucleophilic attack of an alkyl dihalide on a (methylmercapto) phenol derivative followed by ring closure as methyl bromide is removed, is applicable to formation of six membered rings. Method three has been used to produce meta substituted derivatives, inaccessible through electrophilic substitution of phenols, but the meta derivatives are much more reactive, polymerizing in 10 minutes at 40°C (12).

Table 1 is a tabulation of the cyclic sulphonium phenoxides prepared by Hatch, Schmidt and their coworkers. Of the monomers prepared, the polymerization of three have been studied in detail. They are the 1- (3,5 dichloro -4-hydroxy phenyl) tetrahydrothiophenium hydroxide inner salt, the 1-(3-methyl-4-hydroxy phenyl) tetrahydrothiophenium hydroxide inner salt and the 1- (4-hydroxy -1-naphthyl) tetrahydrothiophenium hydroxide inner salt (19), referred to as the dichloro zwitterion, methyl zwitterion

TABLE 1. CYCLIC SULPHONIUM PHENOXIDES



A	B	C	D	n	q	
Cl	H	Cl	H	4	0	dichloro zwitterion
Cl	H	H	H	4	1	
Cl	H	Cl	CH ₃	4	0.5	
H	H	H	H	5	1	
CH ₃	H	H	H	4	2	methyl zwitterion
H	H	H	CH ₃	4	2	
CH ₃	H	CH ₃	H	4	2	
H	H	H	H	4	2	
OCH ₂ CH ₂ OH	H	H	H	4	2	hydroxyethoxy zwitterion
		H	H	4	2	naphthyl zwitterion

and naphthyl zwitterion respectively. Preliminary work on the synthesis and polymerization of the hydroxy ethoxy zwitterion has been reported (20, 21).

The dichloro zwitterion exists as a stable anhydrous crystalline material. The studies of the naphthyl, hydroxyethoxy and dichloro zwitterions were carried out on dihydrates. Table 2 shows the product distributions found for these materials when the crystalline monomers were heated in bulk. The purified dichloro zwitterion produced mostly cyclics when subjected to bulk polymerization but mostly linear polymer when small amounts of nucleophilic materials were present. The other hydrated zwitterions produced predominately polymeric products, the product distribution being relatively unaffected by additives.

The molecular weight of poly dichloro zwitterion was found to be affected by the addition of nucleophiles prior to polymerization, material of $M_n = 46,000$ being reported. The methyl zwitterion showed no trend toward producing higher molecular weight material with added nucleophiles.

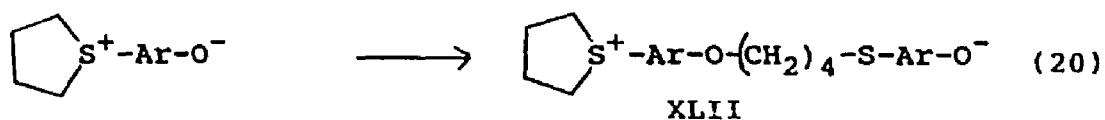
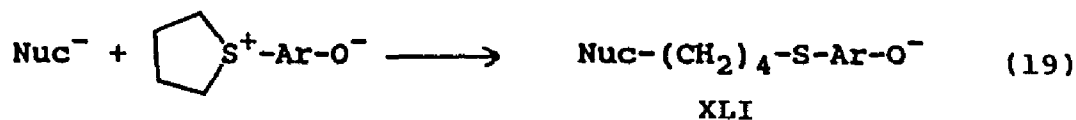
The ability of the dichloro zwitterion to produce higher molecular weight materials and less cyclic by-products when polymerized in the presence of added nucleophiles (Equation 15) was attributed to the lower reactivity of the dichloro phenoxide group compared to the o-methyl phenoxide group.

TABLE 2. PRODUCT DISTRIBUTION PRODUCED BY BULK
POLYMERIZATION OF VARIOUS CYCLIC SULPHONIUM
PHENOXIDES.

ZWITTERION	% CYCLICS	% POLYMER	SPECIFIC VISCOSITY
methyl ¹	20	80	0.20
dichloro ¹	70	30	0.22
naphthyl ²	20	80	Mn = 46,000 (GPC)
hydroxyethoxy	6	94	-----
dichloro + nucleophile ¹	6	94	0.50 Mn = 46,000 (GPC)

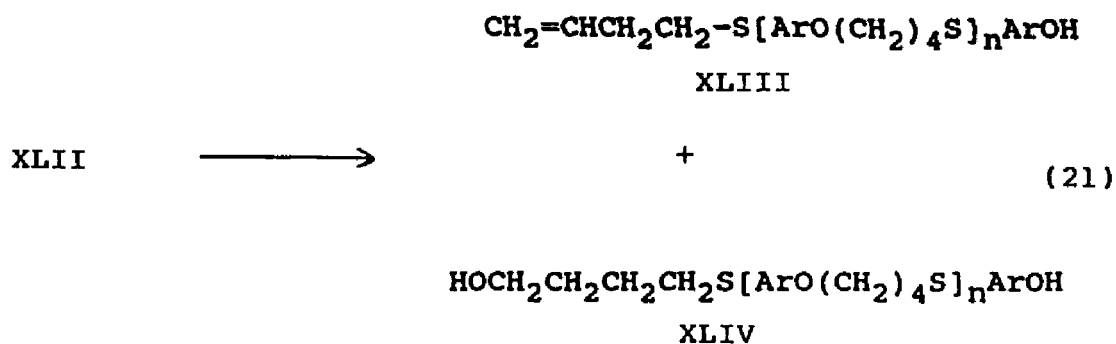
¹ reference 12

² reference 19



When Ar-O^- = the dichloro phenoxide group, the attack of nucleophile upon the tetrahydrothiophenium ring occurs much faster than monomer self reaction, while the reaction of monomer with itself occurred at comparable rate with nucleophile- monomer reaction when Ar-O^- = o-methyl phenoxide (equation 20). The difference of relative nucleophilicity between XLI or XLI^- versus the respective monomer is greater for the dichloro zwitterion than for the methyl zwitterion.

Besides cyclization, beta elimination of the cyclic sulphonium group and substitution with water were found to occur in the case of the naphthyl zwitterion to produce linear molecules containing naphtholic groups at one end and either olefinic or alcoholic groups at the other end (19).



Experimental evidence regarding propagation processes is largely unavailable, although step wise growth has been proposed for the polymerization of the naphthyl zwitterion and methyl zwitterion (12, 19) and a chain type mechanism proposed for the polymerization of the dichloro zwitterion (12). The classification of ring opening polymerizations as either chain or step processes is made on the basis of the relative reactivity of monomers with propagating specie compared to monomer self reactivity. A chain polymerization is characterized as a system in which monomer can react only with reactive specie formed as an intermediate and not with itself (22). For the cyclic sulphonium phenoxides, the monomers will be somewhat less reactive with monomer than with genetic or macro zwitterion specie. The magnitude of the difference in monomer/ propagating specie reactivity will determine whether the polymerization is more similar to a step or

chain polymerization.

A step polymerization is characterized by the slow increase in the product molecular weight, higher molecular weight products being formed only at very high conversions. Chain processes on the other hand produce high molecular weight material very early in the course of the reaction. No attempt has been reported in the literature to determine the product molecular weight versus extent of reaction which would answer this fundamental question concerning the propagation mechanism.

3.0 EXPERIMENTAL SECTION

3.1 Materials. The hydroxyethoxy zwitterion monomer was synthesized and supplied by Dr. Donald Schmidt of Dow Chemical Corporation, Midland, Michigan. $\text{Me}_2\text{SO-d}_6$, 99.9% D, was purchased from ICN Biomedicals Inc, Cambridge Ma. Lithium bromide, p-methoxyphenol, molecular sieves and trifluoroacetic acid were purchased from the Aldrich Chemical Co. and used without further purification. The solvents used were generally ACS grade or better and used without further purification with the exception of N,N-dimethylformamide used for gel permeation chromatography. N,N-dimethylformamide used for gel permeation chromatography was generally recycled material from the instrument. Used solvent was distilled at atmospheric pressure, stored over molecular sieves (3A) and filtered through a 0.5 micron filter prior to being used. The molecular sieves were activated by heating at 350°C for five hours.

3.2 Synthesis and Purification of Monomer. A solution of 68.7 g. (0.779 mol) of tetrahydrothiophene and 0.01 g. iodine in a dry nitrogen atmosphere was cooled to -40°C. using dry ice-methylene chloride and then 300 g. of sulfur dioxide condensed into the solution through a dry ice-methylene chloride condenser. About 20 g. of hydrogen chloride was dissolved in the solution followed by the

addition of 100.7 g.(0.746 mol) of sulfuryl chloride at a rate to maintain the temperature below -15°C . 2-(2-hydroxyethoxy)phenol, 100g.(0.649 mol), was added to this solution which was then allowed to warm to reflux. After refluxing for three hours, water (5 mL) was added and then about 200 mL of sulfur dioxide removed under vacuum. The resulting solution was extracted three times with 100 mL portions of n-hexanol and twice with 100 mL portions of methylene chloride. The aqueous solution was treated with Dowex-2 (hydroxide form) to increase the pH to between 10.5 and 10.7 and the solvent then removed under vacuum. The resulting powder was washed with acetone and dried in a vacuum oven at 40°C to yield 144 g (84% yield) of the dihydrate of the hydroxyethoxy zwitterion. This synthesis was carried out by Dr. Donald Schmidt of Dow Chemical Company (21).

The monomer was purified by first dissolving the monomer at room temperature in a mixture of 5 parts isopropanol and 1 part methanol by volume, adding a small amount of water, filtering off an insoluble tar and precipitating the product with diethyl ether. The product, a white solid, was filtered and air dried to constant weight.

3.3 Polymerization Methods.

3.3.1 Bulk Polymerization. The hydroxyethoxy zwitterion was polymerized using four methods.

a) Forty mg samples of monomer were finely divided using the sharp edge of a spatula, introduced into a test tube, and heated at a specific temperature for 24 hours. Some polymer samples were purified by dissolving the sample in N,N-dimethylformamide and reprecipitating the product by adding diethyl ether. Samples prepared over a temperature range of 60 to 140°C were analyzed by gel permeation chromatography and NMR spectroscopy.

b) Kinetic measurements carried out using TGA and ^1H NMR spectroscopy revealed a dependence of rate of polymerization on both sample size and flow rate of gas above the sample. For this reason, 15 mg samples of the monomer were immersed in octane in a test tube and heated in an oil bath for various amounts of time and analyzed using ^1H NMR spectroscopy in order to run the reaction at essentially constant pressure. Octane was chosen as a solvent because monomer, polymer and cyclic by-products are insoluble in this solvent.

At a given temperature, samples were removed from the oil bath at different times and subsequent reaction slowed by cooling the sample in cold water. The hydrocarbon solvent was decanted from the reaction mass and the sample dissolved in 0.7 mL of $\text{Me}_2\text{SO}-d_6$ and analyzed for composition using ^1H NMR spectroscopy. This kinetic analysis of bulk polymerization samples was carried out over the temperature range of 60 - 80°C.

In one experiment, the samples heated for different times were subjected to NMR analysis as described above and then diluted with N,N-dimethylformamide/LiBr₂ solution and analyzed by gel permeation chromatography to yield molecular weight/conversion data.

c) Samples of the hydroxyethoxy zwitterion were also reacted in the furnace of a thermogravimetric analyzer to monitor the dehydration of the hydrated starting material.

d) Small amounts of additives were incorporated into the bulk polymerization mixture by dissolving the hydroxyethoxy zwitterion monomer and additive in methanol and stripping the solution at room temperature under aspirator vacuum. The resulting film of polymer and additive was then heated at 100°C for two hours and analyzed by gel permeation chromatography.

3.3.2 Solution Polymerization. Five types of solution polymerization experiments were performed.

a) 0.145 molar solutions of monomer were reacted at different temperatures over a range of 60 to 80°C and the composition of the reaction mixture determined as a function of time.

b) At 80°C, solutions of varying initial monomer concentration were reacted and reaction mixture composition as a function of time obtained.

c) At 65°C, a set of monomer solutions, 0.145 M, were reacted in the presence of 3-10 mol percent of initiator,

tetrahydro 1-[4 hydroxy 3-(2-hydroxyethoxy) phenyl] thiophenium trifluoroacetate .

d) At 65°C, a set of samples was reacted in which the amount of initiator added was held constant and the initial monomer content varied from 0.07 to 0.2 mol/L.

e) Solutions of monomer were reacted in an oil bath at different temperatures to determine the the effect of temperature on product and molecular weight distributions. Samples containing initiator and other additives were also reacted in this manner.

Solution polymerized samples were subjected to analysis for the distribution of products formed. After allowing the polymerization to proceed to completion, a sample was analyzed by ^1H NMR spectroscopy and a separate sample diluted and analyzed by GPC. In a separate experiment, monomer (0.6g) was dissolved in Me_2SO (15 mL) and polymerized at 80°C for 2 days. The solvent was removed under vacuum at 80°C and the resulting solid extracted with CH_2Cl_2 . The CH_2Cl_2 -soluble products amounted to 95% of the total and was used for HPLC fractionation of the reaction products.

3.4 Spectroscopic Analysis. Infrared spectra of the monomer, polymer, model compounds and cyclic dimer were obtained for KBr pellet samples using a Beckman 4260 IR spectrometer. 200 MHz ^1H and natural abundance ^{13}C NMR spectra were recorded on an IBM WP 200SY FTNMR

spectrometer using a 5 mm dual $^{13}\text{C}/^1\text{H}$ probe. NMR spectra of monomer samples were obtained at 25°C while spectra of polymer, dimer and model compounds were acquired at 60°C . The spectra were acquired from samples dissolved in $\text{Me}_2\text{SO}-d_6$ using Me_4Si as an internal standard at nominal concentrations of 5% (w/w) for ^1H spectra and 10% (w/w) for ^{13}C NMR spectra.

3.5 Direct NMR Analysis of Solution Polymerization

Mixtures. Direct proton NMR analysis of reaction mixtures undergoing polymerization was accomplished by placing samples of monomer dissolved in $\text{Me}_2\text{SO}-d_6$ in the preheated sample compartment of the spectrometer.

3.5.1 Monitoring Sample Temperature. The temperature experienced by samples in the spectrometer compartment was calibrated using a thermocouple and sample of ethylene glycol. Hydroxylic protons of ethylene glycol show a pronounced effect of temperature on chemical shift while hydrogens bound to alkyl groups show chemical shifts unaffected by changes in temperature. The chemical shift difference between the alkyl and hydroxyl protons serves as an "ethylene glycol thermometer" if suitable calibration data is available (24).

A wire thermocouple probe (type K -model 8520-90, Cole Parmer Instrument Co.) was immersed in ethylene glycol in a 5 mm NMR tube and introduced into the NMR

sample compartment. The instrument was equilibrated at various temperature settings using the variable temperature unit (VTU) and thermocouple temperature readings noted. When the reproducibility of the VTU settings was established, the thermocouple was removed and a sealed capillary tube containing $\text{Me}_2\text{SO-d}_6$ was placed in an ethylene glycol sample to allow an internal deuterium lock on the sample. After equilibrating the sample at various VTU settings and acquiring spectra, the difference in chemical shift between alkyl and hydroxyl protons was measured. A plot of chemical shift difference versus temperature was linear and used for subsequent determinations of spectrometer sample compartment temperature (Fig 2).

3.5.2 Quantitation of Reaction Mixtures. Proton NMR analysis of reaction mixtures was possible due to spectral differences between the linear polymer and higher cyclics, cyclic dimer, and hydroxyethoxy zwitterion in the aromatic region (Fig 3).

Cyclic trimer through pentamer are referred to as higher cyclics. Both higher cyclic species and linear polymer show signals in the region of 6.8 to 7.4 ppm due to 3 protons. Hydroxyethoxy zwitterion exhibits signals in this area due to 2 protons but shows a doublet in the 6.3-6.15 ppm range due to the proton ortho to the phenoate group. Cyclic dimer yields a unique signal in the area

**FIGURE 2. Temperature calibration of NMR Spectrometer
Plot of Chemical Shift Difference Versus Sample
Compartment Temperature.**

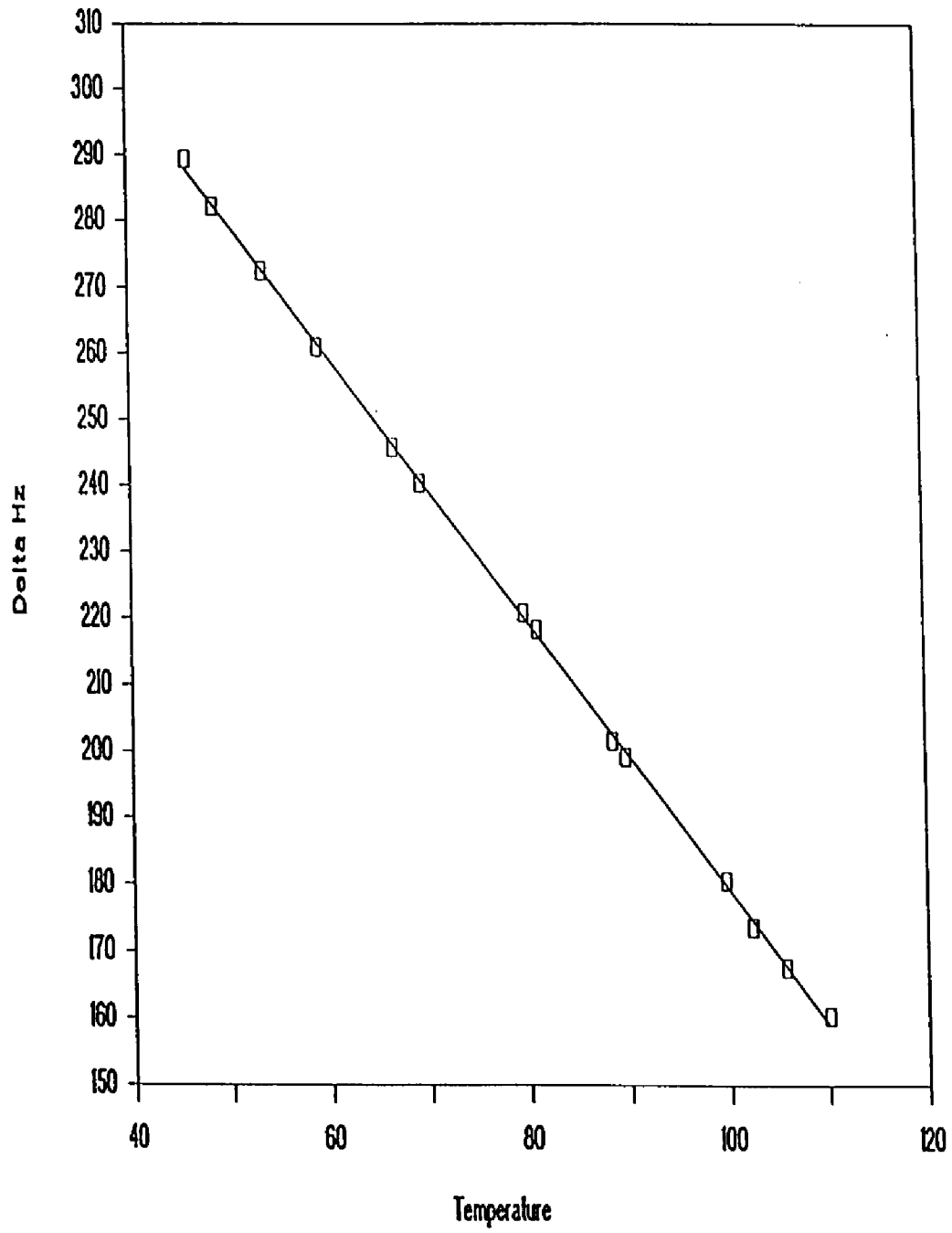
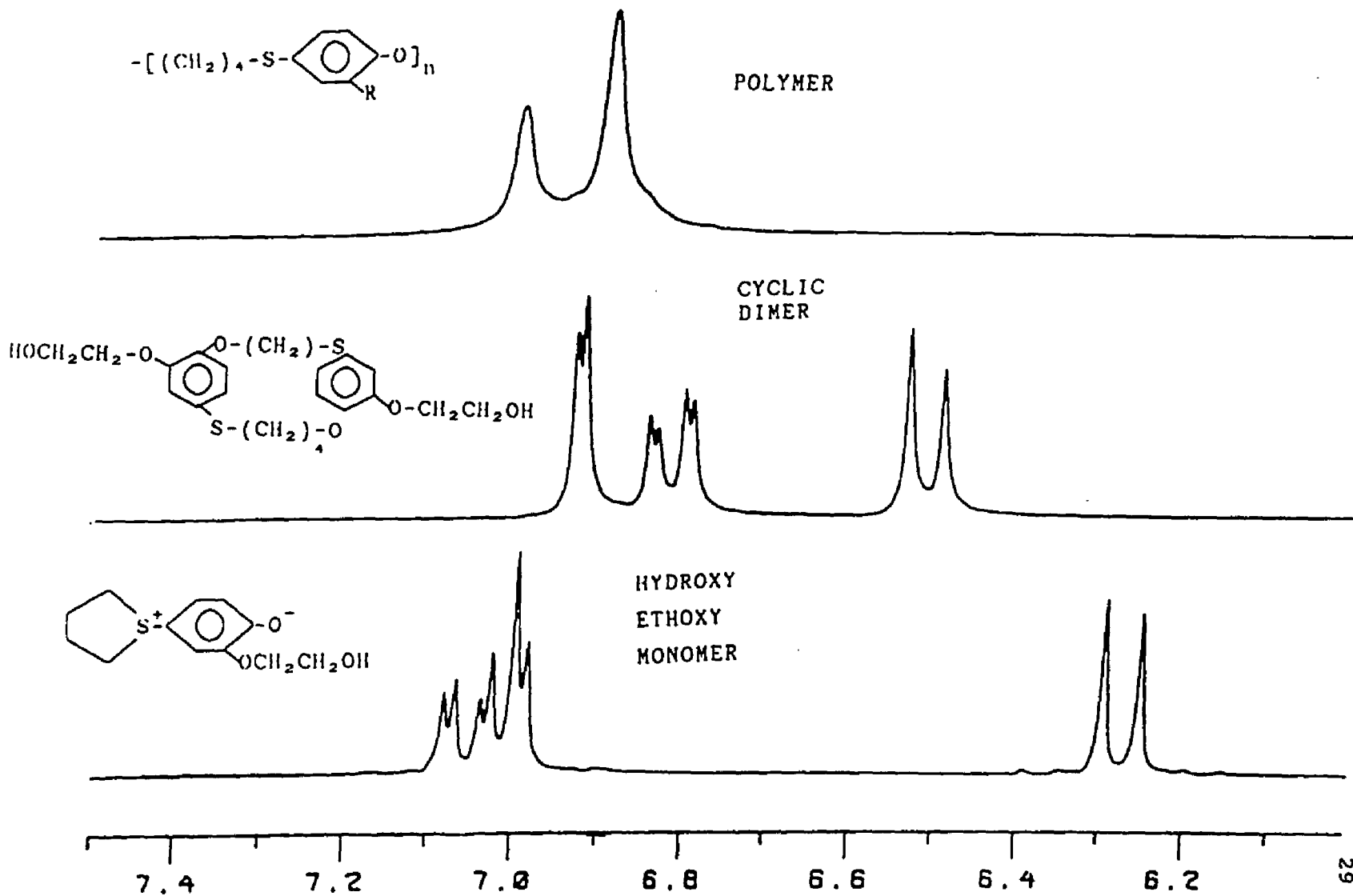


FIGURE 3. ^1H NMR spectra showing the aromatic region of
linear polymer, cyclic dimer and monomer.
Conditions: 0.145 M in DMSO; 45° pulse angle; 65°C ; 2.8
sec. delay between pulses; 32 acquisitions.



from 6.7-6.35 ppm due to the proton ortho to the aryl ether linkage as well as several signals in the region from 6.8-7.4 ppm. This behavior is summarized in table 3.

The area due to one proton was calculated for each of the three classes of material by integration of the three areas shown in Fig 4.

The proton equivalent areas, the area due to a single proton, due to cyclic dimer and zwitterion are B and C respectively. If the proton equivalent area due to polymer plus higher cyclics is defined as D, it may be calculated as:

proton equivalent area due to polymer

$$D = (A-2B-2C)/3$$

The mole fraction of the three classes of materials, monomer, dimer and polymer plus higher cyclics are:

$$M_f = C/(B+C+D); C_f = B/(B+C+D); P_f = D/(B+C+D).$$

3.5.3 Control of Spectra Accumulation. Spectra accumulation as a function of time was controlled using the program shown in Table 4. Variable delay lists appropriate for the temperature and initial monomer concentration were used in these experiments. Samples were analyzed over the range of 0.04 - 0.2 mol/L of monomer over a temperature range of 55 - 80°C.

The sample was placed into the spectrometer at time=0 and the kinetics program started at 10.0 minutes, allowing time for the spectrometer to be locked.

TABLE 3. ¹H NMR ASSIGNMENTS OF ARYL PROTONS USED FOR
POLYMERIZATION MIXTURE QUANTITATION.

region (ppm)	integral	# protons polymer + higher cyclics	# protons cyclic dimer	# protons zwitterion
7.4-6.8	A	3	2	2
6.8-6.35	B	0	1	0
6.35-6.1	C	0	0	1

FIGURE 4. ^1H NMR spectrum of solution polymerization mixture. Conditions as in Figure 1.

SOLUTION POLYMERIZATION
REACTION MIXTURE

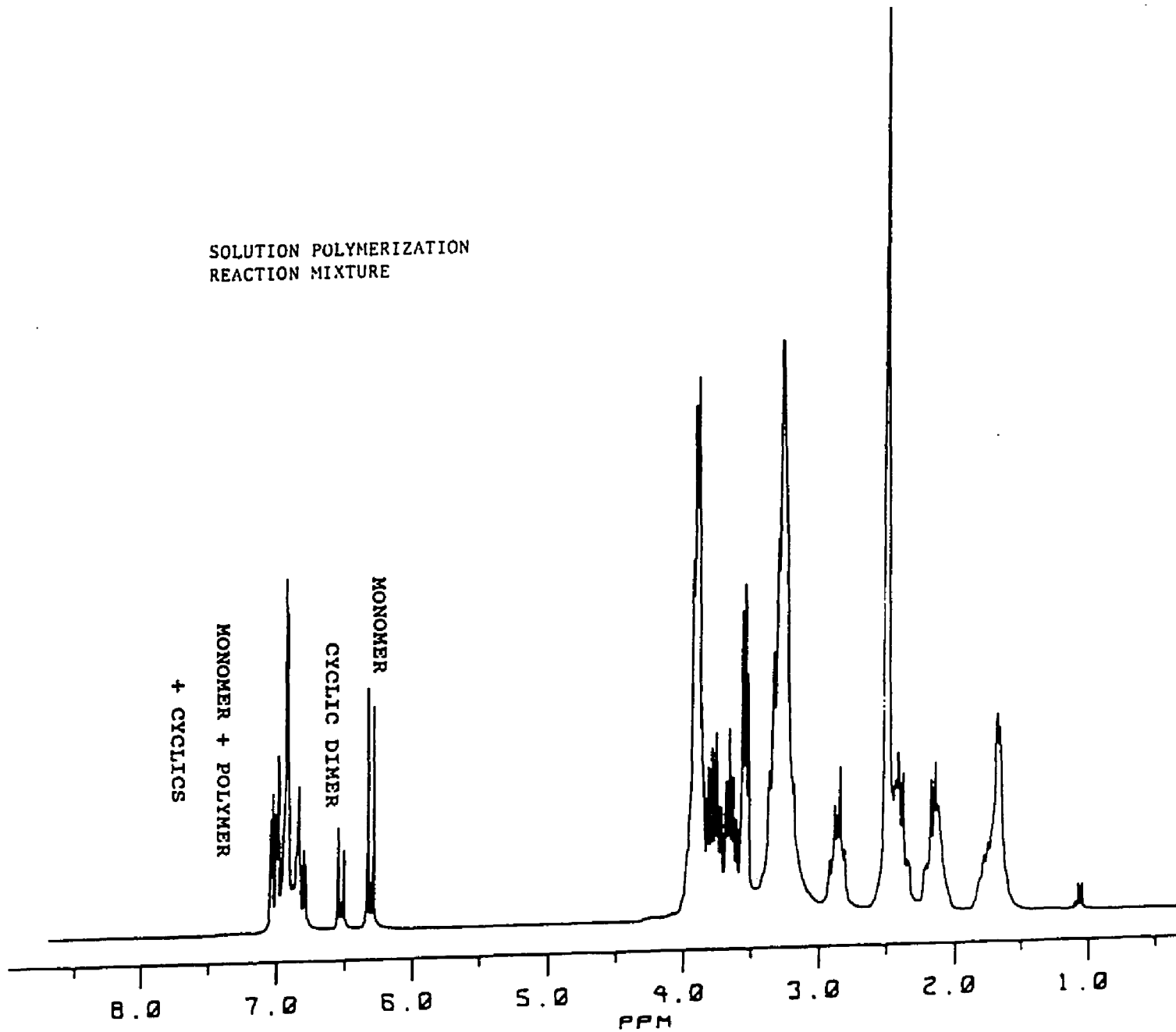


TABLE 4. KINETIC PROGRAM USED TO ACCUMULATE SPECTRA
AS A FUNCTION OF TIME

1	ZE
2	GO=2
3	WR #1
4	IF #1
5	VD
6	IN=1
7	EXIT

3.6 Chromatographic Analysis.

3.6.1 Gel Permeation Chromatography (GPC). GPC analysis of reaction products was carried out at 80 and 100°C on a Waters 150C instrument using N,N-dimethylformamide containing LiBr at 0.05 M levels as the mobile phase. Lithium Bromide was used in the mobile phase to deactivate any polar sites produced by normal degradation of the column. GPC of polar materials is often complicated by a separation based on polarity occurring in the background of the size separation. As a column ages, the retention time of standards and samples can often change due to polar sites within the stationary phase becoming exposed.

Four Ultrastyrigel columns (Waters) of 500, 10³, 10⁴ and 10⁵ Angstrom pore sizes were used as the stationary phase. The GPC calibration for molecular weight determinations was based on polystyrene standards. Gel Permeation Chromatography was also used to fractionate reaction mixtures to estimate product distributions. These experiments were carried out at 100°C using N,N-dimethylformamide without LiBr as the mobile phase. For the fractionation experiments, a 100 angstrom Shodex column was used in addition to the four Ultrastyrigel columns.

3.6.2 High Performance Liquid Chromatography (HPLC).

Analytical HPLC of the CH₂Cl₂ soluble products was performed at ambient temperature with a Waters Associates system consisting of a micro-porasil column, an M-600 solvent

delivery unit, U6K universal chromatography injector, and a 450 variable wavelength UV detector with an 8 microliter flow through cell.

The mobile phase consisted of CH_2Cl_2 - CH_3OH (100:2) vol+vol at a flow rate of 1.0 mL/min. All solvents (HPLC grade, Fischer) were filtered prior to use through an 0.5 micron filter (Millipore). 1 to 10 micrograms of material were injected in volumes of 5 to 25 microliters of mobile phase and detected at a wavelength of 245 nm.

Preparative HPLC was used to fractionate the CH_2Cl_2 soluble portion of polymerization mixtures using a Waters Prep LC system 500 and a Prep Pak-500 silica column with CH_2Cl_2 - CH_3OH (100:1.5) as the mobile phase. A solution of the products, 0.3 g in 10 mL of mobile phase was injected onto the column and eluted at a flow rate of 50 mL/min. Fractions of 100 mL were collected and analyzed for purity by analytical HPLC. After the first two components were eluted, the CH_3OH content of the mobile phase was increased to 2.5 parts. Fractions shown to be pure by analytical HPLC and fractions with one major component plus one or two minor components were combined, concentrated in a rotary evaporator under reduced pressure at 35°C and dried in a vacuum oven at 40°C.

3.7 Thermal Analysis. The water of hydration of the hydroxyethoxy zwitterion was determined by carrying out its polymerization in a thermogravimetric analysis (TGA)

experiment using a Dupont 990 thermal analyzer coupled to a 950 thermogravimetric analyzer module. The zwitterion (10-15 mg) was weighed to the nearest 0.01 mg at ambient temperature in an aluminum cup in the TGA module, heated to 175°C at a rate of 5°C/min, held at 175°C until a constant weight was observed, cooled and weighed at ambient temperature to obtain the water loss due to polymerization. The water of hydration values obtained in this manner were precise to within ± 0.02 mol water per mol of zwitterion.

The kinetics of monomer dehydration was studied using the TGA apparatus isothermally. The temperature experienced by the sample at the experimental temperature setting was determined by inserting a wire thermocouple probe, type K-model 8520-90, Cole Parmer Instrument Co., into the instrument close to the sample pan. It was found that a seven minute period was needed for the sample to equilibrate at the isothermal reaction temperature after insertion into the preheated furnace. The sample was continuously purged with dry nitrogen (100 mL/min) during the analysis.

3.8 Synthesis of Model Compounds.

3.8.1 Synthesis of Tetrahydro 1-[4 hydroxy 3-(2-hydroxyethoxy) phenyl] thiophenium acetate (HEZ SALT). The salt of the monomer and acetic acid was prepared by dissolving 2 g of hydroxyethoxy zwitterion in 10 mL of methanol at room temperature, adding an excess of acetic acid (2 g) and adding diethyl ether to precipitate the

tetrahydrothiophenium acetate salt. The product, mp 115-116°C, was air dried at room temperature to constant weight. ¹H NMR spectroscopy (Me₂SO-d₆) shows the following signals: 7.21-7.30 (m, 1, aromatic), 7.12 (s, 1, aromatic), 6.76-6.86 (d, 1, aromatic), 3.41-4.14 [m, 9, CH₂-OH, +S(CH₂)₂, aryl-O-CH₂], 2.07-2.55 [m, 4, (CH₂)₂], 1.72 ppm (s, 3, COCH₃). Infrared absorption (KBr pellet) is seen at 1575 (COO⁻ Carbonyl) and 1250 cm⁻¹ (aromatic COH).

The salt was converted to the corresponding ester, 2-hydroxyethoxy-4-(4-acetoxy butanthio) phenol, by heating a sample of the solid above its melting point.

3.8.2 Synthesis of Tetrahydro 1-[4 hydroxy 3-(2-hydroxy -ethoxy) phenyl] thiophenium trifluroacetate (TFA SALT).

0.50 g of hydroxyethoxy zwitterion was dissolved in 7 mL of isopropanol/methanol (5 + 1 parts by volume) and 1 mL of trifluroacetic acid was added to the solution and the salt precipitated by adding 50 mL of diethyl ether. The salt was filtered off and air dried to constant weight producing 577 mg of the salt, mp 127-128°C, (78% of theoretical). Elemental analysis calculated for C₁₄H₁₇F₃O₅S: C-47.43, H-4.80, F-16.09, S-9.03%; found: C-47.33, H-4.87, F-15.82, S-9.05. ¹H NMR spectroscopy (Me₂SO-d₆) shows the following signals: 10.45-10.82 (s, broad, 1, aryl-OH), 7.33-7.52 (m, 2, aromatic), 7.02-7.14 (d, 1, aromatic), 4.82-5.40 (s, broad, 1, CH₂-OH), 3.53-4.18 [m, 8, aryl-O-CH₂, +S(CH₂)₂, CH₂-OH], 2.11-2.49 ppm [m, 4, (CH₂)₂]. Infrared absorption

(KBr pellet) at 1690 (COO^- Carbonyl) and 1290 cm^{-1} (aromatic COH).

3.8.3 Synthesis of 2-Hydroxyethoxy-4-(4-hydroxy butanthio) phenol (Phenolic Diol). 2.0 g of the HEZ SALT was heated in an 80°C oil bath for three hours. The resulting phenolic ester was dissolved in 15mL of 3 M sodium hydroxide and heated under reflux overnight. The sodium hydroxide solution was rendered just acid to litmus paper, 25 mL of 5% NaHCO_3 solution added and the resulting neutral solution extracted twice with 25 mL portions of CHCl_3 . The aqueous portion was retained, acidified with 6N HCl and extracted with CHCl_3 . The organic extracts were dried and stripped to yield 0.39 g from the neutral extract and 0.21 g in the case of the acidic extract. Material recovered from the neutral extract was found to consist of a mixture of the target compound and impurities thought to be oligomeric. The acidic extract contained essentially pure target compound, exhibiting a melting point of $88-91^\circ\text{C}$.

3.8.4 Synthesis of 2-Hydroxyethoxy-4-(4-butenylthio) phenol (Vinyl Phenol). 15 mL of 3M NaOH was added to a solution of 1.5 g of hydroxyethoxy zwitterion in 15 mL of water and the mixture heated under reflux for three hours. The reaction mixture was neutralized using 6N HCl and buffered using 15 mL of 5% sodium bicarbonate solution. The neutral solution was extracted twice with 25 mL portions of methylene chloride. The target compound was located in the

neutral extract and isolated from a silica gel column using 60/40 (v/v) 2-butanone - cyclohexane as the eluting solvent.

3.8.5 Synthesis of Cyclic Dimer. A solution of 1.4 g of hydroxyethoxy zwitterion and 250 mL of N,N-dimethyl formamide was heated at reflux for four hours. After removing approximately 90% of the N,N-dimethylformamide in a rotary evaporator, the concentrated solution was added to methanol to precipitate higher molecular weight materials. The solvent was stripped from the filtered mother liquor, the solid dissolved in hot methanol and filtered. The hot methanol solution was reduced in volume and cooled to produce crystalline material, mp 127-130°C.

4.0 RESULTS AND DISCUSSION

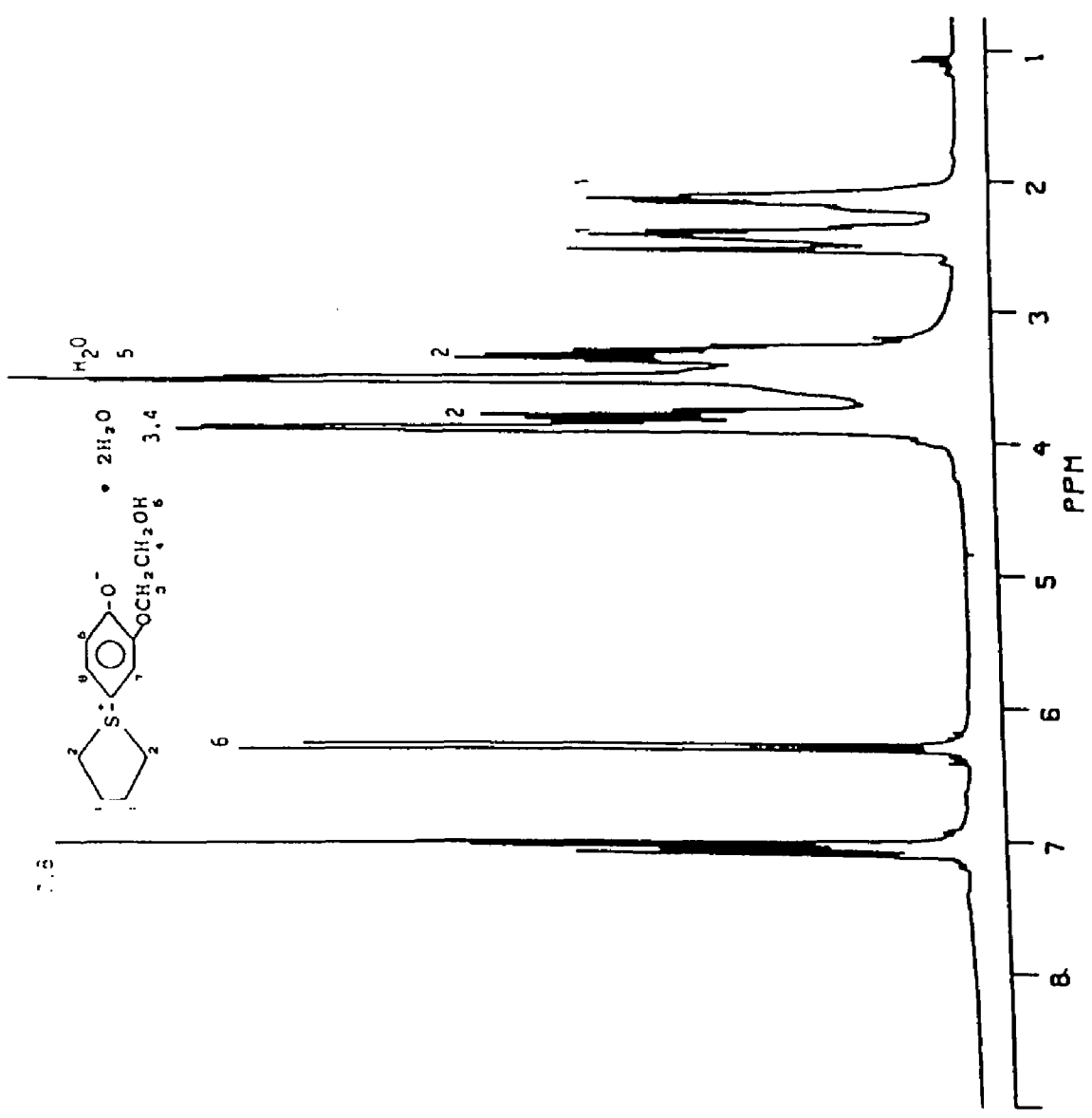
4.1 CHARACTERIZATION OF MONOMER. Support for the structure of the hydroxyethoxy zwitterion was found in NMR spectroscopy and thermogravimetric analysis. The infrared spectrum of monomer was also consistent with the proposed structure.

4.1.1 Proton NMR Spectrum. ^1H NMR spectroscopy (Fig 5) shows signals in the area of 7 ppm, assigned as protons 7 and 8. Examination of the signal at 7.17 ppm shows a doublet and is assigned as proton 7, the splitting due to weak coupling with proton 8 situated meta with respect to proton 7. The signal seen at 7.08 ppm is a pair of doublets as expected for proton 8. Proton 8 is split due to coupling with the ortho proton 6, and then split again due to coupling across the ring with proton 7. The ortho aromatic proton is deshielded and seen as a doublet in the area of 6.3 ppm. The area from 3 to 4 ppm is complex and contains signals due to methylene adjacent to aryl ether (protons 3), methylene adjacent to alcohol (protons 4) and alcoholic protons exchanged with water at 3.87, 3.82 and 3.55 ppm respectively.

The internal methylene protons (protons 1) of the tetrahydrothiophenium ring are nonequivalent and show as a

FIGURE 5. ^1H NMR Spectrum of the Hydroxyethoxy Zwitterion.

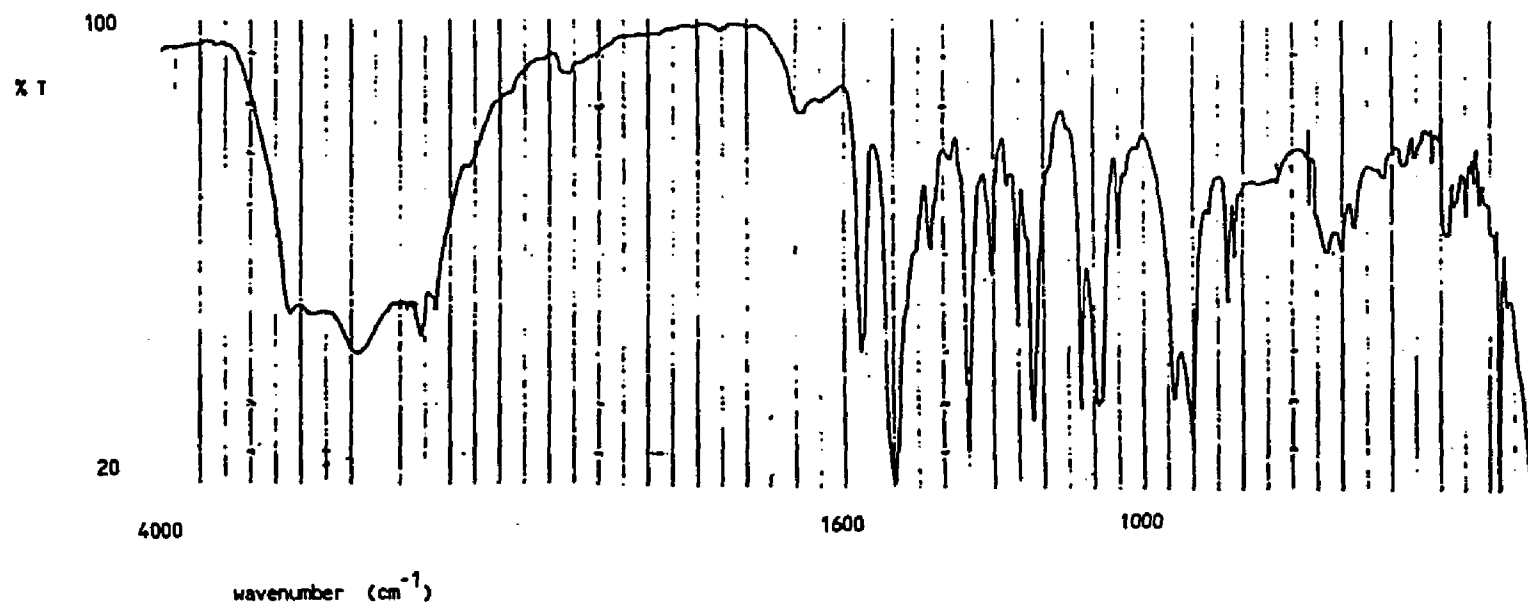
Conditions: 0.145 M in $\text{Me}_2\text{SO-d}_6$; 45° pulse angle; 25°C ;
2.8 sec. delay between pulses; 32 acquisitions.



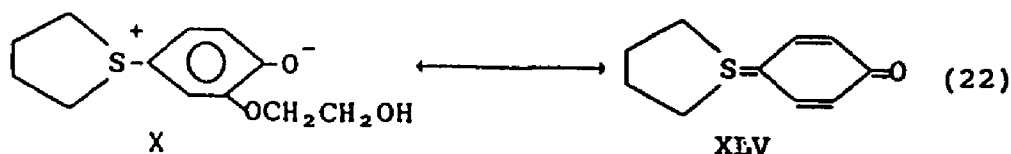
complex doublet at 2.17 and 2.45 ppm. The methylene protons adjacent to sulfur (protons 2) appear as a complex doublet at 3.35 and 3.65 ppm. Signals due to residual solvents (2-propanol and diethyl ether) are seen in the area of 1.0 ppm.

4.1.2 Infrared Spectrum. The infrared spectrum of the hydroxyethoxy zwitterion (Fig 6) showed many absorption peaks. Some of the absorption peaks were easily assigned: broad absorption at 3500-2500 cm^{-1} (OH of alcohol and H_2O); 3494 cm^{-1} (OH); 3026 cm^{-1} (aromatic C-H); 2984, 2951, 2912, 2855 cm^{-1} (aliphatic C-H); 1566, 1506 cm^{-1} (aromatic C=C); 895, 823 cm^{-1} (1, 2, 4-trisubstituted benzene C-H). Absorptions at 1422, 1342, 1305, 1252, 1218, 1094, 1081 and 1057 cm^{-1} are attributable to C-O (from aryl alkyl ether, alcohol, aryloxide), methylene twisting and wagging vibrations. Some absorption peaks (1680, 939, 720, 625 cm^{-1}) were more difficult to assign. All of the latter except the 1680 cm^{-1} absorption are compatible with structure II and can be attributed to a combination of aromatic, CH_2 and C-S bond excitations. The 1680 cm^{-1} absorption could be attributed to an aromatic overtone peak were it not a lone, strong peak. Overtone peaks typically occur as a group of several weak peaks, weaker than the observed peak at 1680 cm^{-1} . The strong absorption at 1680 cm^{-1} may indicate the important contribution of the quinoid resonance form VII to the structure of the

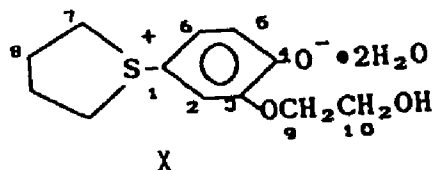
FIGURE 6. Infrared Spectrum of the Hydroxyethoxy
Zwitterion. KBr Pellet.



zwitterion



4.1.3 ^{13}C NMR Spectrum. The ^{13}C NMR spectrum of the monomer is consistent with the structure proposed. Ten signals are observed, the assignments given in Figure 7.

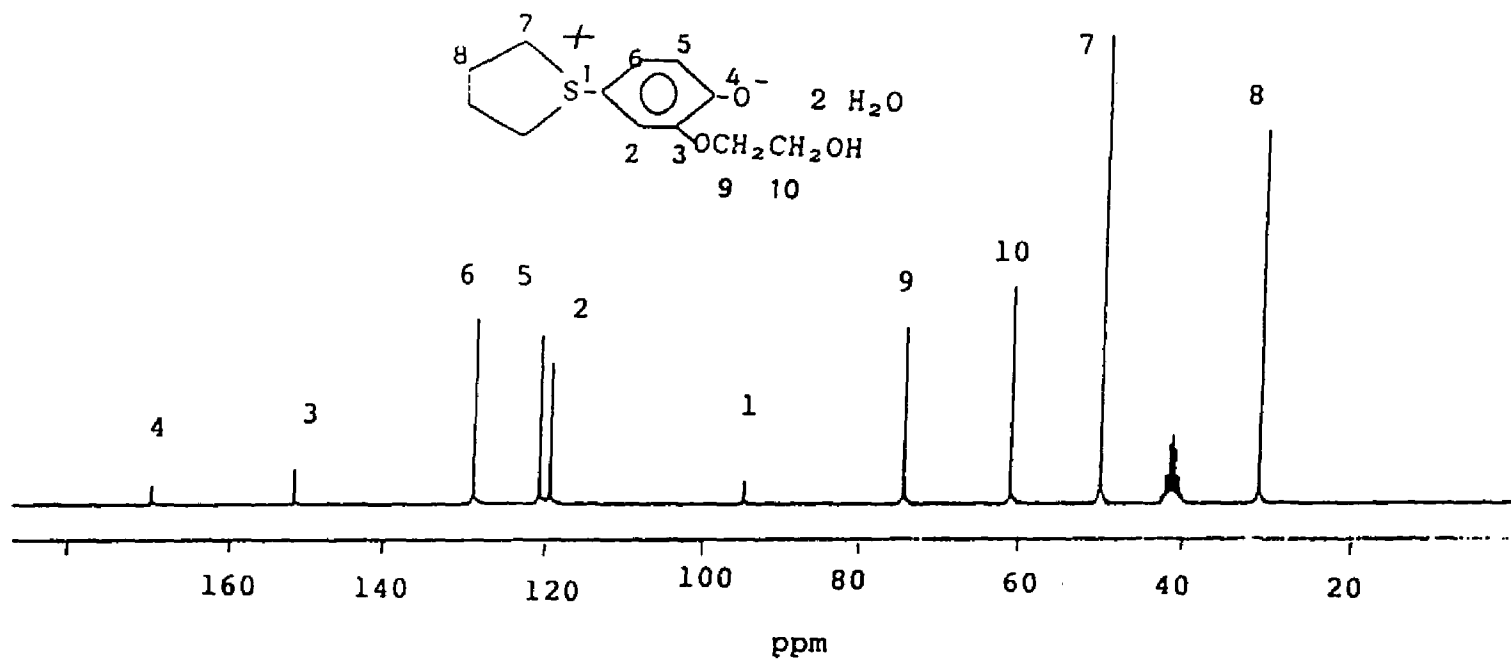


The aliphatic portion of the spectrum shows 4 signals. Signal 8 (28.13 ppm) is due to two equivalent internal methylene carbons of the tetrahydrothiophenium ring. Signal 7 (48.66 ppm) is due to the two equivalent ring methylene carbons adjacent to sulfur. Signal 10 (60.18 ppm) is assigned to the side chain carbon bearing the alcohol group. Signal 9 (73.75 ppm) is assigned to the aliphatic carbon of the aryl-alkyl ether linkage.

Three of the aromatic signals are readily identified from examination of a coupled ^{13}C NMR spectrum and consideration of the relative electronic environments.

FIGURE 7. ^{13}C NMR Spectrum of the Hydroxyethoxy
Zwitterion.

Conditions: 0.145 M in $\text{Me}_2\text{SO}-d_6$; 45° pulse angle;
 25°C ; 2.2 sec. delay between pulses; 10000 acquisitions.



Signal 1 , a singlet in the coupled ^{13}C NMR spectrum, is shifted far upfield to 94.60 ppm, and is assigned as the quaternary aryl carbon substituted with the positively charged tetrahydrothiophenium group. Signal 4, shifted far down field at 169.53 ppm, also appears as a singlet in the coupled spectrum and is assigned as the ring carbon bearing the negatively charged phenoate group. Signal 3, a singlet in the coupled spectrum appearing at 151.83 ppm, is assigned as the aryl carbon of the aryl-alkyl ether group.

Previous workers (23) used single frequency off resonance decoupling experiments (SFOR) to characterize the monomer and polymer. In the case of the monomer, hetero-nuclear SFOR experiments were performed.

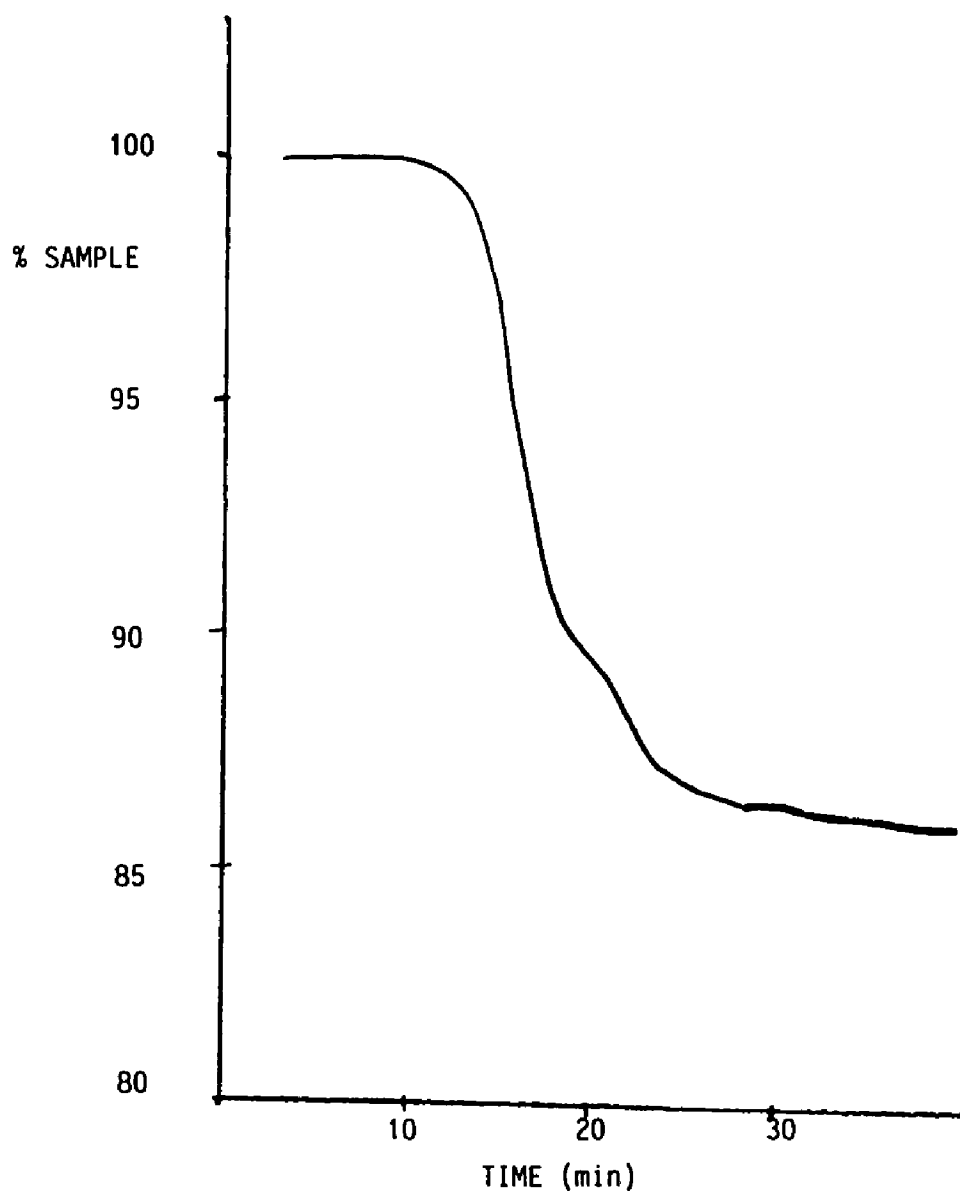
The protonated carbons, 2, 5 and 6 (118.72, 120.28 and 128.56 ppm), were assigned by accumulating coupled spectra while irradiating at frequencies associated with the protons at each position of the ring and observing which carbon signal exhibited enhanced intensity.

In this manner, irradiating at a frequency associated with the proton adjacent to the phenoate group at 6.25 ppm produced an enhancement of signal 5.

Signals 2 and 6 were assigned in the same manner by these workers.

4.1.4 Thermal Analysis. Thermogravimetric analysis (Fig 8) shows a weight loss indicative of 2.02 ± 0.05

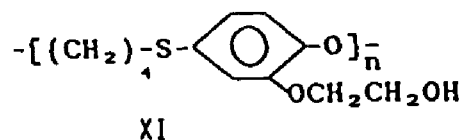
FIGURE 8. Thermogram Showing Water Loss of the
Hydroxyethoxy Zwitterion.



moles of water per mole of hydroxyethoxy zwitterion. The average of eight determinations yielded $13.17\% \text{ H}_2\text{O} \pm 0.13\%$. The theoretical moisture content of the dihydrate is 13.04% . The presence of water is also seen in the proton NMR spectra of the hydroxyethoxy zwitterion, as well as the infrared spectrum.

4.2 POLYMER CHARACTERIZATION. When a sample of crude polymerization mixture is dissolved in N,N-dimethylformamide and reprecipitated by the addition of methanol, small proton NMR signals due to the presence of oligomeric impurities disappear.

Analysis of the purified polymer by ^{13}C and ^1H NMR spectroscopy and infrared spectroscopy indicate the structure of this material to be:



The spectral assignments are given in Table 5 and figures 9 and 10.

Elemental analysis is consistent with the above repeat unit. Found: $59.67\% \text{ C}$; $6.51\% \text{ H}$; $13.10\% \text{ S}$. Theoretical: $60.00\% \text{ C}$; $6.67\% \text{ H}$; $13.33\% \text{ S}$.

4.2.1 Proton NMR spectrum. ^1H NMR spectroscopy

Table 5. ^{13}C NMR SPECTRAL ASSIGNMENTS

Carbon #	Polymer	Phenolic Diol	Vinyl Phenol	Dimer
1	126.97	124.64	124.40	126.63
2	114.97	115.88	115.64	113.27
3	148.71	146.78	146.78	148.74
4	147.43	146.05	146.21	147.83
5	116.90	116.89	117.13	120.62
6	122.87	124.13	124.07	126.22
7	33.50	34.56	33.91	35.21
8	25.12	25.41	32.74	26.34
9	27.46	31.25	136.45	27.39
10	68.28	60.17	115.85	67.33
11	70.72	70.78	70.72	71.90
12	59.40	59.60	59.50	61.22

FIGURE 9. ^{13}C NMR Spectrum of Poly(hydroxyethoxy zwitterion).

Conditions: 0.145 M in $\text{Me}_2\text{SO}-d_6$; 45° pulse angle; 65°C ; 2.2 sec. delay between pulses; 15000 acquisitions.

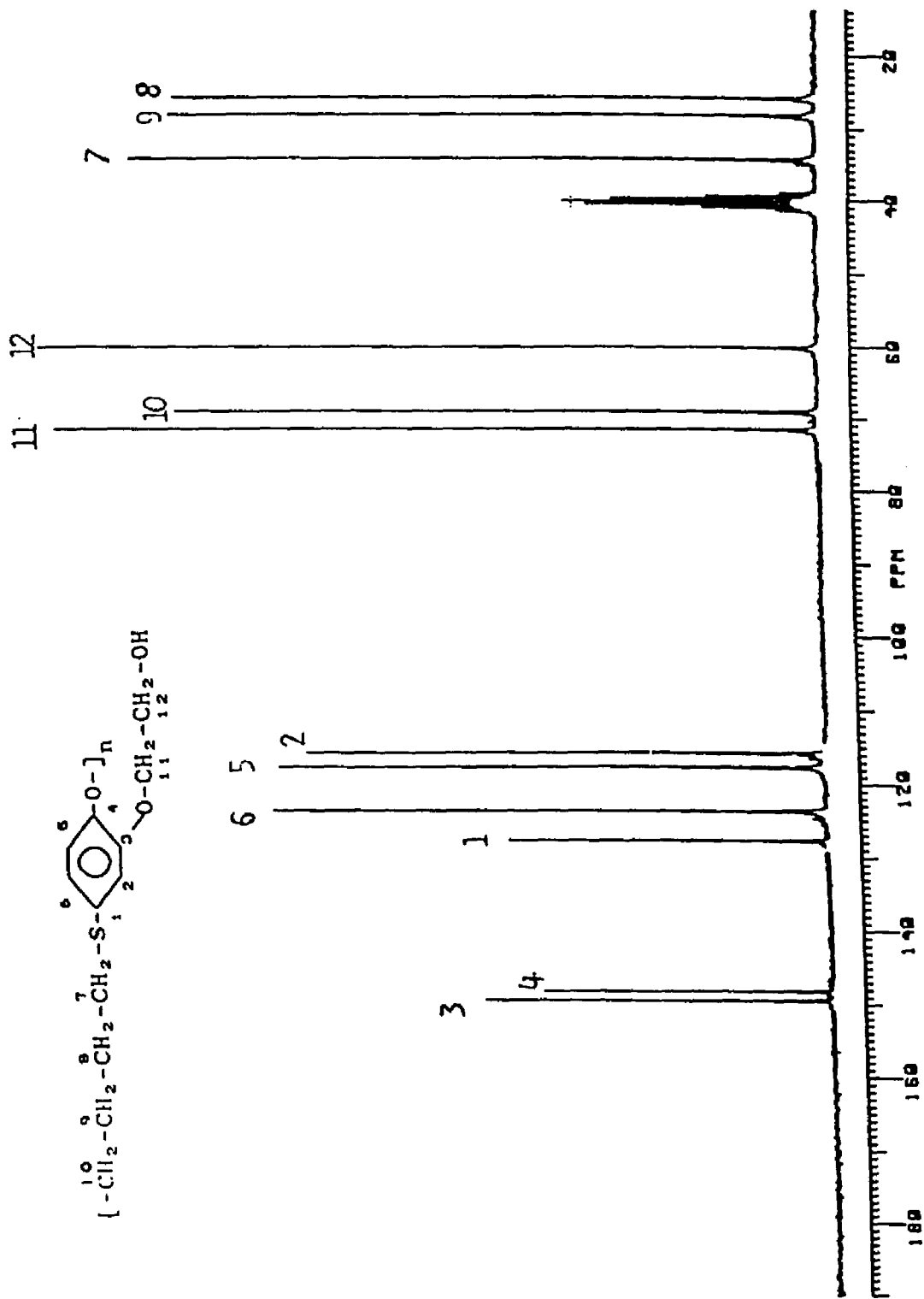
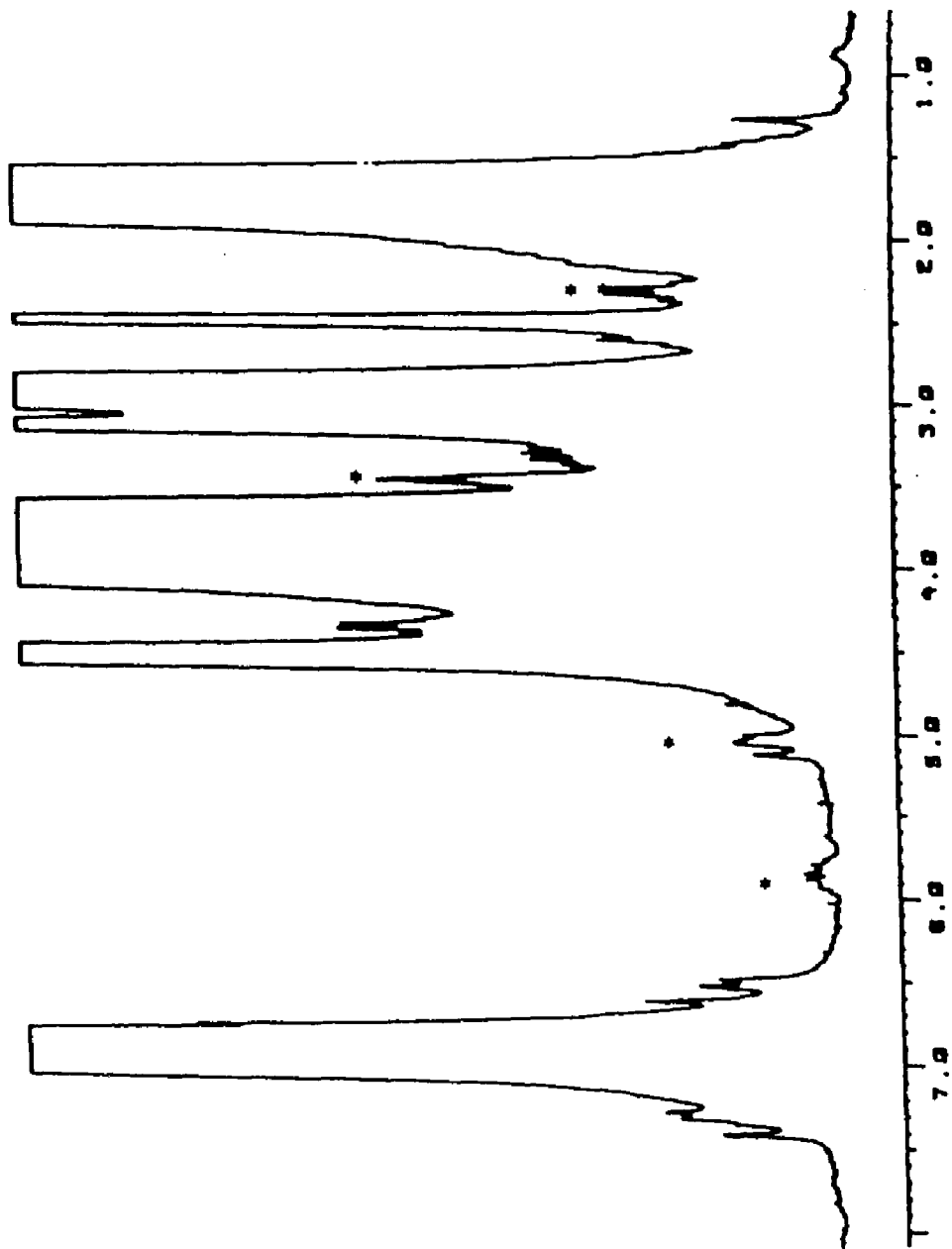


FIGURE 10. ^1H NMR Spectrum of Poly(hydroxyethoxy
zwitterion).

Conditions: 10% in $\text{Me}_2\text{SO}-d_6$; 45° pulse angle; 65°C ; 2.8
sec. delay between pulses; 1000 acquisitions.

FIGURE 10a. ^1H NMR Spectrum of Poly(hydroxyethoxy zwitterion).

Conditions: 10% in $\text{Me}_2\text{SO}-d_6$; 45° pulse angle; 65°C ; 2.8 sec. delay between pulses; 1000 acquisitions.



(Fig 10) shows signals consistent with the proposed structure, poly [oxytetramethylenethio-(2-[2-hydroxyethoxy])-1,4-phenylene]. Signals due to each type of hydrogen expected for this compound are present. Integration of the signals show the proper proportion of each type of proton, with the exception of the alcohol proton, which exchanges slightly with residual moisture.

Signals due to three aryl protons, assigned as protons 6, are seen in two signals at 7.05 and 6.95 ppm. A signal, accounting for 0.85 protons is seen at 4.50 ppm and is assigned to the alcohol proton, 5. This signal shows a dependency of chemical shift on temperature as expected for an alcoholic proton which can engage in hydrogen bonding. A signal equivalent to four protons is seen at 4.05 ppm. This signal is due to protons 2 and 3, both of which are protons of an aryl-alkyl ether linkage. protons 4, the methylene protons adjacent to the alcohol are observed at 3.65 ppm, equivalent to two protons.

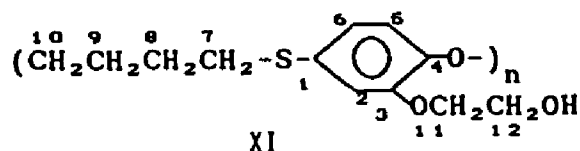
The spectrum gives clear indications that the tetrahydrothiophenium ring has been opened. The methylene adjacent to the sulfur is seen at 2.95 ppm with an integral equivalent to two protons. The internal methylene protons, 1, are seen as a signal at 1.90 ppm. The tetrahydrothiophenium ring methylene protons in the monomer are observed as a pair of multiplets.

Besides evidence of structure based on chemical shift

and signal integration, previous workers (23) have gathered evidence from homonuclear single frequency off-resonance decoupling experiments.

Off-resonance decoupling of signal 1, the internal methylene protons, produced simplification of signals 2 and 3, the ether methylene protons and methylene protons adjacent to sulfur. Irradiation of signal 4, the methylene protons adjacent to alcohol, produced simplification of signals 5 and 3, the alcohol proton and methylene protons adjacent to the ether linkage. Irradiation of signal 3 produced simplification of signals 1 and 4, the internal methylene protons and the methylene protons adjacent to the alcohol group.

4.2.2 ^{13}C NMR spectrum. The ^{13}C NMR spectrum of the polymer (Figure 9) exhibits twelve signals, as expected for the proposed structure.



The ^{13}C NMR spectrum was assigned by analogy to the ^{13}C NMR spectrum of the hydroxyethoxy zwitterion and consideration of relative chemical environment.

Of the aromatic signals, 2, 3, 5 and 6 are only slightly shifted (2-6 ppm) in the polymer spectrum when compared to the spectrum of monomer. Signals 1 and 4 are

shifted 35 and 23 ppm respectively. At these sites, bonds are being broken or formed producing drastic changes in electronic environment at these carbons. The chemical shift observed for signal 4 is close to the value seen for signal 3. This is to be expected as both signals are due to aryl carbons substituted with an alkyl ether. The carbon responsible for signal 1, the aryl carbon bonded to sulfur, is no longer in an electropositive environment and is shifted down field.

The aliphatic portion of the polymer spectrum exhibits differences when compared to the spectrum of the monomer.

The signals due to aliphatic side chain carbons of the ether and alcohol, 11 and 12, remain at the same position only slightly shifted.

A new signal, similar in chemical shift to signal 11, an aliphatic carbon involved in an alkyl-aryl ether linkage appears as signal 10. The carbon adjacent to sulfur is no longer in a strained ring and is shifted down field to 34.90 ppm.

The internal methylene carbons are no longer equivalent and are seen as two signals, 9 and 8. The internal methylene carbon closest to the ether linkage is assigned as signal 9.

4.3 PRODUCT DISTRIBUTION OF THE POLYMERIZATION. The polymerization of the hydroxyethoxy zwitterion yields

linear and cyclic products. The product distribution of the polymerization, the distribution of products into either linear higher molecular weight species or low molecular weight cyclics, shows different behavior for bulk polymerized samples compared to samples polymerized in $\text{Me}_2\text{SO-d}_6$. The bulk polymerization yields mostly linear polymer and is relatively unaffected by purposely added impurities. The polymerization of the hydroxyethoxy zwitterion in dilute solutions of $\text{Me}_2\text{SO-d}_6$ was carried out with and without added initiator. Solutions of the hydroxyethoxy zwitterion to which no added initiating specie was introduced are referred to as thermal polymerization samples. Experiments involving mixtures of monomer and the trifluoroacetate salt of the hydroxyethoxy zwitterion are referred to as initiated polymerization. The discussion of section 4.3 is limited to uninitiated polymerizations.

The solution polymerization yields larger amounts of cyclics. Temperature showed little effect on the product distribution of the reaction while solution polymerized samples produced more linear polymeric species as the reaction temperature was increased.

4.3.1 Bulk Polymerization. When monomer crystals are heated in bulk, polymerization occurs spontaneously and water of hydration is lost as water vapor. The polymerization mixture consists of linear high molecular

weight polymer and 3-7% of oligomeric products. A large portion of the oligomeric fraction is cyclic dimer and is seen as minor signals, a doublet at 6.46 and 6.55 ppm, in the ^1H NMR spectra of crude polymer (Figure 11). Cyclization is probably limited in the polymerization of the hydroxyethoxy zwitterion due to steric hindrance caused by the presence of the flexible ortho hydroxyethoxy group. Cyclization of the naphthyl analogue of this monomer under similar conditions results in the formation of 20-30% of cyclic oligomers.

Reaction temperature over a range of 70 to 140°C has the effect of increased molecular weight of the product with decreased temperature as indicated in Table 6. Thus the number average molecular weight obtained on the high molecular weight fraction produced in bulk polymerization mixtures varied from 57,700 to 94,100 daltons relative to anionic polystyrene standards at polymerization temperatures of 140 and 70°C.

In the case of the naphthyl zwitterion (19) number average molecular weights ranging from 6,300 to 21,700 were attained over a similar temperature range.

4.3.2 Solution Polymerization. In dilute solution, cyclization competes much more effectively with linear growth and much larger quantities of cyclic materials are formed. The relative quantities of cyclic dimer and trimer formed depends on the initial monomer concen-

FIGURE 11. ^1H NMR Spectrum of a Bulk Polymerization
Mixture.

Conditions: 0.145 M in $\text{Me}_2\text{SO}-d_6$; 45° pulse angle; 65°C ;
2.8 sec. delay between pulses; 32 acquisitions.

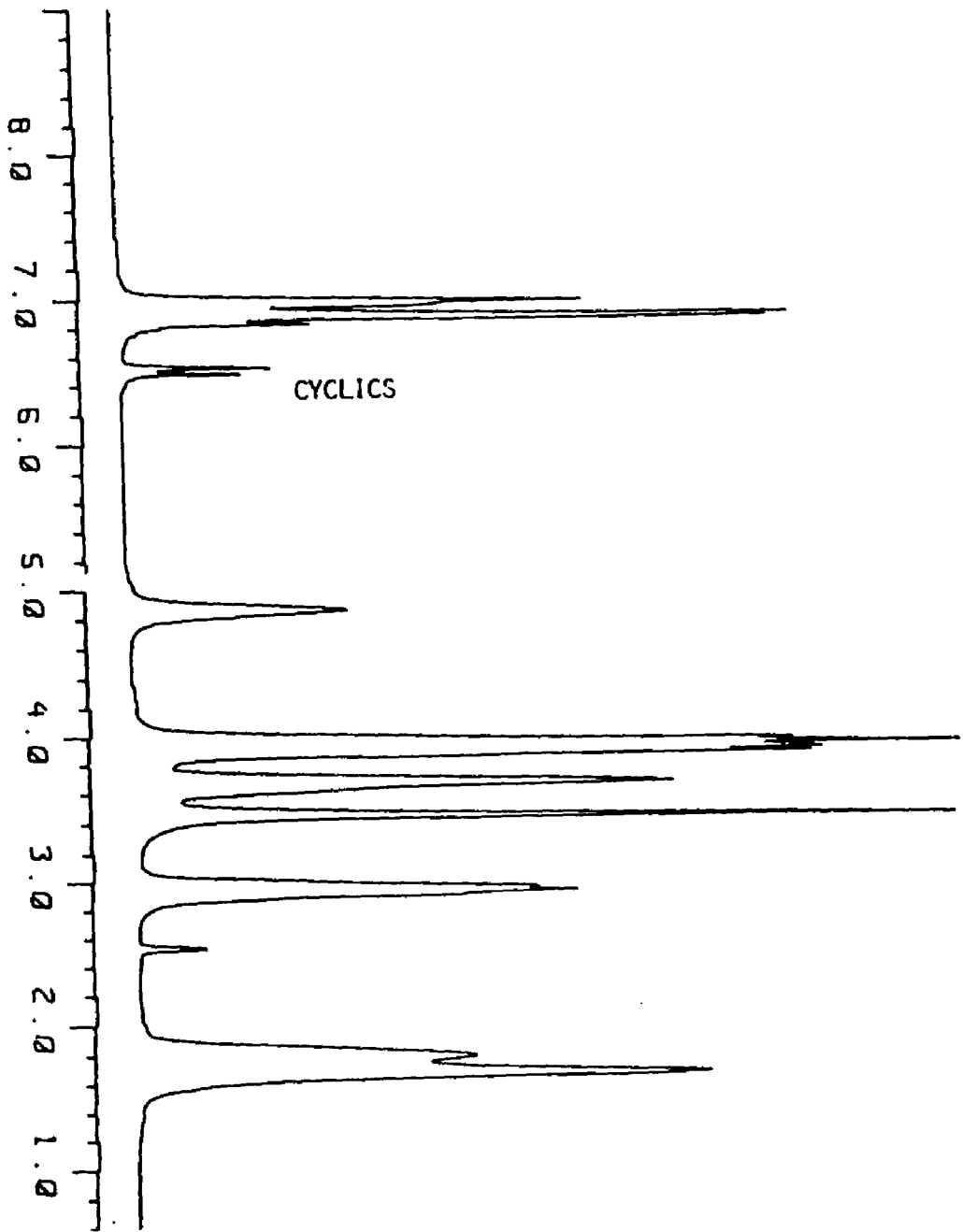


TABLE 6. EFFECT OF REACTION TEMPERATURE ON THE
MOLECULAR WEIGHT OF BULK POLYMERIZED SAMPLES

Temperature	\bar{M}_w	\bar{M}_n	\bar{M}_w/\bar{M}_n
140	100,400	57,700	1.74
100	146,500	71,400	2.05
70	290,500	94,100	3.08

tration. Table 7 shows trends of reduced cyclic trimer and increased cyclic dimer production at the completion of the reaction as the initial monomer content of reaction mixtures was decreased. The cyclic oligomers are referred to as C2, C3, C4, and C5 representing cyclic dimer through cyclic pentamer.

The solubility of monomer in the reaction solvent, Me₂SO-d₆, limited prepared reaction mixtures to 0.208 M solutions. Analysis of cyclic dimer spectroscopically (¹H NMR) generally yielded cyclic dimer results 10% lower than chromatographic analysis of the mixture using a GPC fractionation and an area percent analysis of the differential refractive index signal of the detector.

As the initial monomer concentration of the reaction mixture was decreased from 0.208 M to 0.020 M, the cyclic dimer content of the reaction mixture increased by 46% and the polymer content decreased by 50%. The relative quantities of cyclic trimer and cyclic tetramer decreased with lowered initial monomer concentration while the cyclic pentamer content showed little change over the concentration range of monomer employed.

Temperature exerts only a small effect on the relative amount of cyclic dimer formed (Table 8). The cyclic dimer contents found in reaction products over a temperature range of 65 to 140°C are identical within the limits of experimental uncertainty. The ratio of polymer

TABLE 7. EFFECT OF INITIAL MONOMER CONCENTRATION ON
PRODUCT DISTRIBUTION IN FINAL REACTION MIXTURE ¹

<u>NMR ANALYSIS</u>						
M_0	Mole Fraction		Mole Fraction			
	Cyclic Dimer		Polymer & Higher Cyclics			
0.208	0.410/0.485		0.590/0.515			
0.145	0.563		0.437			
0.101	0.572/0.581		0.427/0.419			
0.060	0.617		0.383			
0.0404	0.637/0.604		0.363/0.396			

<u>SIZE EXCLUSION CHROMATOGRAPHY</u>						
M_0	<u>Cyclic Oligomers</u>					<u>Polymer</u>
	C2	C3	C4	C5	Total Cyclics	
0.208	0.503	0.237	0.065	0.031	0.836	0.164
0.145	0.597	0.208	0.049	0.021	0.875	0.124
0.101	0.622	0.159	0.038	0.021	0.840	0.161
0.060	0.715	0.142	0.032	0.019	0.908	0.093
0.040	0.703	0.090	0.028	0.029	0.850	0.150
0.020	0.773	0.085	0.033	0.031	0.922	0.077

¹ Solution polymerized samples at 80°C.

TABLE 8. EFFECT OF TEMPERATURE ON PRODUCT
DISTRIBUTION IN FINAL REACTION MIXTURE ¹

<u>NMR ANALYSIS</u>						
Temp	Mole Fraction		Mole Fraction			
°C	Cyclic Dimer		Polymer & Higher Cyclics			
65	0.495/0.490		0.495/0.510			
80	0.563		0.437			
100	0.577/0.550		0.423/0.450			
140	0.579/0.520		0.421/0.480			

<u>SIZE EXCLUSION CHROMATOGRAPHY</u>						
Temp	<u>Cyclic Oligomers</u>				Total	<u>Polymer</u>
	°C	C2	C3	C4		
65	0.585	0.231	0.055	0.022	0.893	0.106
80	0.597	0.208	0.049	0.021	0.875	0.124
100	0.628	0.154	0.037	0.019	0.838	0.163
140	0.599	0.127	0.022	0.022	0.777	0.215

¹ The initial monomer concentration was 0.145 M in
DMSO-d₆

to cyclics in the bulk polymerization of the naphthyl zwitterion (19) was also rather insensitive to temperature over the temperature range of 100 to 200°C. The amount of higher molecular weight product as measured by GPC increases with increased reaction temperature at the expense of higher cyclic species.

4.4 ANALYSIS OF REACTION BY-PRODUCTS. The products of the polymerization of the hydroxyethoxy zwitterion were analyzed by fractionating a sample of a reaction mixture prepared in solution at 80°C using preparative HPLC. The separated components were examined by ¹H NMR and mass spectroscopy to identify individual components. All of the separated low molecular weight materials proved to be cyclic oligomers. Cyclic dimer, trimer, tetramer and pentamer were isolated in the preparative HPLC experiment. A higher molecular weight specie believed to be cyclic hexamer is also observable in GPC fractionation.

Larger amounts of purified cyclic dimer were obtained by reacting a dilute solution (0.020M) of the hydroxyethoxy zwitterion in Me₂SO-d₆ and isolating the product by recrystallization. The larger quantities of purified cyclic dimer available allowed for characterization of the material by ¹³C NMR and infrared spectroscopy.

4.4.1 Characterization of Cyclic Dimer. The structure of the cyclic dimer was established using

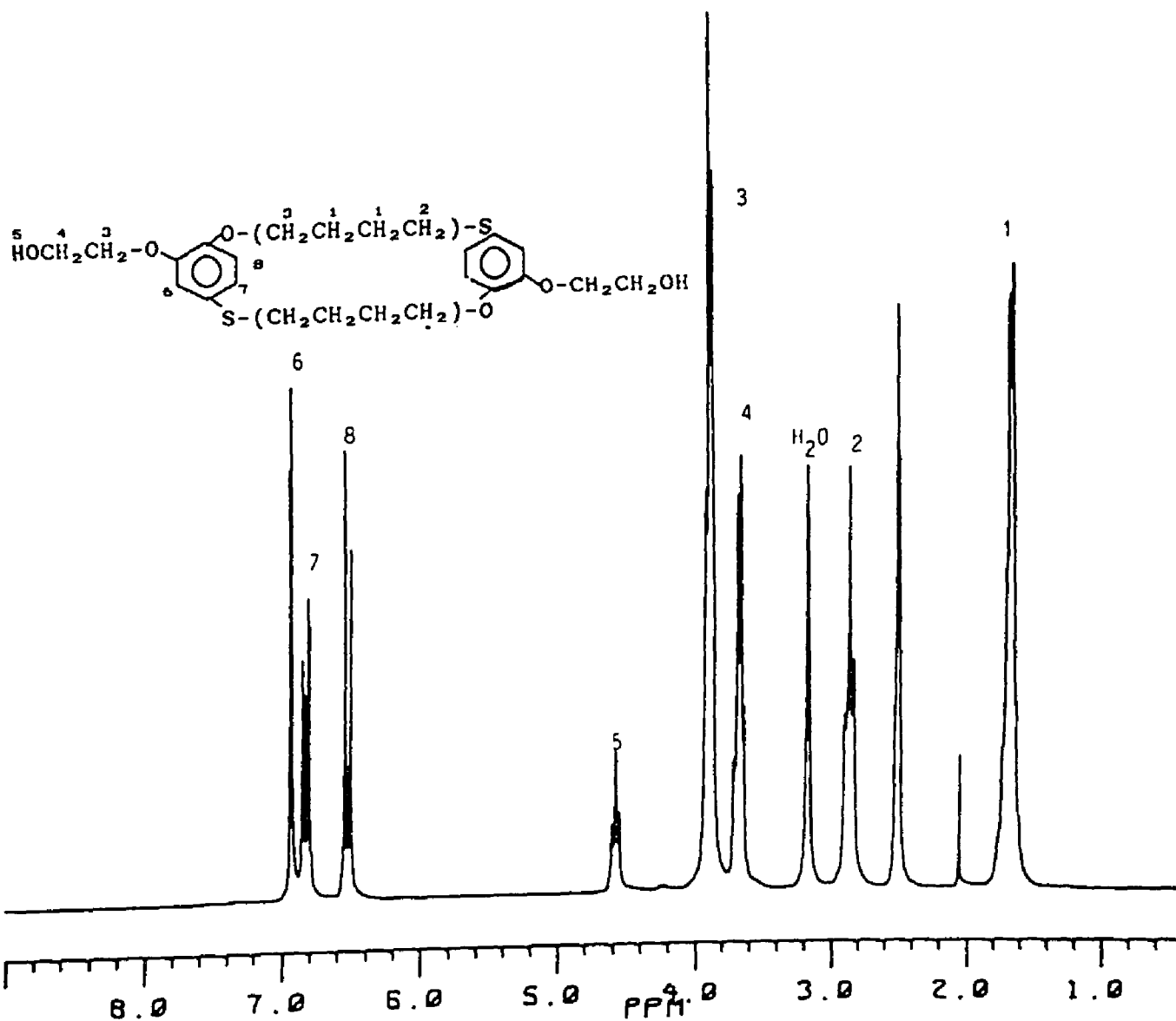
elemental analysis, mass spectroscopy, and NMR spectroscopy. Elemental analysis: Theory: 60.00% C, 6.67% H, 13.33% S; Found: 60.17% C, 6.82% H, 13.58% S.

Mass spectroscopy, carried out at the laboratories of Dow Chemical, detected a parent ion, molecular mass 480 g/mol; 480 g/mol calculated. The NMR spectra show no evidence of any end groups. End groups are expected to be easily discernible for a linear molecule of only two repeat units molecular mass. The absence of end groups is taken as strong evidence of the cyclic nature of the isolated dimer.

4.4.1.1 Proton NMR Spectrum. The proton NMR spectrum of cyclic dimer (Fig 12) is consistent with the proposed structure of this material. The tetrahydrothiophenium ring has clearly been opened as can be seen from the internal methylene signals seen at 1.74 ppm and the methylene adjacent to sulfur at 2.93 ppm. Other signals easily assigned are methylene protons adjacent to alcohol at 3.67 ppm, methylene protons adjacent to aryl ether at 3.98 ppm and aromatic signals (3 protons) seen from 6.4 to 7.0 ppm. The aryl protons show the splitting pattern expected for this structure. The coupling constants were measured as $J_{ortho} = 8.4$ Hz., $J_{meta} = 2.0$ Hz. and $J_{para} < 0.2$ Hz. These values are in good agreement with the reported ranges of: J_{ortho} 5-9 Hz., J_{meta} 2-3 Hz. and J_{para} 0-1 Hz (24).

FIGURE 12. ^1H NMR Spectrum of Cyclic Dimer.

Conditions: 0.145 M in $\text{Me}_2\text{SO}-d_6$; 45° pulse angle; 65°C ;
2.8 sec. delay between pulses; 32 acquisitions.



The most conclusive evidence relating to the cyclic nature of the dimer is the absence of any proton NMR signals that could be attributable to end groups.

4.4.1.2 Infrared Spectrum. The infrared spectra of polyhydroxyethoxy zwitterion and the cyclic dimer are very similar (Figures 13 and 14). Both compounds show IR absorption bands at 3060 cm^{-1} (aromatic C-H); $2930, 2870\text{ cm}^{-1}$ (aliphatic C-H); $1580, 1500\text{ cm}^{-1}$ (aliphatic C=C); $895, 800\text{ cm}^{-1}$ (1,2,4 trisubstituted benzene). Bands at 1300 and 1040 cm^{-1} are consistent with the O-H bend and C-O stretch for the primary alcohol and signals at 1255 and 1215 cm^{-1} are assignable as due to the C-O stretch of the aryl-alkyl ether.

While the absorption bands of the cyclic dimer are sharper than the signals seen in the polymer spectrum, all major signals are observed in both spectra with the exception of the OH signal in the area of $3400 - 3600\text{ cm}^{-1}$.

The polymer shows a broad signal centered at 3460 cm^{-1} which is typical for alcohols. The cyclic dimer shows a sharp signal at 3450 cm^{-1} superimposed on the broad OH stretch in this region. While the sharpness of this band is reminiscent of a phenolic O-H stretch, ^1H NMR spectroscopy shows no evidence of a phenolic proton and the sample is insoluble in aqueous alkali.

The sharpness and position of the O-H stretch of the

FIGURE 13. Infrared Spectrum of Poly(hydroxyethoxy zwitterion). KBr Pellet.

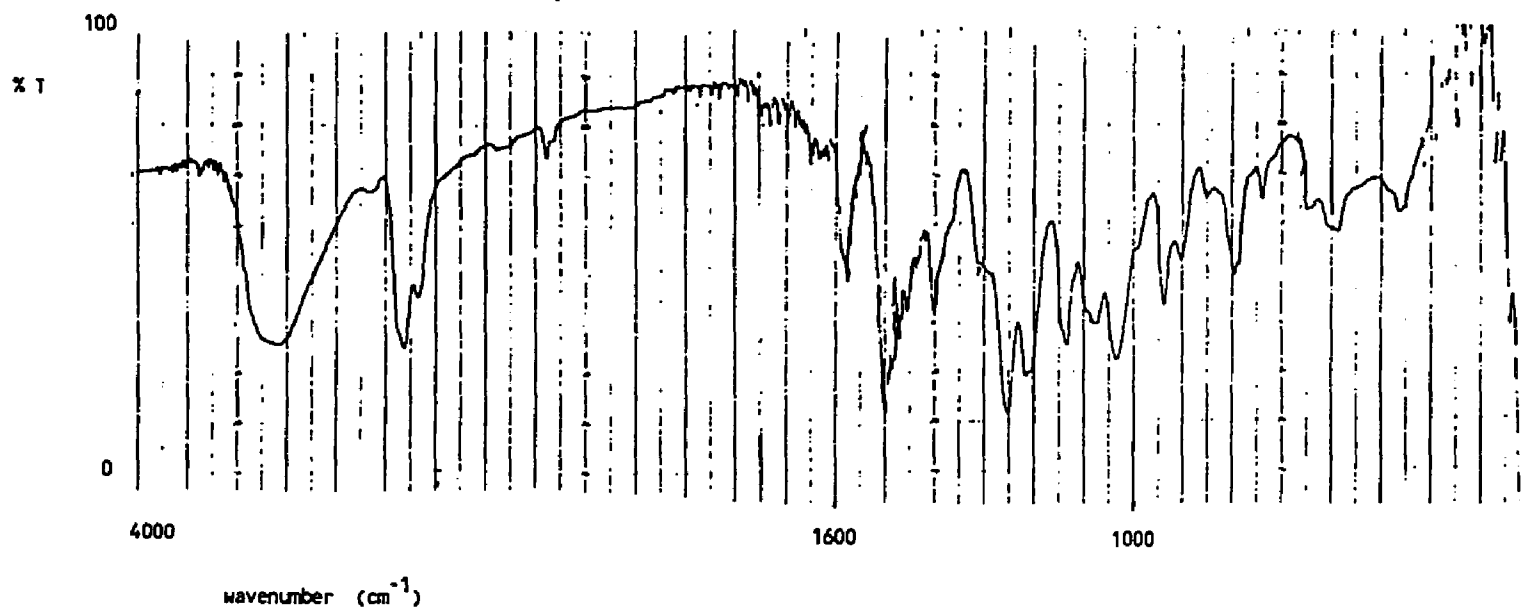
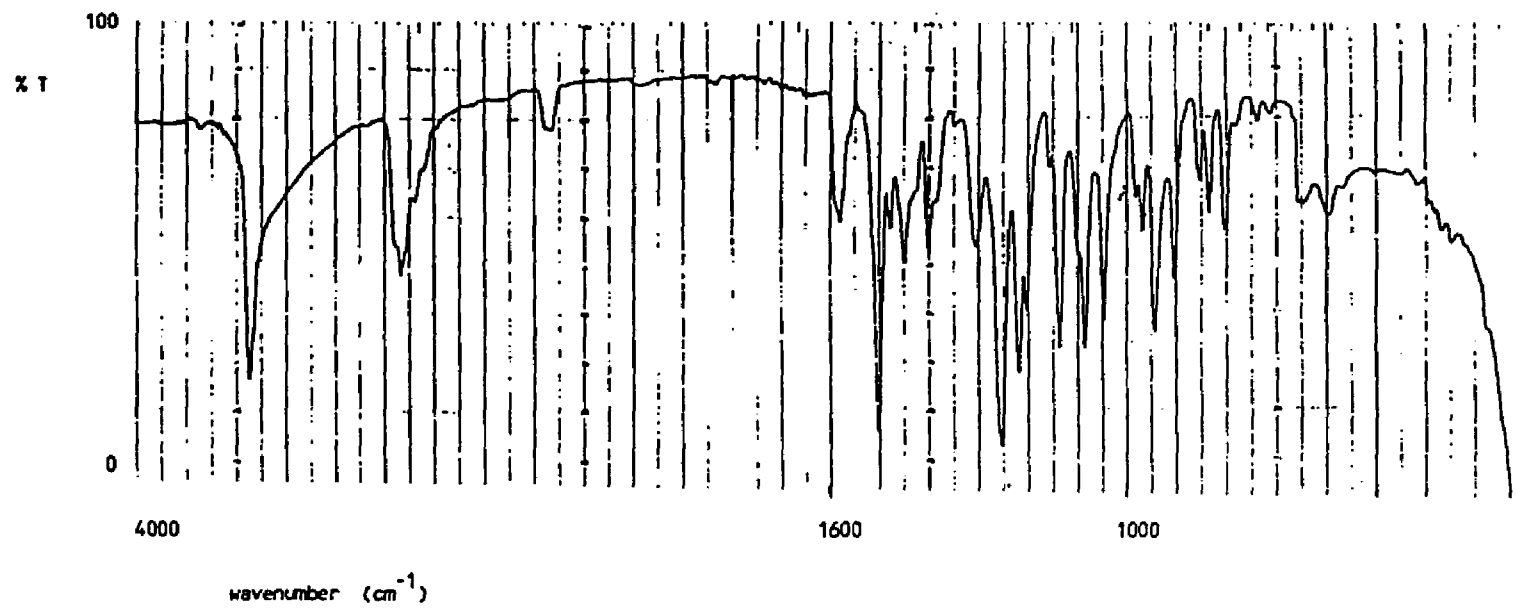
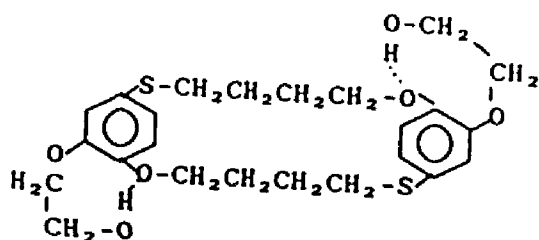


FIGURE 14. Infrared Spectrum of Cyclic Dimer.
KBr Pellet.



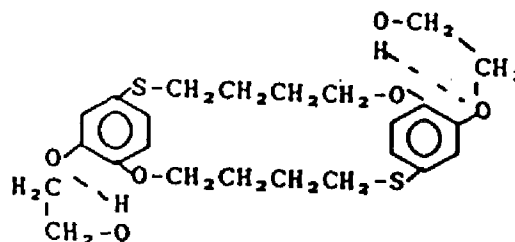
dimer may be assigned to intramolecular hydrogen bonding. Examination of spatial models of the cyclic dimer indicates that hydrogen bonding between the hydroxyl proton and the oxygen para to the sulfur group is favored sterically over hydrogen bonding involving the alcohol and the oxygen meta to the sulfur.



XLVI

sterically favored

VII



XLVII

sterically prohibited

IX

4.4.1.3 ^{13}C NMR Spectrum. Like the Infrared spectrum, the ^{13}C NMR spectrum of the cyclic dimer is similar to the carbon spectrum of the polymer. The signals are easily assigned from analogy to the polymer spectrum (Figure 15, Table 5). Again no signals identifiable as end groups were discerned.

4.4.2 Characterization of the Higher Cyclics. The methylene chloride soluble fraction of the reaction products from the solution polymerization of the hydroxyethoxy zwitterion at 80°C was analyzed by HPLC. Analytical HPLC showed the presence of five different compounds in this oligomer fraction (Figure 16).

FIGURE 15. ^{13}C NMR Spectrum of Cyclic Dimer.

Conditions: 0.145 M in $\text{Me}_2\text{SO}-d_6$; 45° pulse angle;
 65°C ; 2.2 sec. delay between pulses; 15000 acquisitions.

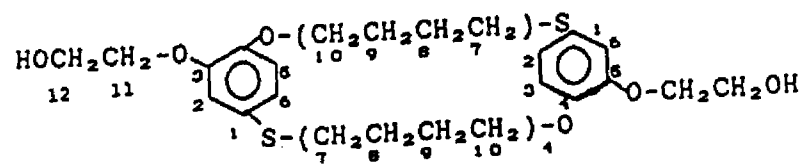
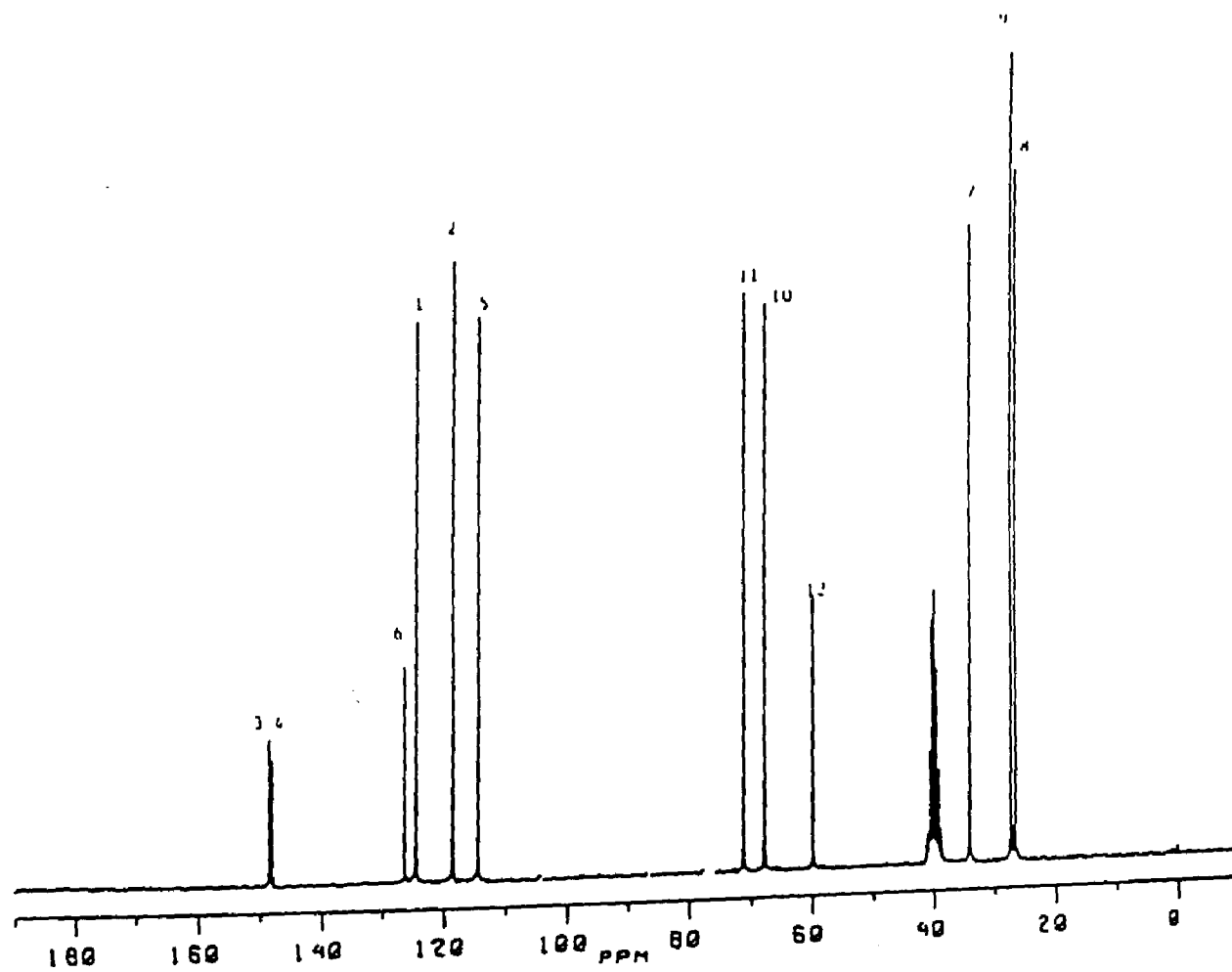
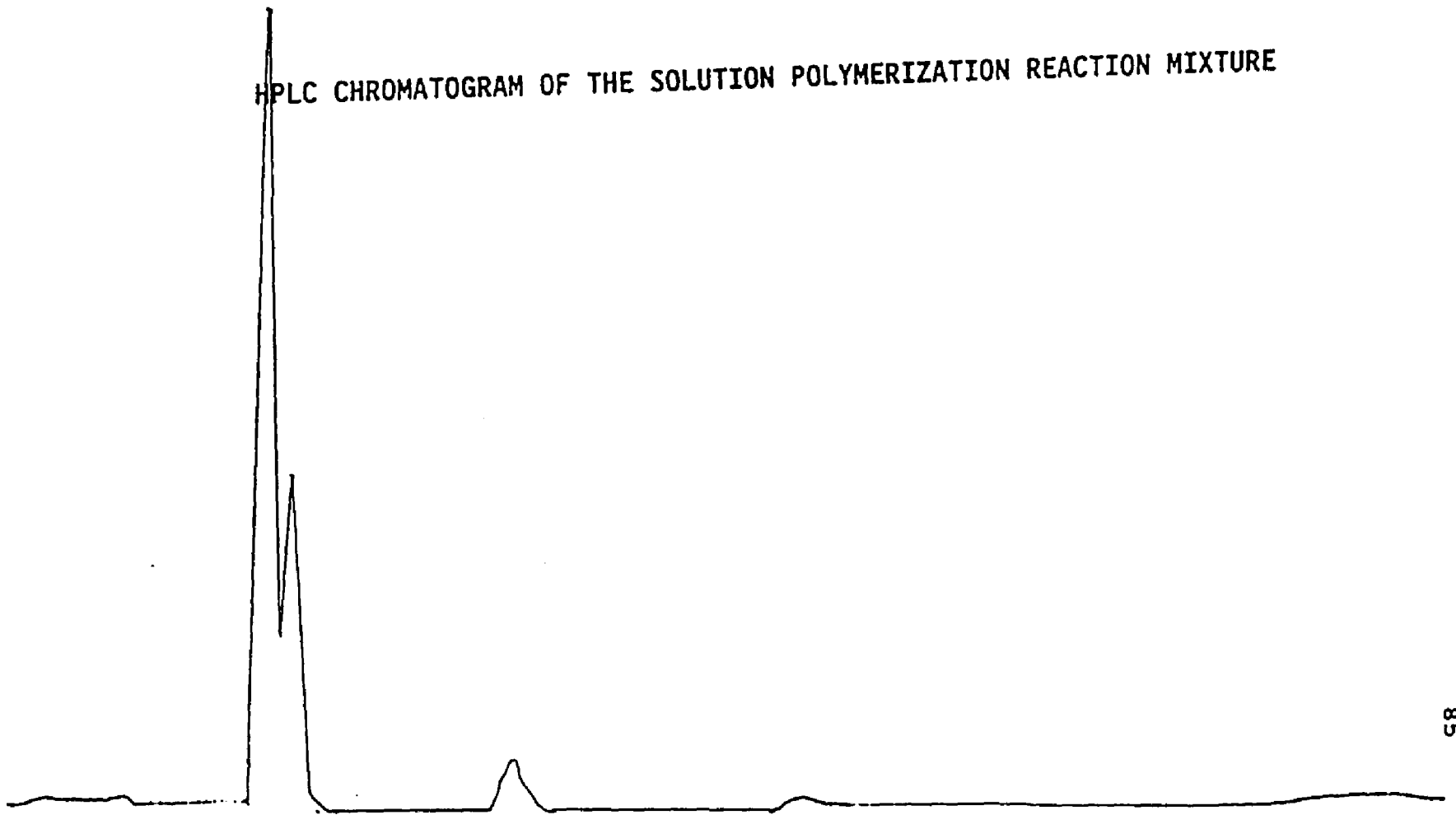


Figure 16. High Performance Liquid Chromatogram of the Methylene Chloride Soluble Fraction of the Solution Polymerized Reaction Mixture.

Conditions: 0.145 M solution of monomer reacted at 80°C for two days.

HPLC CHROMATOGRAM OF THE SOLUTION POLYMERIZATION REACTION MIXTURE



The methylene chloride soluble portion of the reaction mixture was fractionated by preparative HPLC and three fractions enriched in cyclic dimer, trimer, tetramer and pentamer were obtained.

Cyclic dimer was obtained in pure form, while the cyclic trimer, tetramer, and pentamer were enriched to 70, 87, and 70% purities, respectively, as shown by analytical HPLC.

The assignment of cyclic oligomers to these materials are based on the absence of end groups detectable by ^1H NMR spectroscopy, and the molecular masses indicated by mass spectroscopy.

The ^1H NMR spectra of the isolated higher cyclics were very similar. On all three samples signals were observed at 1.83 (m, CH_2CH_2), 2.90 (m, SCH_2 , OH), 3.99 (m, Ph-O-CH_2 -), 6.76 (d, aryl H), and 6.97 ppm (m, aryl H). In these higher cyclic species, the aryl protons are different from both the hydroxyethoxy zwitterion and the polymer, a signal appearing at 6.76 ppm compared to 6.42 ppm in the case of the cyclic dimer under these conditions. No signals were observed to indicate any chemical linkage different than the linear polymer, i. e., the materials are indicated to be cyclic by ^1H NMR spectroscopy.

Mass spectra of the samples enriched in cyclic dimer, trimer and tetramer support this conclusion as protonated

molecular ions were observed at M/Z 481, 721, and 961, respectively.

4.4.3 Calculation of Product Distribution by

^1H NMR Spectroscopy and GPC. Samples of cyclic dimer through pentamer isolated by HPLC were also analyzed by GPC. The GPC analysis of the enriched fractions obtained from preparative HPLC showed that the species were separated by size in the GPC experiments as expected. At 65°C using N,N-dimethylformamide as the mobile phase without added LiBr, peaks with elution times of 49.67, 48.25, 47.05, 46.17, and 45.42 minutes were identified as cyclic dimer, trimer, tetramer, pentamer, and hexamer, respectively (Figure 17). The cyclic hexamer was not isolated but identified in the HPLC and GPC experiments by analogy to the other species isolated and identified.

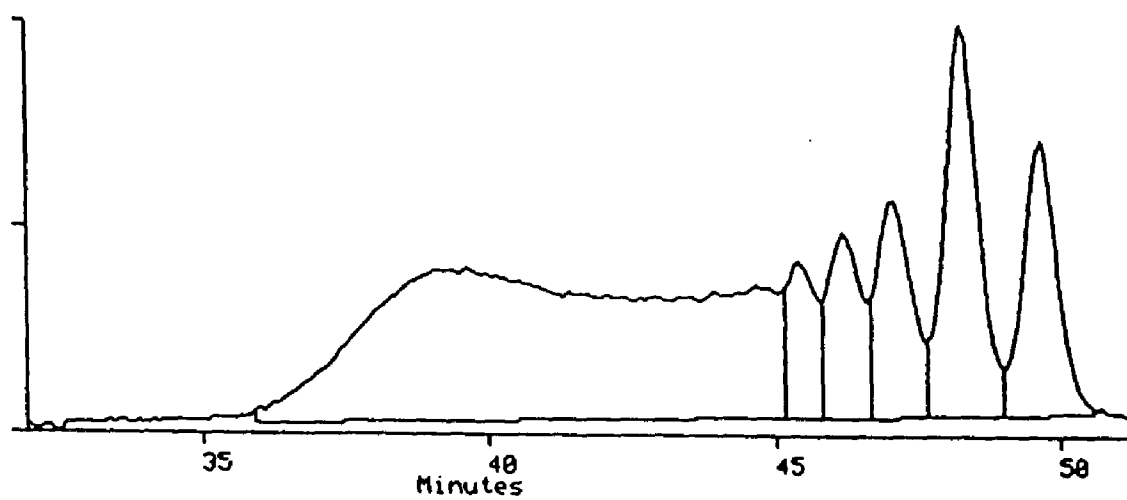
The signal areas of the GPC peaks were proportional to the relative weights of the components present and in agreement with the results of ^1H NMR measurements. Recrystallized cyclic dimer and polymer, obtained from a bulk polymerization and purified by reprecipitation, were used to prepare a 50:50 mixture and subjected to analysis by GPC and ^1H NMR spectroscopy. GPC analysis by peak area yielded a calculated ratio of 51:49 (polymer to dimer) and ^1H NMR analysis carried out as described in Section 3.5.2 yielded a calculated ratio of 48:52 (polymer to dimer).

The GPC analysis is probably not as accurate when

Figure 17. Gel Permeation Chromatogram of Reaction Mixture
After Polymerization in $\text{Me}_2\text{SO-d}_6$ Solution
(0.145M) at 65°C for Three Days with 4.6 mol%
of TFA Salt Initiator.

POLYMER

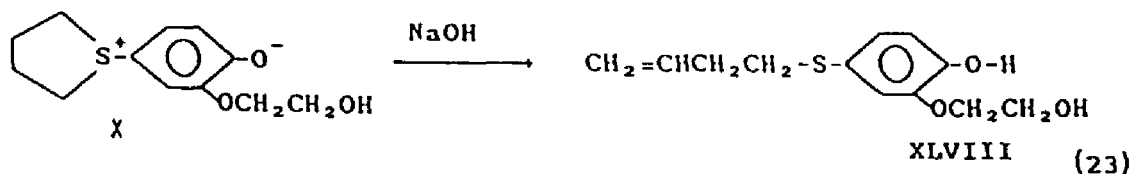
CYCLIC OLIGOMERS



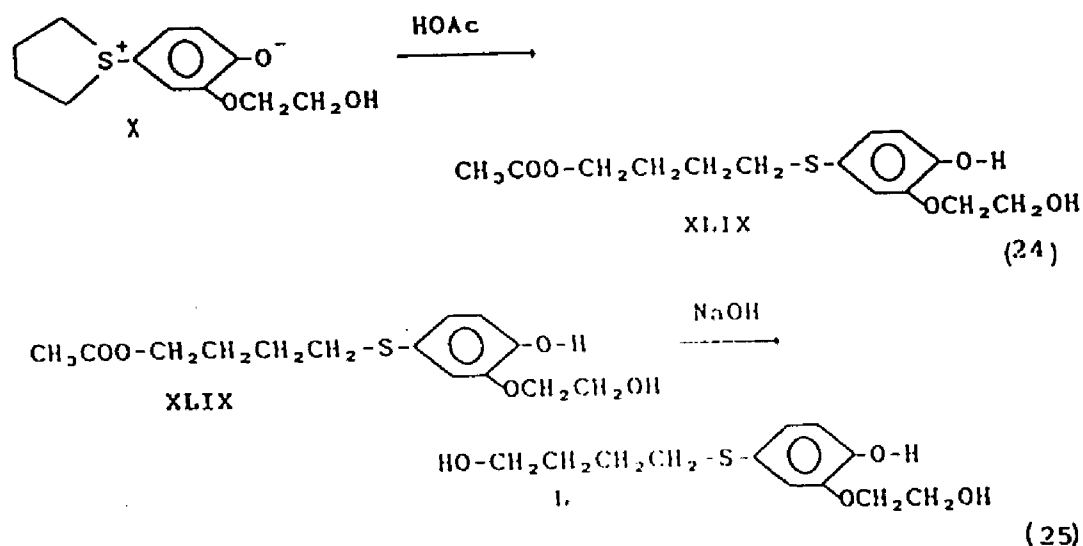
applied to the more complex mixtures analyzed which contain appreciable amounts of all six components, but is an indicator of the relative amounts present. Standard additions of recrystallized cyclic dimer to a solution polymerization reaction mixture previously analyzed by ^1H NMR yielded results within 8% relative to the calculated values of monomer, cyclic dimer, and polymer plus higher cyclics.

4.5 CHARACTERIZATION OF COMPOUNDS MODELING POLYMER END GROUPS.

Low molecular weight compounds were prepared which serve as models for the expected endgroups. 2-Hydroxyethoxy-4-(4-butenylthio) phenol, referred to subsequently as vinyl phenol, was prepared by ring opening elimination at the sulfur of the tetrahydrothiophenium ring in the monomer using an excess of aqueous sodium hydroxide.



2-Hydroxyethoxy-4-(4-hydroxybutanthio) phenol, referred to subsequently as phenolic diol, was prepared from the acetate ester of the monomer as outlined below.



4.5.1 Phenolic Diol. The carbon spectrum of the phenolic diol (Figure 18) is consistent with the expected structure. 12 signals were observed, the assignments given in Table 5. As expected, 11 of the signals are very similar to the polymer spectrum; a second alcoholic carbon signal is seen at 60.17 ppm and the ether carbon, seen in the spectrum of polymer at 68.28 ppm is no longer observed. The proton NMR spectrum (Figure 19) is also indicative of the phenolic diol. Methylene protons attached to carbon bearing an alcohol group appear at 3.41 ppm. The phenolic proton can be seen in dry samples at 8.65 ppm in $\text{Me}_2\text{SO-d}_6$. The low field position of the phenolic chemical shift is solvent dependent. This is analogous to the behavior of p-methoxy phenol which shows a phenolic proton in this region when run in $\text{Me}_2\text{SO-d}_6$, but

FIGURE 18. ^{13}C NMR Spectrum of 2-Hydroxyethoxy-4-(4-hydroxy butanthio) phenol.

Conditions: 0.145 M in $\text{Me}_2\text{SO-d}_6$; 45° pulse angle;
 65°C ; 2.2 sec. delay between pulses; 15000 acquisitions.

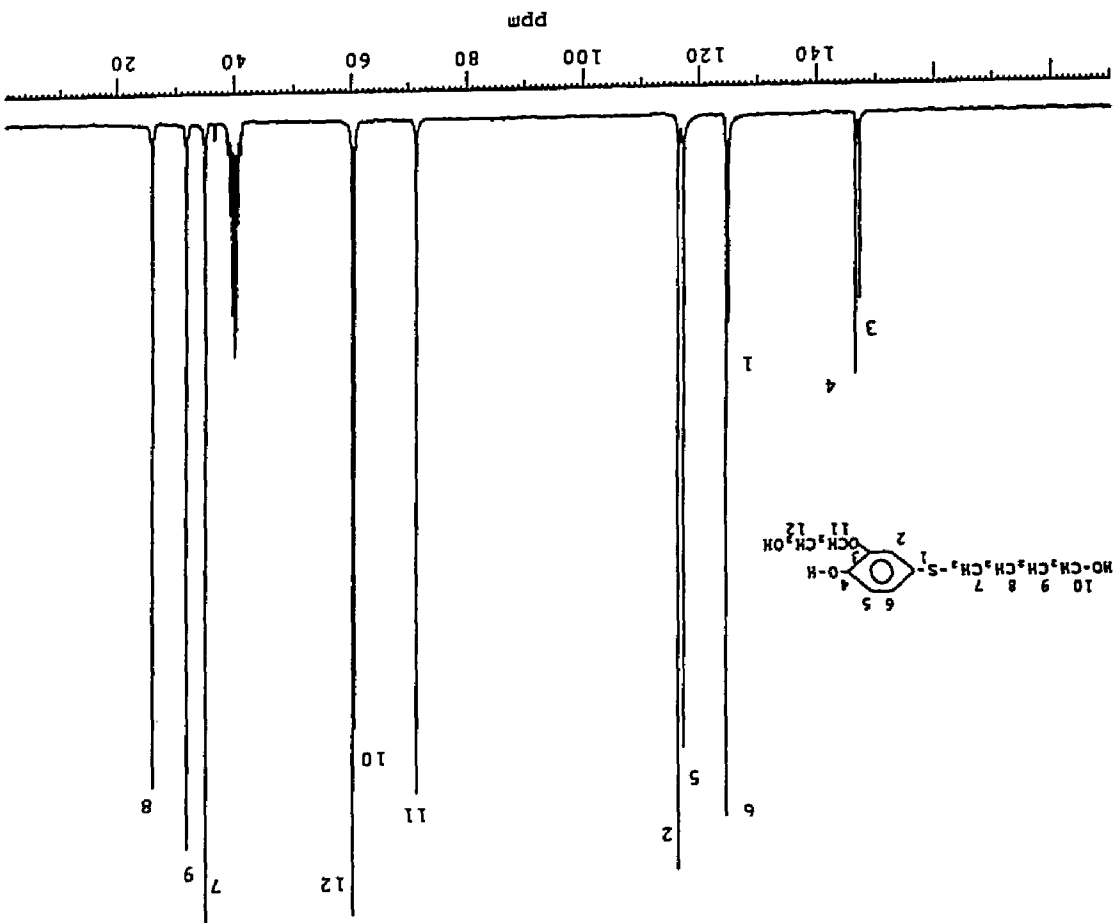
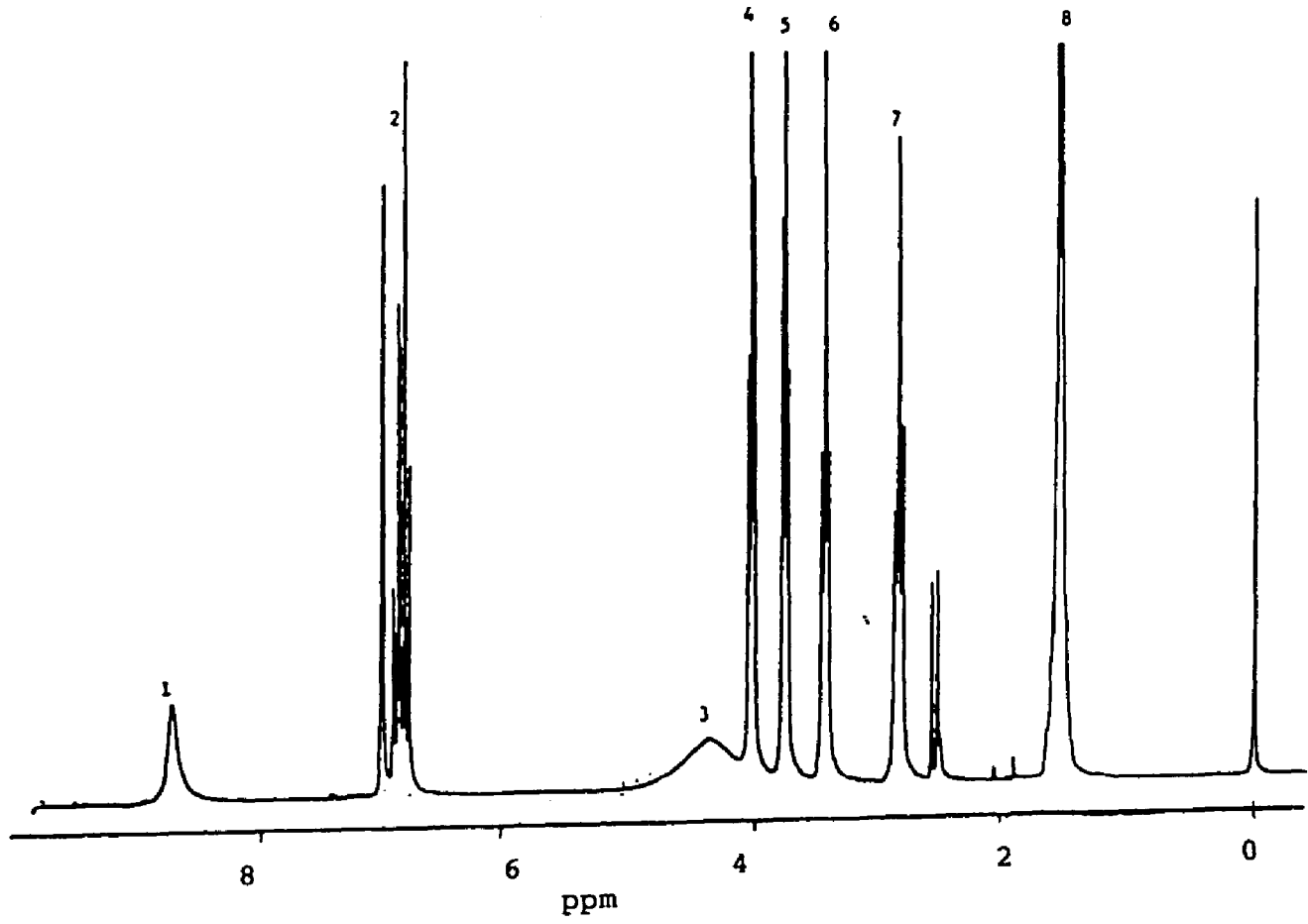
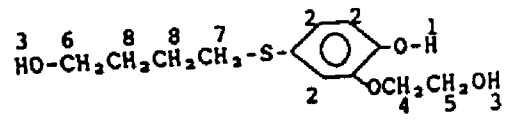


FIGURE 19. ^1H NMR Spectrum of 2-hydroxyethoxy-4-(4-hydroxy butanthio) phenol.

Conditions: 0.145 M in $\text{Me}_2\text{SO-d}_6$; 45° pulse angle; 65°C ; 2.8 sec. delay between pulses; 32 acquisitions.



shows a signal shifted to 4.5 ppm in CDCl_3 .

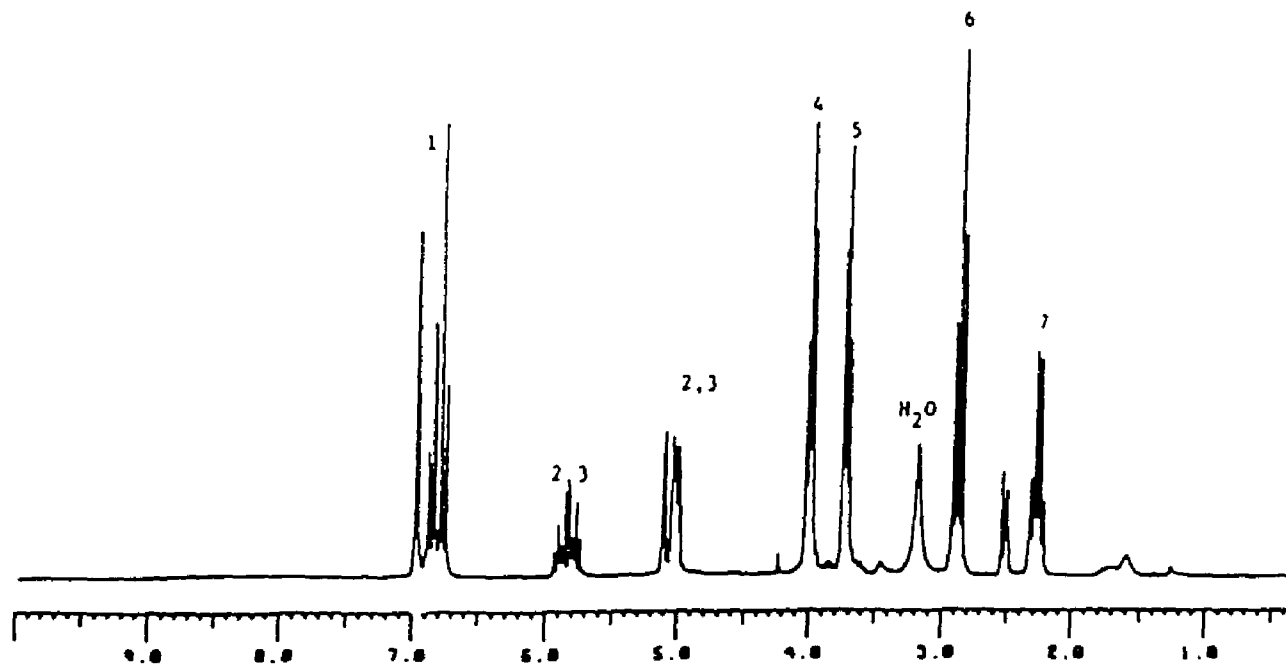
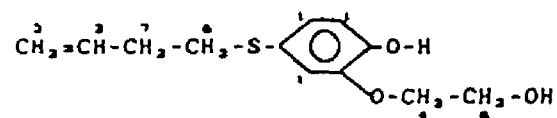
Elemental analysis of this material yielded 55.36% C; 7.18% H; 12.41% S; Theoretical: 55.81% C; 6.98% H; 12.40% S.

4.5.2 The Vinyl Phenol. The vinyl phenol was not purified as effectively as the phenolic diol, as can be seen in the proton NMR spectrum (Fig 20). A trace of phenolic diol is discernible as well as an unknown substance giving rise to a signal at 4.30 ppm. The purity is greater than 90%, however, and the effect of the vinyl group is seen in signals centered at 5.9 and 5.0 ppm. The methylene protons adjacent to the vinyl group are shifted down field to 2.34 ppm. The ^{13}C NMR spectrum (Fig 21) is also consistent with the expected structure yielding 12 signals, tabulated in table 5. As expected, significant effects are seen in the vinyl protons and the adjacent methylene carbon, when analogous carbons of polymer and model compound are compared.

4.6 EXAMINATION OF POLYMER END GROUPS. Weak endgroup signals are observed in purified polymer samples. Figure 10a is a proton NMR spectrum of polymer prepared at 70° and purified by dissolution in *N,N*-dimethylformamide followed by reprecipitation with added diethyl ether. The end group signals, observed at scale settings 150 times more sensitive than those used to observe the gross spectrum, provide evidence of side reactions which termin-

FIGURE 20. ^1H NMR Spectrum of 2-hydroxyethoxy-4-(4-butenylthio) phenol.

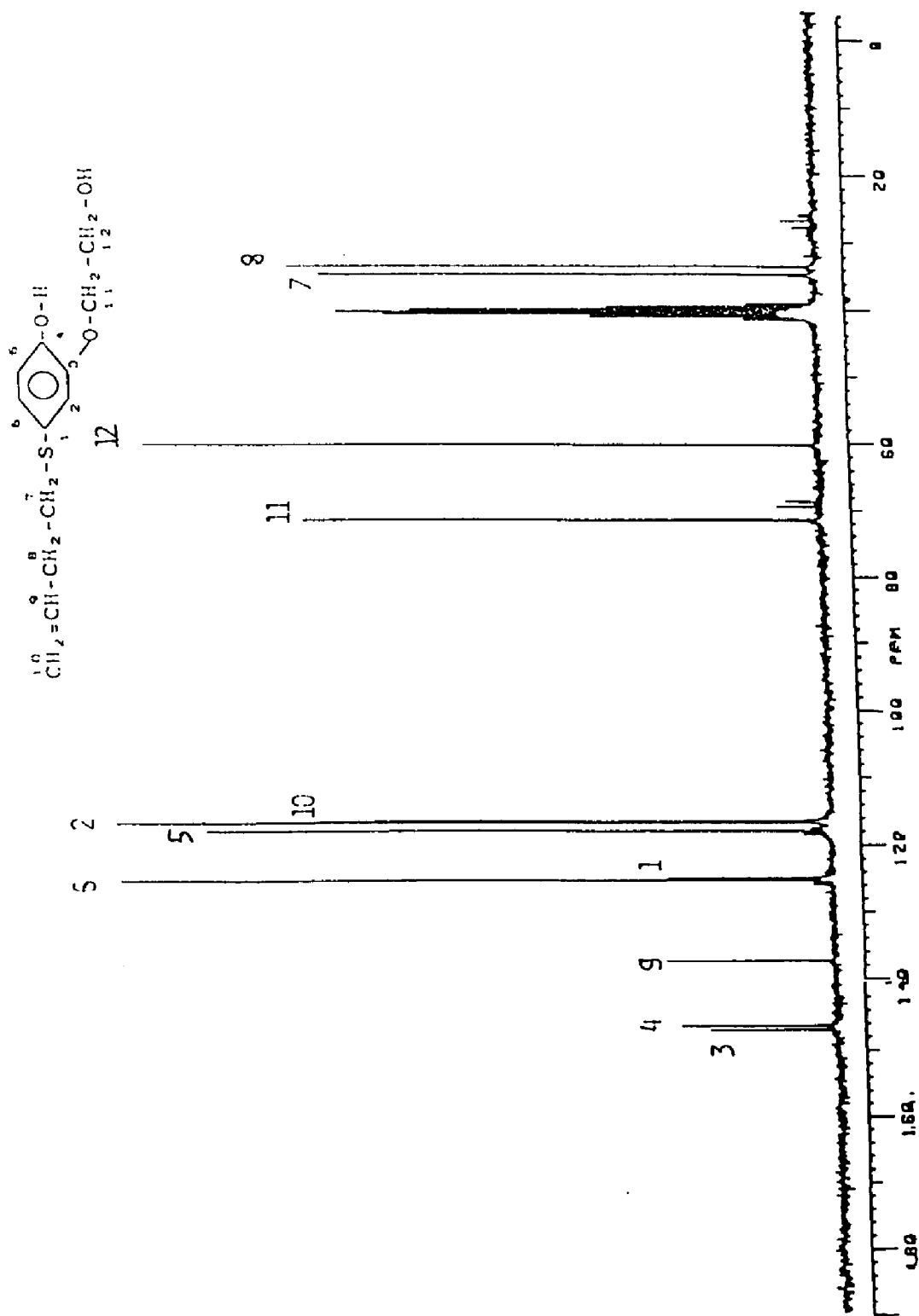
Conditions: 0.145 M in $\text{Me}_2\text{SO-d}_6$; 45° pulse angle; 65°C ; 2.8 sec. delay between pulses; 32 acquisitions.



¹H NMR SPECTRUM OF 2- HYDROXYETHOXY-4-(4-BUTENYLTHIO) PHENOL

FIGURE 21. ^{13}C NMR Spectrum of 2-hydroxyethoxy-4-(4-butenylthio) phenol.

Conditions: 0.145 M in $\text{Me}_2\text{SO}-d_6$; 45° pulse angle;
 65°C ; 2.2 sec. delay between pulses; 15000 acquisitions.



ate linear growth and limit product molecular weight.

Nucleophilic attack of phenoxide ion upon an aryl tetrahydrothiophenium salt in aqueous media might reasonably be expected to yield by-products resulting from addition of water as a competing nucleophile, and elimination of the tetrahydrothiophenium ring due to the alkaline nature of the aquated phenoxide. This pathway is expected to yield the hydroxyl and vinyl terminated poly hydroxyethoxy zwitterion detected in both bulk and solution polymerized samples.

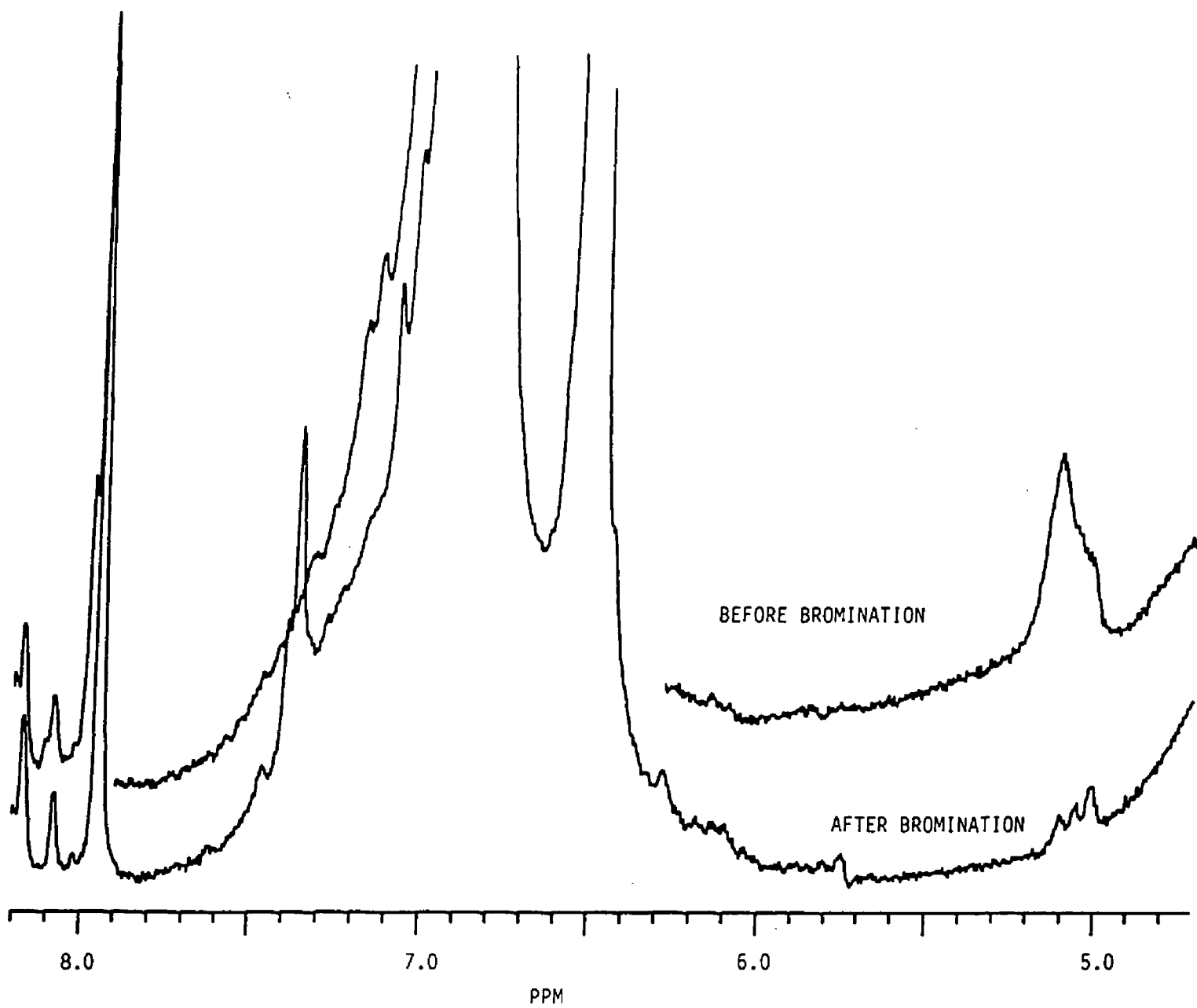
4.6.1 Evidence from ^1H NMR spectroscopy . Signals observed in the ^1H NMR spectrum of the polymer at 5.9, 5.0 and 2.34 ppm (Fig 10a) are reasonable for the vinyl protons and methylene protons adjacent to the vinyl grouping and are in fact observed as major signals in the spectrum of vinyl phenol (Fig 20). Addition of a slight excess of bromine to a sample dissolved in $\text{Me}_2\text{SO}-d_6$ caused the signals at 5.9 and 5.0 ppm to disappear giving further strength to the assignments of these signals as olefinic protons (Fig 22).

Signals centered at 3.40 ppm are consistent with methylene protons of the carbon bearing the alcohol endgroup, and in fact a major signal is seen at 3.41 ppm in the spectrum of phenolic diol (Fig 17).

The ^1H NMR spectra of purified polymer also indicated the presence of terminal phenol groups. A broad, weak

FIGURE 22. Overlay of Polymer Spectra Before and
After Bromination. ^1H NMR Spectra

Conditions: 10% in $\text{Me}_2\text{SO}-d_6$; 45° pulse angle; 65°C ; 2.8
sec. delay between pulses; 1000 acquisitions.



signal is seen at 8.65 ppm which displays a variability of chemical shift with temperature as would be expected for a hydroxylic proton. The ^1H NMR spectra of phenolic diol exhibits a phenolic proton at 8.67 ppm at the same temperature using $\text{Me}_2\text{SO}-d_6$ as the solvent.

4.6.2 Evidence From ^{13}C NMR Spectroscopy.

Additional evidence for vinyl and alcohol endgroups is found in the ^{13}C NMR spectrum of purified polymer. Three trace signals were observed which are consistent with either alcohol or vinyl endgroups at 146.8, 124.1 and 115.6 ppm. Additional trace signals assigned to an alcohol endgroup were observed at 146.1, 124.6 and 34.6 ppm. Trace signals consistent with vinyl group termination were seen at 124.4, 33.9 and 32.7 ppm. The signal expected for the methine carbon of the vinyl endgroup (carbon 9) expected at 136.5 ppm was not observed. The signal is weak in the spectrum of the model compound however, and the evidence from ^1H NMR spectroscopy for the vinyl endgroup is compelling.

4.6.3 Evidence of Unidentified End Group.

The proton and carbon spectra of the purified polymer indicate that one important functional group present in trace quantities is unaccounted for. A proton end group signal is seen at 4.33 ppm and a carbon end group signal at 70.3 ppm. Both of these signals are indicative of an alkyl-aryl ether linkage.

Sometimes samples of poly hydroxyethoxy zwitterion were found to be intractable; common solvents would not dissolve the entire sample. This phenomena was observed under the following circumstances:

1) Occasionally samples which appeared to be dissolved in N,N-dimethylformamide were impossible to filter through an 0.5 micron membrane for analysis by GPC.

2) Bulk polymerized samples which were initially soluble in N,N-dimethylformamide were found to exhibit N,N-dimethylformamide and Me₂SO insoluble fractions after being stored either in jars on the bench top or a desiccated environment for approximately three weeks or longer.

3) samples of the hydroxyethoxy zwitterion polymerized in Me₂SO-d₆ and stored dissolved in NMR tubes produced a Me₂SO-d₆ insoluble fraction after being stored for approximately two months or more.

The purity of the sample influenced the degree to which cross linking occurred. The product of the bulk polymerization of crude hydroxyethoxy zwitterion, monomer purified as described in the experimental section on a 0.5 g scale, and hydroxyethoxy zwitterion recrystallized on a 5 g scale were compared qualitatively. The 5 g scale purification involved a direct 10 time scale-up of glassware, crude monomer employed, and quantities of solvent (CH₃OH/isopropanol), non-solvent (diethyl ether)

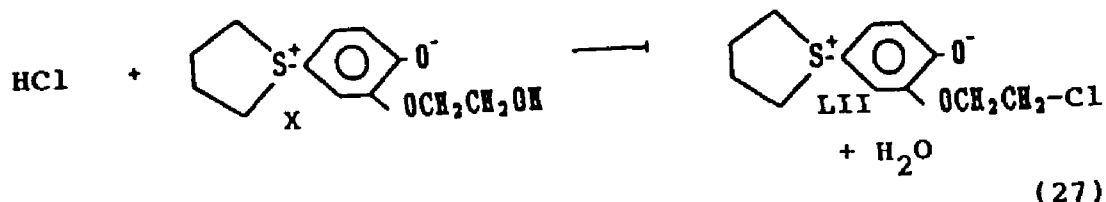
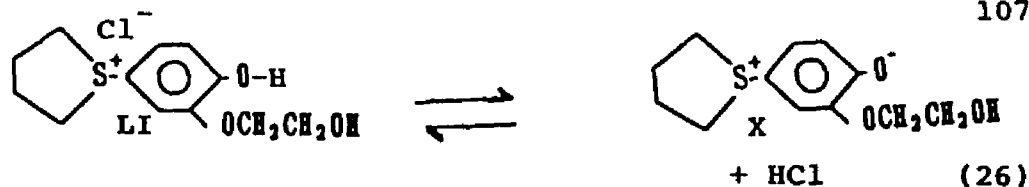
and water. The 5 g scale purification gave a slightly higher yield as expected from loss minimization on glassware and filter paper surfaces.

The crude monomer gave the largest amount of insoluble gel. Monomer recrystallized on a 5 g scale produced insoluble gel in lower quantities. 5 g quantities recrystallized twice yielded less gel than material recrystallized a single time.

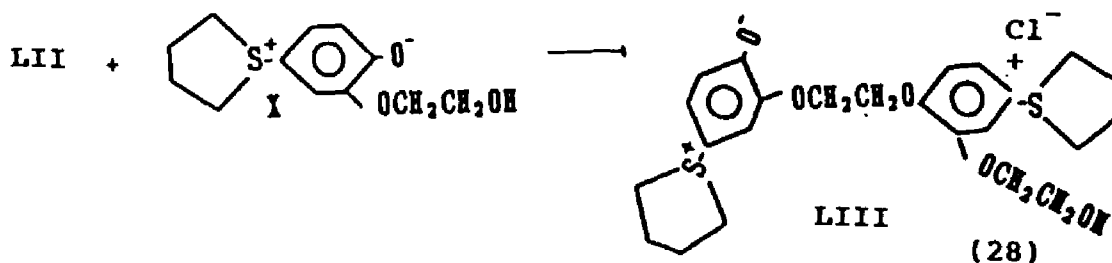
Monomer samples recrystallized on an 0.5 g scale (either once or twice) produced no insoluble material. Samples allowed to polymerize in bulk for extended periods of time past quantitative conversion still yielded an insoluble fraction.

While no direct experimental evidence is available, halide ion, an impurity from residual intermediate hydrochloride salt of the hydroxyethoxy zwitterion could provide a pathway to branching during the course of the reaction if present in small amounts, or slower grafting after the bulk of the reaction is complete could occur if halide ions were present in trace quantities.

The hydrochloride of the hydroxyethoxy zwitterion may produce transient levels of HCl from the equilibrium of equation 26.



The HCl could be capable of converting the pendant alcohol group into an alkyl halide (equation 27). The aryl ether resulting from the reaction of the alkyl halide and hydroxyethoxy zwitterion through the phenoxide linkage could produce branch points which lead to formation of insoluble product (equation 28). Once formed, the halide ion is regenerated to repeat the process.



If the concentration of halide ion is very small, this reaction may proceed too slowly to compete with the linear polymerization. At the end of the polymerization

phenol end groups, trace HCl and pendant alcohol groups may combine slowly through the alkyl halide intermediate to form an insoluble graft polymer. Again, no net HCl would be consumed, allowing the grafting to continue until the concentration of phenol end groups is consumed.

4.7 ADDITIVE STUDIES. The reaction of other sulphonium arene oxides have been reported to be very sensitive to added materials (9,11,12). For this reason, a group of additives were screened to search for effects upon the reaction. Analysis of product molecular weight by Gel Permeation Chromatography was used to assess the effect of additive candidate on the bulk polymerization of monomer. Analysis of the reaction mass for product distribution by ^1H NMR spectroscopy was the primary tool used to assess the effect of additives on the solution polymerization of monomer.

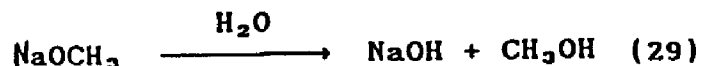
Screening experiments showed that the solution polymerization of the hydroxyethoxy zwitterion was effected by both electrophilic and nucleophilic additives, the bulk polymerization showing little effect when either sodium methoxide or trifluoroacetic acid were added to reaction mixtures. The activity of trifluoroacetic acid discovered lead to the studies of the initiated solution polymerization reaction product distributions and kinetics.

4.7.1 Bulk Polymerization. An electrophilic and nucleophilic additive were used to examine the sensitivity of the bulk polymerization to additives. Gel Permeation Chromatography was used to asses the effect of additive on the molecular weight distribution of the high molecular

weight fraction product of the bulk polymerization mixture.

a) Added nucleophile. Table 9 is a compilation of weight and number average molecular weight of product produced by adding varying amounts of sodium methoxide to the monomer prior to polymerization. The data shows a steady decrease in product molecular weight with added nucleophile. Schmidt has shown that additions of this nucleophile to the dichloro zwitterion produced higher molecular weight material. The methoxide ion, a stronger nucleophile than phenoxide, opened the tetrahydrothiophenium ring producing capped initiating specie of much greater reactivity than monomer.

In the case of the hydroxyethoxy zwitterion, a crystalline hydrate, sodium methoxide is quickly decomposed by moisture to yield hydroxide ion, a weaker nucleophile than phenoxide.



The hydroxide would be ineffective at competing with phenoxide in opening the tetrahydrothiophenium ring, but available to lead to early terminations to alcohol or vinyl endgroups. As a result, the product molecular weight decreases as the sodium methoxide content of the starting material increases.

TABLE 9. BULK POLYMERIZATION IN THE PRESENCE OF ADDED
SODIUM METHOXIDE ¹

mole % NaOCH ₃	\bar{M}_w	\bar{M}_n	\bar{M}_w/\bar{M}_n
0	136,000	59,500	2.30
0.33	116,000	46,500	2.50
1.0	80,600	37,900	2.13
2.0	74,600	30,800	2.42
5.0	62,500	29,600	2.11

¹ All samples were polymerized at 100°C

b) Added electrophile. Table 10 shows that added trifluoroacetate salt of monomer also produces product of progressively lower molecular weight as the additive content is increased.

The trifluoroacetate salt, while more electrophilic than the monomer is essentially monofunctional as the phenol end of the molecule is protonated and unable to compete effectively with the phenoxide functionality of the monomer in propagation. The decrease in product molecular weight versus additive content is thought to be due to the stoichiometric imbalance produced by incorporating the additive.

A pure hydroxyethoxy zwitterion sample contains an equivalent amount of phenoxide and cyclic sulphonium functional groups. Addition of the TFA salt of the monomer produces a mixture containing more cyclic sulphonium groups than phenoxide groups and the stoichiometric imbalance limits the molecular weight the mixture is capable of attaining.

4.7.2 Solution Polymerization. Definite effects on the course of the reaction were detected when added nucleophilic and electrophilic additives were incorporated into solution polymerization mixtures.

The most effective initiator found was trifluoroacetic acid. Table 11 shows the results of screening experiments for additives in solution polymerization.

TABLE 10. BULK POLYMERIZATION IN THE PRESENCE OF ADDED
TFA SALT ¹

mole % TFA salt	\overline{M}_w	\overline{M}_n	$\overline{M}_w/\overline{M}_n$
0	130,000	59,500	2.18
0.40	93,700	48,200	1.94
0.79	105,400	50,400	2.09
1.26	99,700	49,500	2.01
3.96	67,900	35,600	1.91

¹ All samples were polymerized at 100°C.

TABLE 11. SCREENING OF ADDITIVES IN SOLUTION
POLYMERIZATION ¹

Additive	Loading ²	Mole Fraction Cyclic Dimer
none	-----	0.55
pyridine	8.9%	0.57
dimethylamino ethanol	22.6%	0.50
sodium bicarbonate	saturated sol'n	0.44
quaternary phenoxide	11.2%	0.39
phenolic diol	23.0%	0.17
trifluoroacetate salt	10.5%	0.07

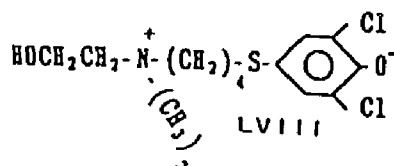
¹ All samples were 0.145 molar monomer solutions in Me₂SO-d₆ reacted at 100 °C.

² ([additive]/[monomer])100

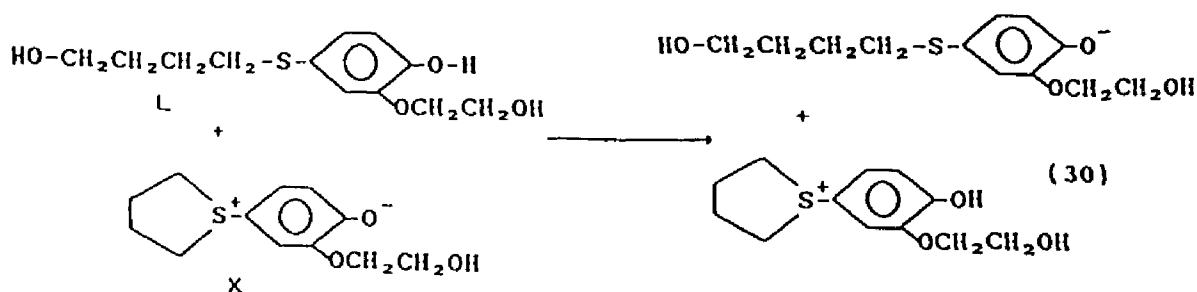
Addition of the trifluoroacetate salt of the hydroxyethoxy zwitterion to the reaction mixture was effective in reducing the cyclic dimer content of the solution polymerization mixture. This initiator was studied in detail and reported on in sections 4.8 and 4.10.3.

The tertiary amines produced only little effect on the product distribution of the polymerization, presumably because the alkylation of tertiary amine by the tetrahydrothiophenium group was slow compared to ring opening by monomer phenoxide functionalities.

A quaternary ammonium phenoxide was prepared from the dichloro zwitterion and dimethylamino ethanol and screened for activity as an additive for solution polymerization (11). This quaternary phenoxide was somewhat more effective in reducing the quantity of cyclic dimer produced. The difference in reactivity between the dichloro quaternary phenoxide and the hydroxyethoxy zwitterion as nucleophiles probably causes this reduction in cyclic dimer content as any propagating species formed from the dichloro quaternary phenoxide is incapable of intramolecular cyclization.



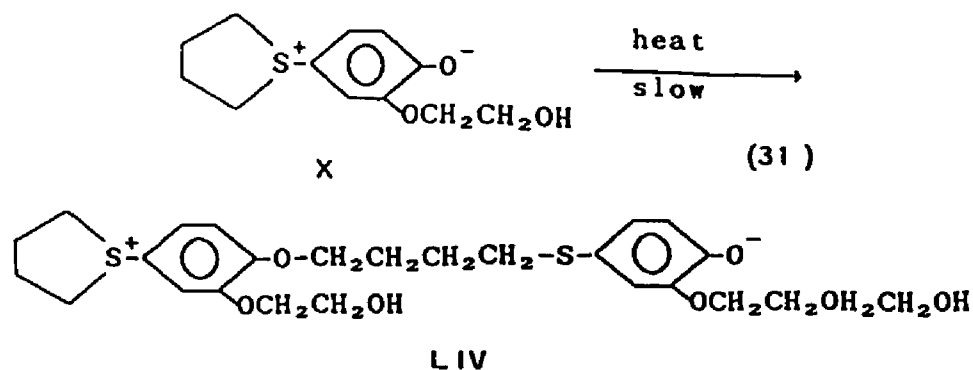
The phenolic diol was also effective in significantly reducing the cyclic content of the reaction mixture. Equilibration of the phenolic diol with monomer is expected to yield more reactive forms of both monomer and diol.



4.8 MOLECULAR WEIGHT AND PRODUCT DISTRIBUTION OF INITIATED POLYMERIZATION.

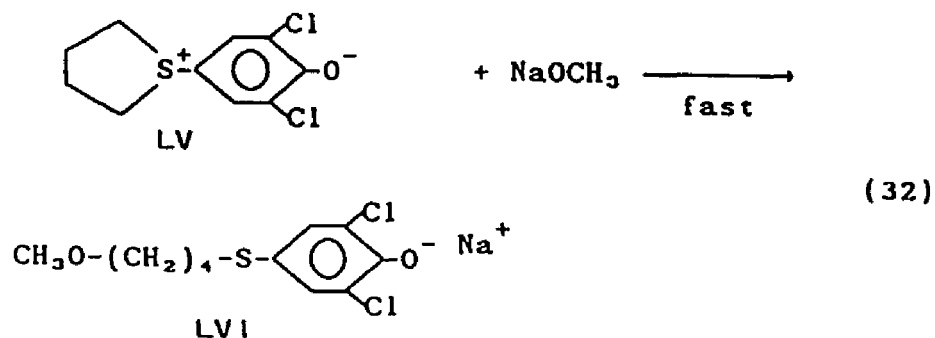
As shown, the uninitiated thermal polymerization of the hydroxyethoxy zwitterion in $\text{Me}_2\text{SO}-d_6$ produces large amounts of low molecular weight cyclics. The rate

determining step is thought to be second order initiation involving a bimolecular reaction of monomer to form an activated propagating specie (LIV) which reacts quickly relative to initiation to either decay to cyclics or add on additional monomer units to form linear polymer. LIV is more reactive than the hydroxyethoxy zwitterion.



The positive and negative sites of the hydroxyethoxy zwitterion are dispersed over the area of the ring due to the contribution of the quinoid tautomer, and as a result, the thiophenium group of the hydroxyethoxy zwitterion is less electrophilic than LIV and the phenoxide group of the hydroxyethoxy zwitterion is much less nucleophilic than LIV.

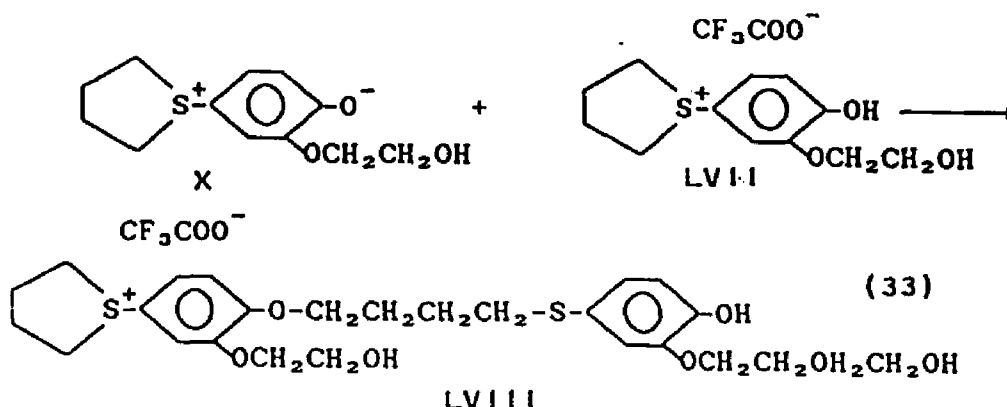
In previous work, Schmidt enhanced the ability of the dichloro zwitterion analogue, LV, to achieve higher quantities of linear material by adding small amounts of sodium methoxide to the reaction mixture forming an activated propagating specie, LVI, very quickly.



The propagating specie, LVI was more nucleophilic than the dichloro zwitterion and produced a larger amount of higher molecular weight product and less cyclic by products than uninitiated reactions.

It is possible to activate the electrophilic portion of the hydroxyethoxy zwitterion. The approach taken was to use a salt of the hydroxyethoxy zwitterion bearing a relatively non nucleophilic counter ion.

The hydroxyethoxy zwitterion trifluoroacetate, LVII, is suited to provide initiation for the polymerization due to its more reactive electrophilic functionality. The tetrahydro thiophenium grouping is no longer conjugated to a negatively charged para group and should be more readily attacked by monomer to produce propagating specie, LVIII.

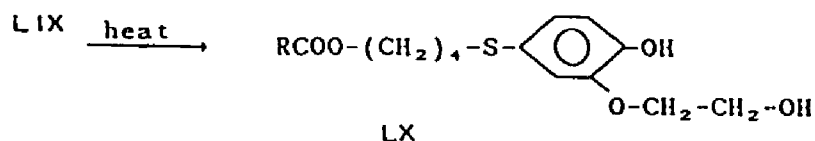
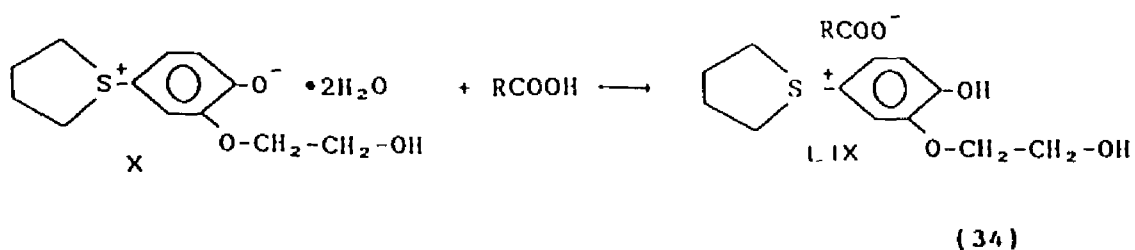


4.8.1 Reactivity of Hydroxyethoxy Zwitterion Carboxylates. The choice of trifluoroacetate as the catalyst counter anion is of the utmost importance to minimize side reactions which could limit molecular weight and destroy catalyst during the course of the reaction. The relative reactivities of the hydroxyethoxy zwitterion acetate (LXI) and trifluoroacetate (LVII) observed in these studies show the trifluoroacetate salt to be less nucleophilic, less prone to decompose to ester, than the acetate.

The thiophenium phenoxides form crystalline carboxylate salts, LIX, which decompose to phenolic esters, LX, upon heating.

Infrared spectroscopy is useful for studying the formation and reactivity of these substances as distinct and well resolved carbonyl IR bands are observed for carboxylic acids, carboxylate salts, and esters. The infrared spectra of the salts show that a distinct salt has formed rather than a physical mixture of carboxylic

acid and the hydroxyethoxy zwitterion as a carboxylate carbonyl signal is seen rather than a carboxylic acid carbonyl signal. The formation of ester linkages or generation of carboxylic acid is easily detectable by IR spectroscopy.



The hydroxyethoxy zwitterion acetate salt (LXI) was prepared and isolated, the infrared spectrum (Fig 23) showing clearly the presence of a carboxylate salt from a band at 1575 cm^{-1} . The acetate salt, when melted (115°C) and cooled, exhibited an infrared spectra (Fig 24) indicative of the Phenolic ester, LX, as evidenced by a strong signal at 1730 cm^{-1} .

FIGURE 23. Infrared Spectrum of Tetrahydro 1-[4
hydroxy 3-(2-hydroxyethoxy) phenyl]
Thiophenium Acetate. KBr Pellet.

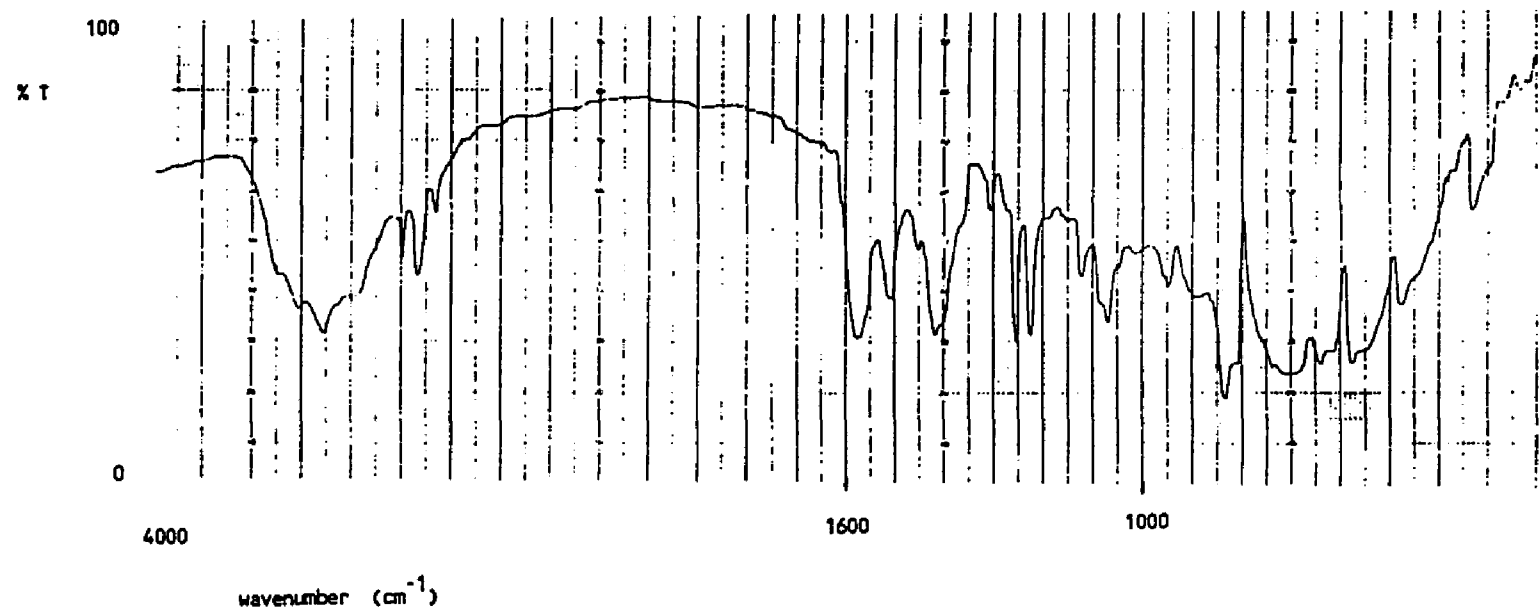
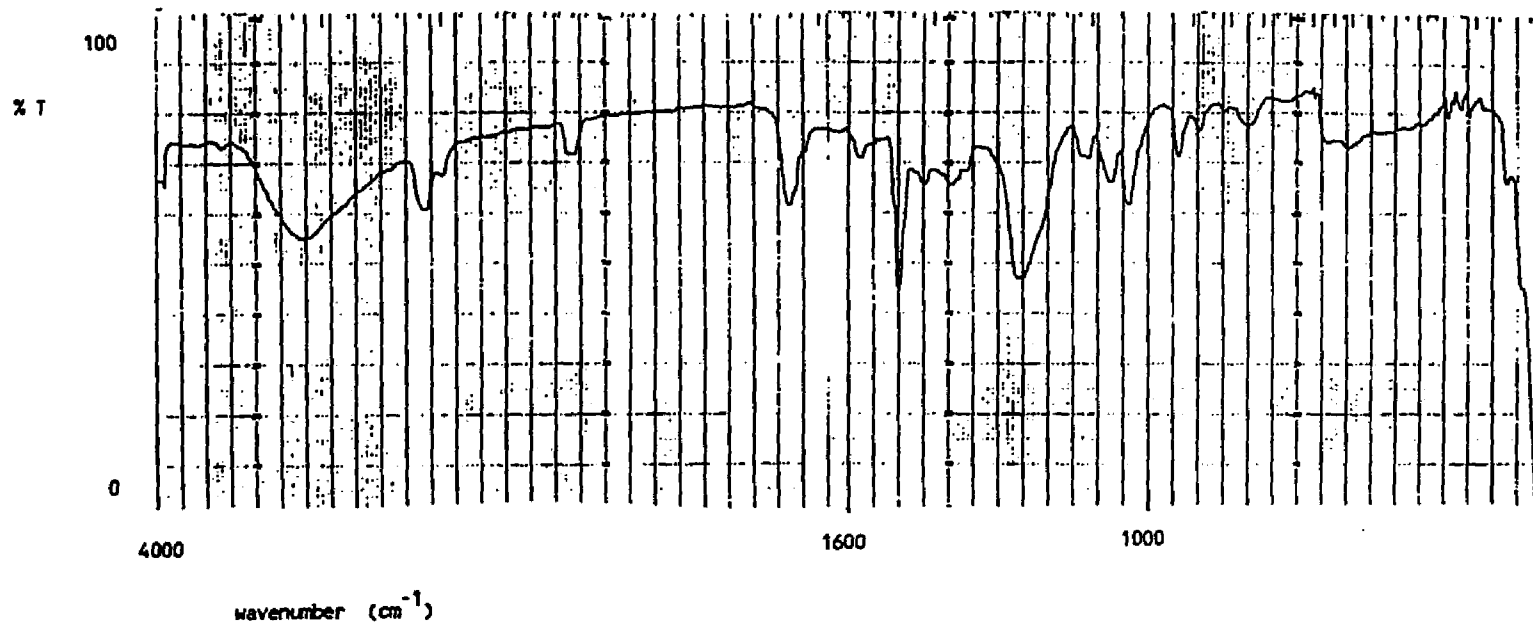
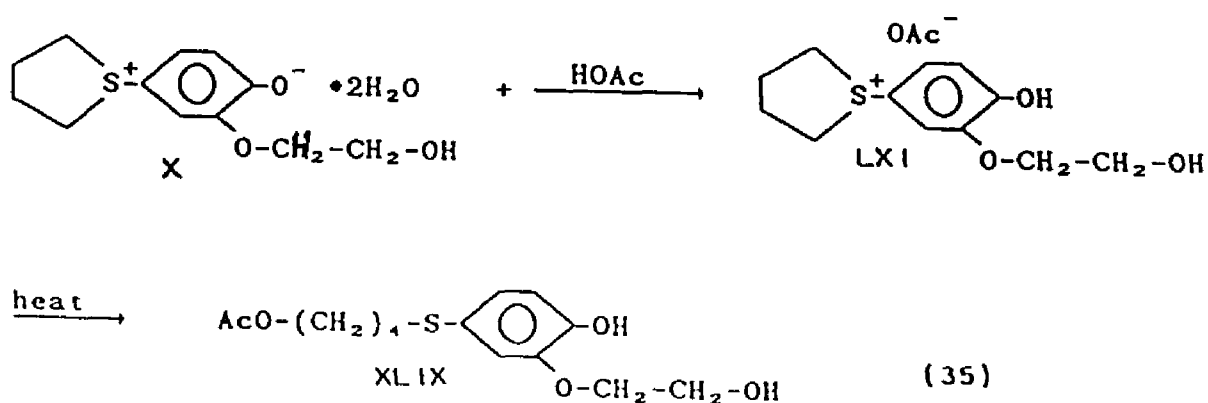
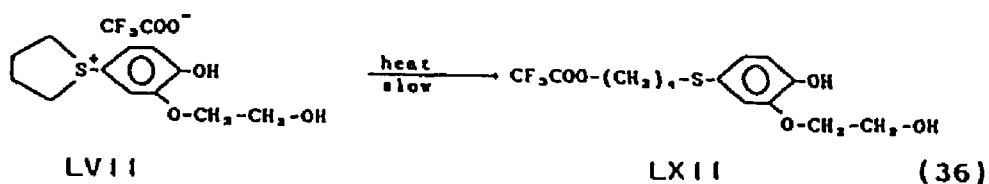


FIGURE 24. Infrared Spectrum of Tetrahydro 1-[4
hydroxy 3-(2-hydroxyethoxy) phenyl]
Thiophenium Acetate After Melting.
KBr Pellet.





The hydroxyethoxy zwitterion trifluoroacetate, LVII (carbonyl frequency 1684 cm^{-1}), when melted at 127°C and cooled produced considerably less ester, LVIII (carbonyl frequency 1780 cm^{-1}), and showed much residual carboxylate salt by IR spectroscopy (Figs 25,26).



Inductive effects of the C-F bonds effectively disperse the negative charge of the trifluoroacetate anion over a larger area which results in the poor nucleophilicity of trifluoroacetate.

4.8.2 Effect of Initiator on Cyclic Content.

Trifluoroacetic acid, added to the polymerization mixture in the form of the trifluoroacetate salt of the hydroxyethoxy zwitterion severely limits cyclization. The

FIGURE 25. Infrared Spectrum of 1-[4 hydroxy 3- (2
-hydroxyethoxy) phenyl] Thiophenium
Trifluoroacetate.
KBr Pellet.

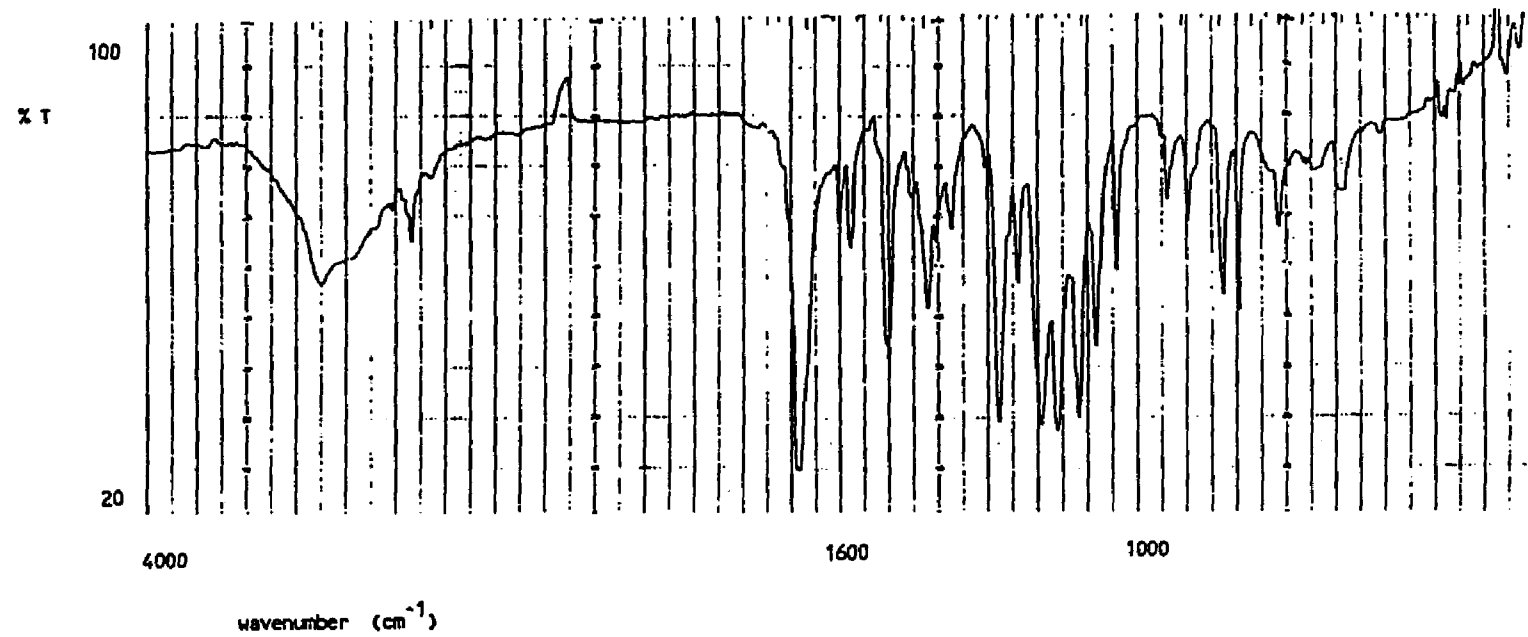
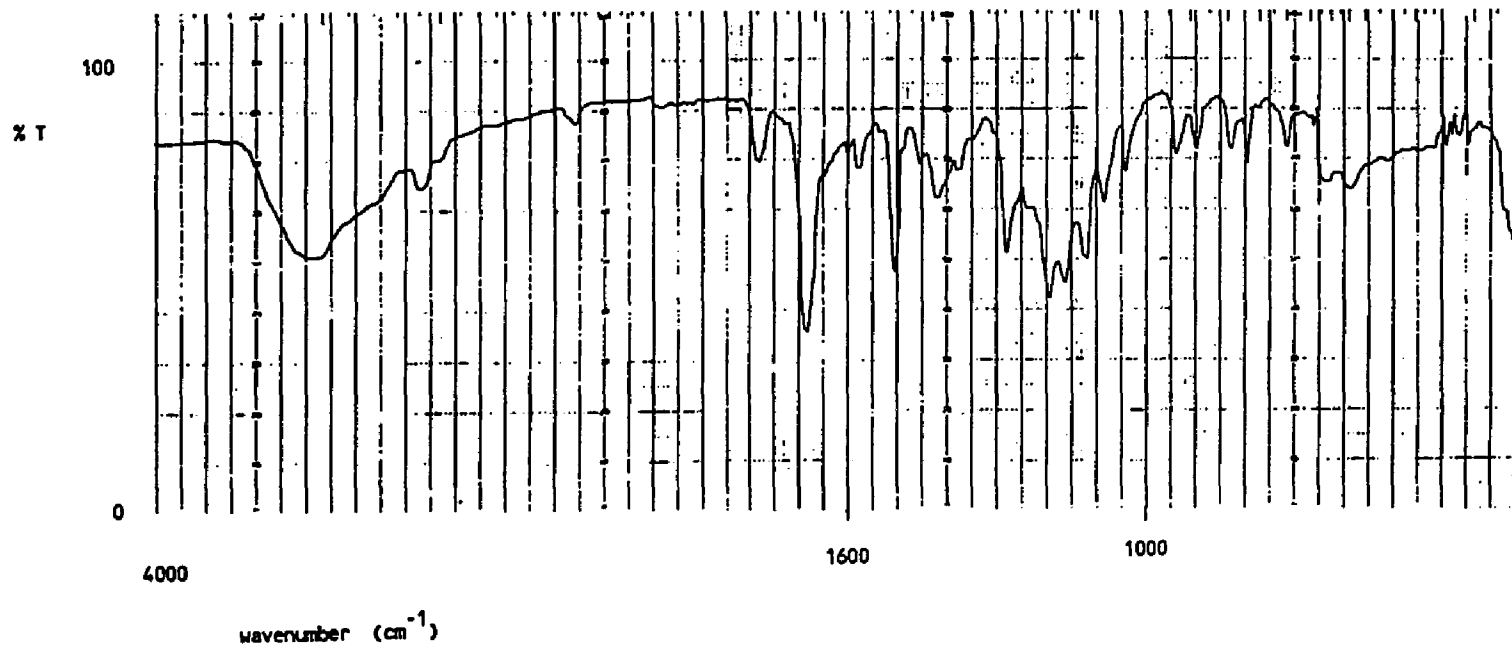
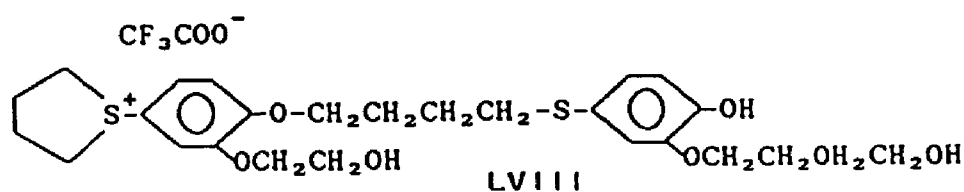


FIGURE 26. Infrared Spectrum of 1-[4 hydroxy 3- (2-
hydroxyethoxy) phenyl] Thiophenium
Trifluoroacetate After Melting.
KBr Pellet.



propagating species produced by the attack of monomer on initiator is far less prone to cyclization than the specie produced by the attack of monomer with itself.



As the relative amount of initiator increases relative to monomer, cyclic production is suppressed. As seen in Table 12, with the initial monomer concentration held constant in polymerizations carried out at 65°C, the quantity of cyclic dimer produced quickly drops off as the initiator loading is increased. Fractionation of reaction mixtures by GPC shows a six-fold increase in the amount of polymer formed, with the relative quantities of dimer, trimer and tetramer dropping off. This chromatographic and spectroscopic evidence is consistent with the formation of propagating species less prone to cyclization in initiated polymerizations.

Table 13 shows the effect of varying monomer concentration on the reaction when the initial initiator concentration is held constant. The trend toward slightly higher cyclic dimer production as the initial monomer concentration increases is in stark contrast to the behavior illustrated in Table 7 for uninitiated solution

polymerization. Tables 12 and 13 show that the relative initiator concentration, I_0/M_0 , is the main determinant of product distribution. The relative amount of cyclic dimer, as measured by ^1H NMR spectroscopy, generated decreases as the ratio of initiator to monomer present at the start of the reaction increases. This trend is seen whether initial concentrations of monomer or initiator are held constant.

4.8.3 Effect of Initiator on Molecular Weight of Linear Product. Table 14 shows that that the molecular weight of polymeric product exhibits a maximum at initiator loadings of less than 10%. At the lowest loading of initiator employed, the molecular weight of product is unchanged within the experimental limits of uncertainty of $\pm 10\%$ relative expected for molecular weight determinations by gel permeation chromatography.

The average molecular weight of linear products falls off at initiator loadings greater than 5 mol %.

4.8.4 Effect of Initiator on Solution Polymerization Kinetics. Incorporating initiator into solution polymerization mixtures causes dramatic effects in both the rate and order of reaction of monomer loss.

The orders of reaction for the polymerization of the hydroxyethoxy zwitterion in solution with and without added initiator are conveniently compared by constructing plots of $\ln[\text{MONOMER}]$ vs. time and $[\text{MONOMER}]^{-1}$ vs. time for

TABLE 12. EFFECT OF INITIATOR LOADING ON THE PRODUCT
DISTRIBUTION OF SOLUTION POLYMERIZATION ¹

NMR ANALYSIS

I_0/M_0 $\times 10^2$	Mole Fraction	
	Cyclic Dimer	Polymer & Higher Cyclics
0	0.494	0.506
0.41	0.381	0.619
0.55	0.323	0.677
0.83	0.340	0.660
4.0	0.094	0.906
4.87	0.079	0.921
6.4	0.062	0.932
7.8	0.050	0.950
8.6	0.043	0.957
10.0	0.038	0.962

SIZE EXCLUSION CHROMATOGRAPHY

I_0/M_0 $\times 10^2$	<u>Cyclic Oligomers</u>					Total Cyclics	<u>Polymer</u>
	C2	C3	C4	C5	Total		
0.41	0.485	0.283	0.080	0.037	0.885	0.101	
0.83	0.385	0.296	0.104	0.056	0.841	0.136	
4.0	0.115	0.160	0.098	0.068	0.441	0.504	
6.4	0.079	0.117	0.077	0.067	0.340	0.601	
8.6	0.077	0.099	0.077	0.067	0.320	0.620	

¹ The initial monomer concentration was 0.145 M in DMSO-d₆; reacted at 65°C for 3 days.

TABLE 13. EFFECT OF INITIAL MONOMER LOADING ON THE PRODUCT
DISTRIBUTION OF TFA INITIATED SOLUTION
POLYMERIZATION ^{1,2}

NMR ANALYSIS

Mole Fraction

M_0	Cyclic dimer	I_0/M_0
0.203	0.104	0.031
0.152	0.099	0.0404
0.073	0.061	0.085

¹ $I_0 = 6.3 \times 10^3$ M; Temperature = 65°C

NMR ANALYSIS

Mole Fraction

M_0	Cyclic dimer	I_0/M_0
0.208	0.090	0.032
0.145	0.081	0.046
0.101	0.061	0.100

SIZE EXCLUSION CHROMATOGRAPHY

M_0	<u>Cyclic Oligomers</u>					Total Cyclics	<u>Polymer</u>
	C2	C3	C4	C5+C6	Total		
0.208	0.108	0.150	0.089	0.117	0.464	0.537	
0.145	0.103	0.143	0.085	0.118	0.449	0.552	
0.101	0.108	0.141	0.090	0.140	0.479	0.521	

² $I_0 = 6.7 \times 10^3$ M; Temperature = 65°C

TABLE 14. EFFECT OF INITIATOR LOADING ON PRODUCT MOLECULAR WEIGHT IN INITIATED SOLUTION POLYMERIZATIONS ^{1,2}

mole % TFA salt	\overline{M}_w	\overline{M}_n	$\overline{M}_w/\overline{M}_n$
0	7,500	5,200	1.44
0.55	7,200	4,900	1.47
4.87	11,900	6,900	1.72
7.80	10,700	6,800	1.57
10.0	8,300	6,000	1.38

¹ All samples were polymerized at 65°C.

² Values from GPC carried out at 100°C using 0.05M LiBr in N,N-dimethylformamide as the mobile phase.

reactions monitored by ^1H NMR spectroscopy as a function of time. A first order process will yield a linear plot for $\text{Ln}[\text{MONOMER}]$ vs. time and a second order process will yield a linear plot if $[\text{MONOMER}]^{-1}$ is plotted vs. time (27)

When the order of reaction is assessed by plotting concentration-time data according to behavior expected for simple second order and simple first order behavior, it is seen that uninitiated monomer decay exhibits a better experimental fit with second order behavior as a plot of inverse monomer concentration versus time is linear (Fig 27).

The same technique (Fig 28) used for initiated polymerization show the initiated polymerization to behave in a manner more closely resembling first order loss of monomer with respect to monomer concentration.

The rate of reaction is strongly dependent on the initiator loading. Figure 29 is a comparison of monomer loss versus time for the uninitiated polymerization and initiated polymerizations carried out with varying initiator loadings at a constant monomer loading. The calculated first order rate constant varies with initiator loading and is linear with respect to initial initiator concentration as shown in Figure 30.

The solution polymerization kinetics were therefore examined in greater detail to deduce mechanistic

Figure 27. Second Order Monomer Loss in Uninitiated
Solution Polymerization.

Conditions: 0.145 M solution in $\text{Me}_2\text{SO-d}_6$; 80°C .

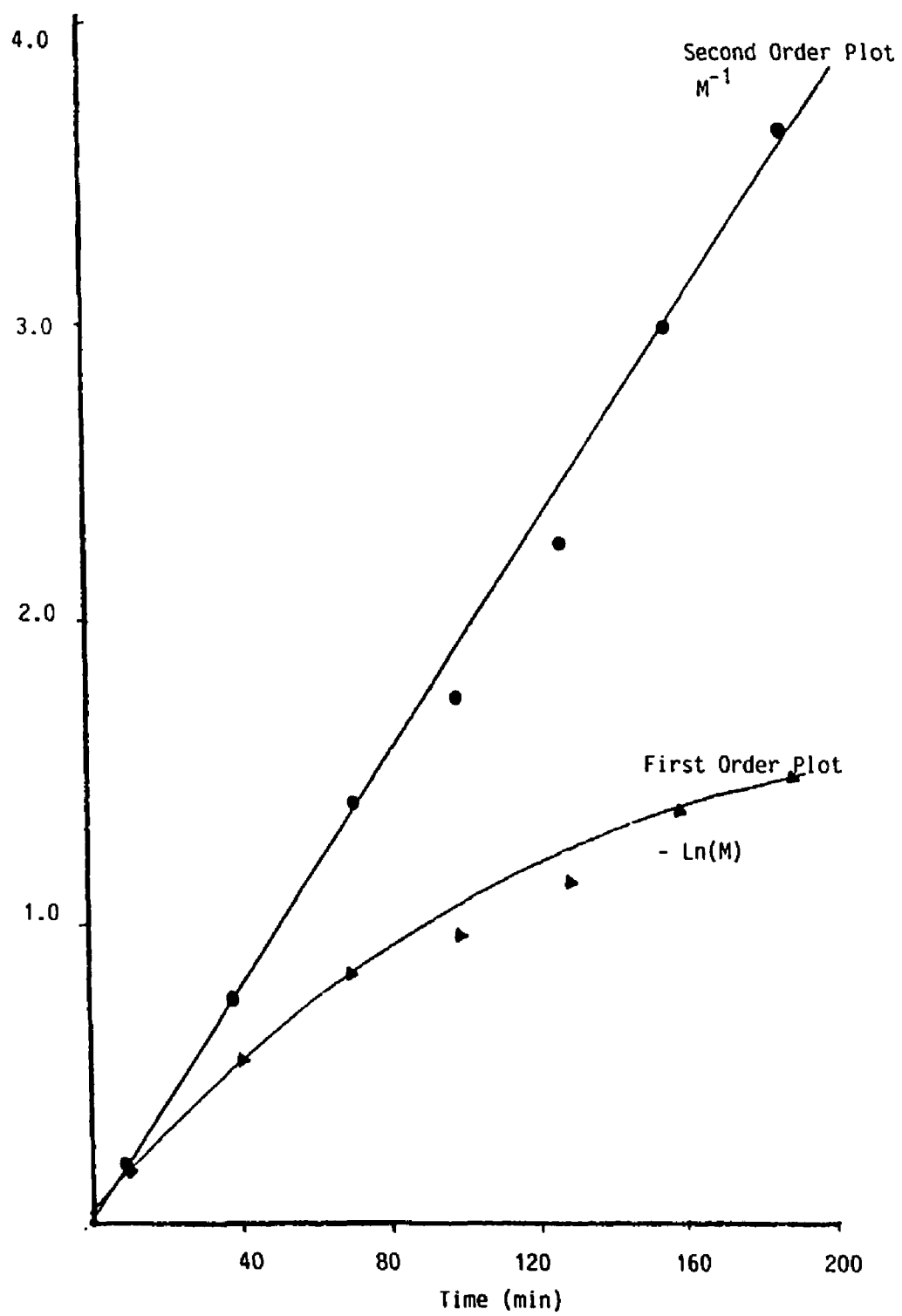


Figure 28. First Order Monomer Loss in Initiated
Solution Polymerization.

Conditions: 0.145 M monomer; 4.80×10^{-3} M initiator in
 $\text{Me}_2\text{SO-d}_6$; 65°C .

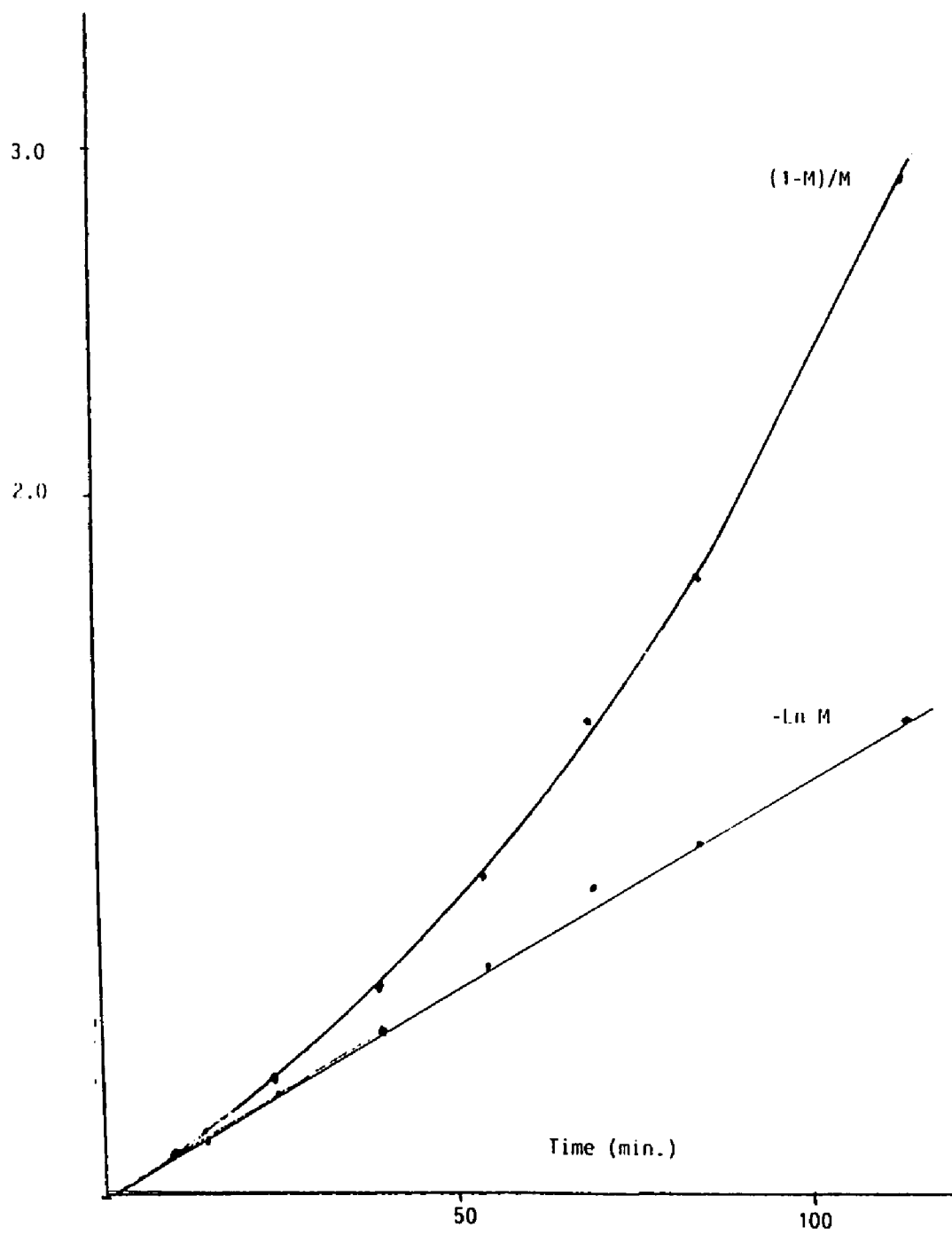


Figure 29. Comparison of Initiated and Uninitiated Reaction Rates.

Conditions: 0.145 M Monomer; $\text{Me}_2\text{SO-d}_6$; 65°C ;

● ; $I_0/M_0 = 0.0$

■ ; $I_0/M_0 = 0.05$

◀ ; $I_0/M_0 = 0.10$

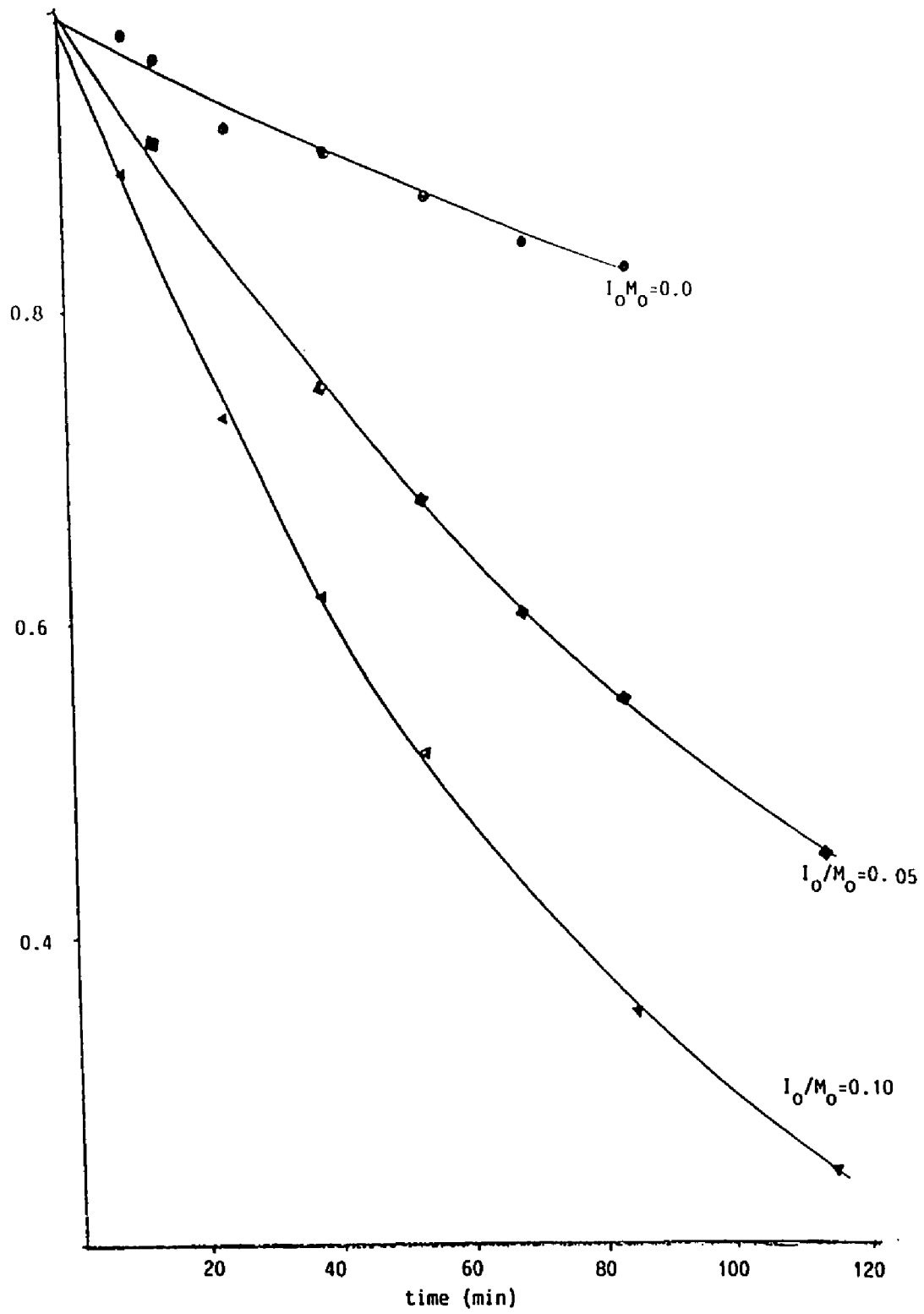
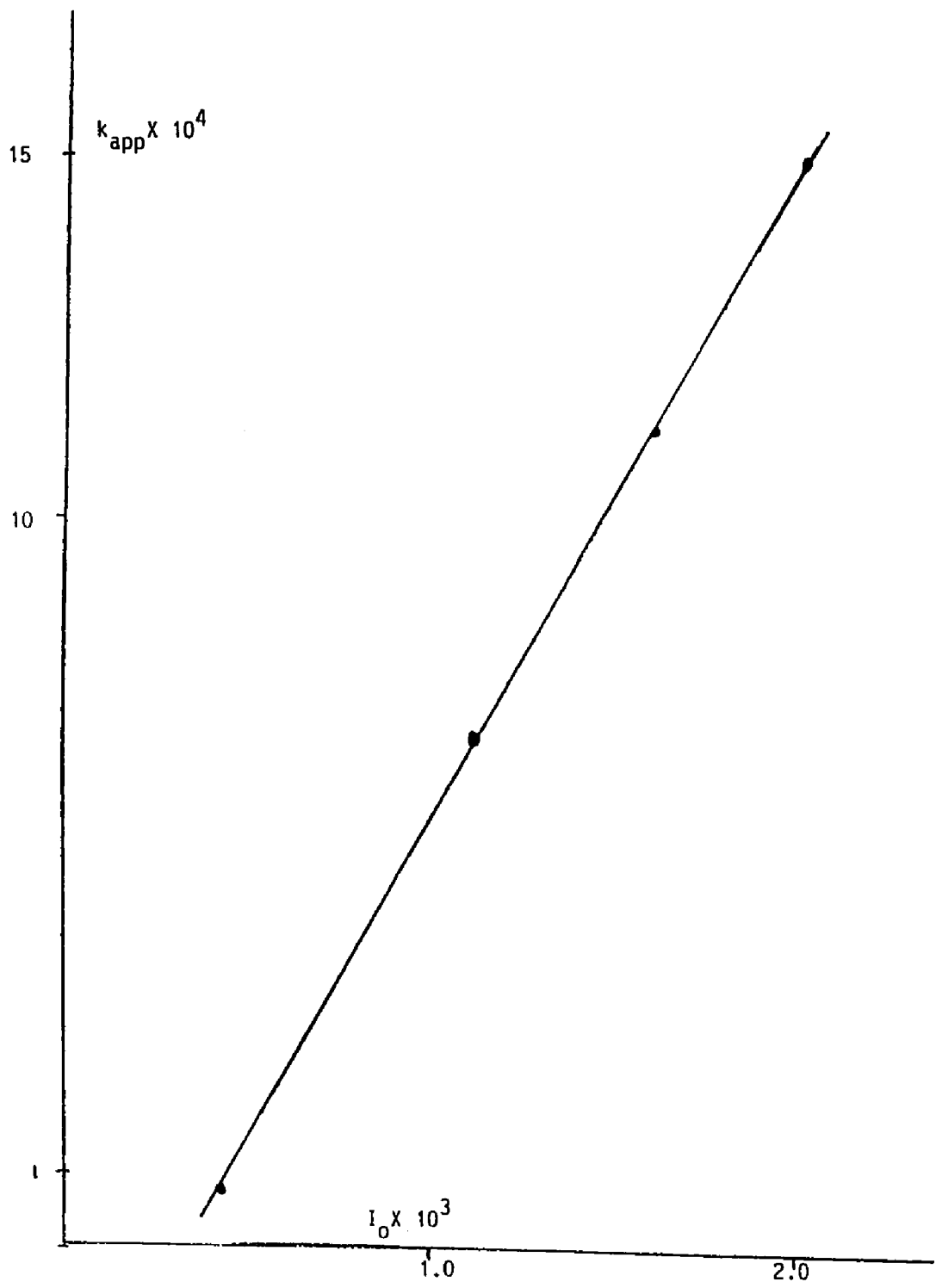


Figure 30. Apparent First Order Rate Constants of
Initiated Polymerization as a Function of
Initial Initiator Concentration.

Conditions: First order rate constants calculated from
data in Fig. 29. All samples polymerized in $\text{Me}_2\text{SO-d}_6$ at
0.145M loadings of hydroxyethoxy zwitterion at 65°C .



differences. These results are reported in detail in section 4.10.

4.9 KINETICS OF BULK POLYMERIZATION. When the hydroxyethoxy zwitterion, a crystalline dihydrate, is heated in bulk, water is evolved and polymerization occurs. Microscopic examination of crystals of hydroxyethoxy zwitterion being heated show, early in the course of heat treatment, well defined crystallites which conduct light and are visible when viewed with crossed polarizers. As the reaction proceeds, the conduction of light becomes progressively weaker until the specimens cannot be seen through the crossed polarizing lenses.

The observation of zero order kinetics is generally ascribed to either geometric or physico/chemical properties of the reacting substrate.

Solid propellants, for example, are purposely fabricated shapes producing a constant surface area as the reaction proceeds (26). The surface decomposition of a donut shaped sample produces a reaction system in which the surface area of the reactant/product interphase remains approximately constant. The surface area of the reacting interphase decreases along the surface of the outer diameter, but this decrease in reaction area is exactly offset by the increase in surface area produced by the decay of the inner diameter of the donut shaped substrate. These offsetting factors give rise to kinetics

in which the amount of substrate consumed is directly proportional to time. The rate of reaction is constant, or shows no dependence on the amount of substrate remaining at any time as is generally seen in chemical reaction kinetics.

A constant rate of reaction is also observed when the product does not provide an effective barrier to further chemical change (26). For this circumstance, rate is independent of product layer thickness and the rate of reaction does not decelerate. Such behavior is observed for the alkali and alkaline earth metal oxidations for which product oxide volumes are less than that of the original metals. Since the product layer undergoes contraction, cracks are developed in the product layer which permit continued access of gas to the metal surface and the weight of product is directly proportional to time for reactions at constant pressure.

Although no crazing of the reaction surface was directly observed by microscopic examination of reacting hydroxyethoxy zwitterion samples, the reaction was observed to proceed with contraction of volume and exhibited zero order kinetics.

The kinetics of monomer dehydration and polymerization reveal identical energies of activation within the limits experimental error (ca 4 Kcal/mole). A study of the degree of polymerization as a function of

extent of reaction reveals that relatively high molecular weight material is produced early in the course of the reaction.

4.9.1 Molecular Weight Versus Extent of Reaction.

Samples of hydroxyethoxy zwitterion heated under a covering of n-octane at constant temperature for various time intervals were analyzed by ^1H NMR spectroscopy and gel permeation chromatography. The data is shown in Figure 31.

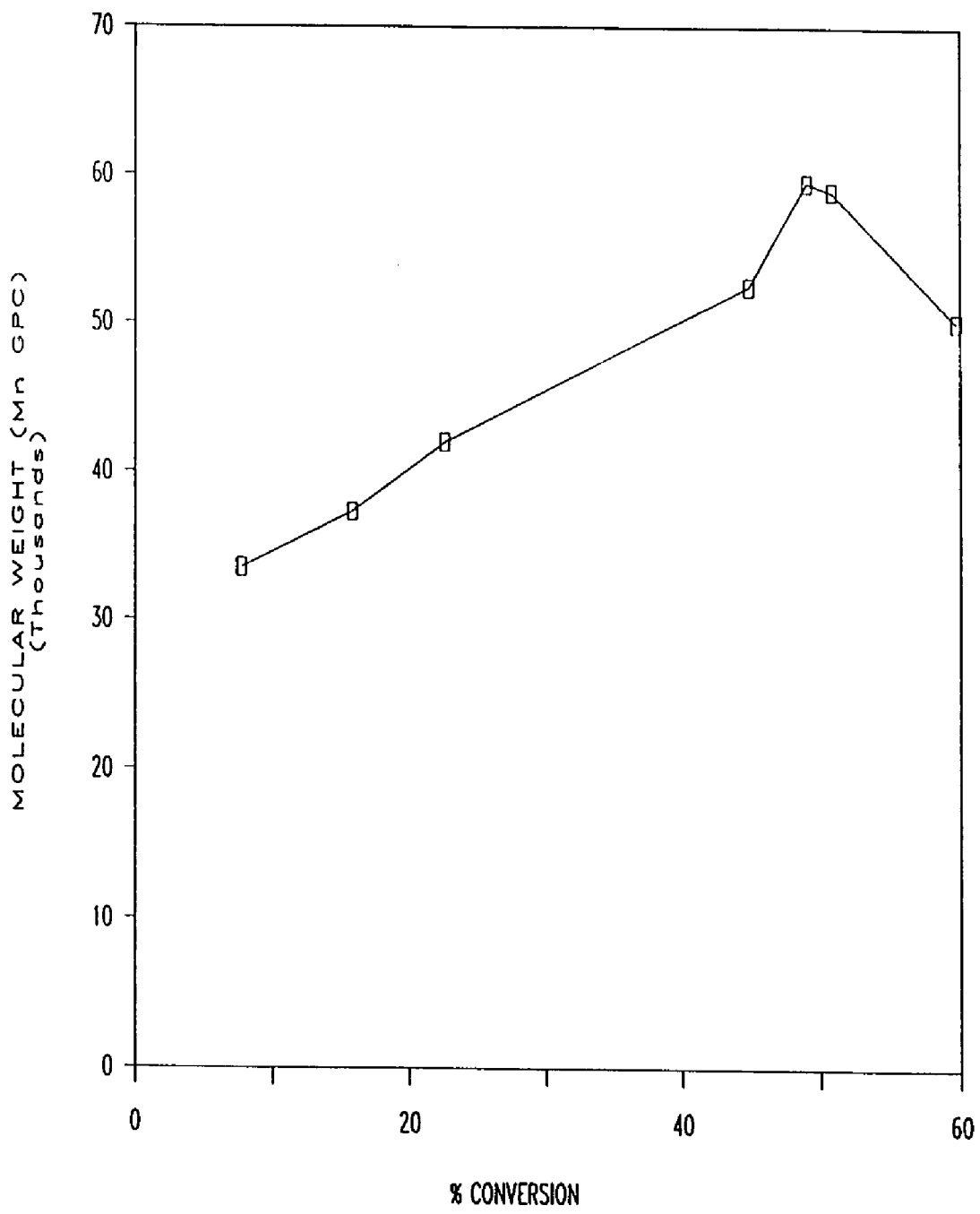
The kinetic experiments run under a covering of n-octane yielded more reproducible results than experiments attempted without the inert hydrocarbon layer. n-Octane was chosen because monomer, cyclics and polymer are all insoluble in this solvent. The inert hydrocarbon covering provides for uniform and efficient heat transfer throughout the reaction mass. The experiments run under n-octane tended to yield slower rates of reaction and lower product molecular weights than samples run in an open test tube. The hydrocarbon covering probably maintains a constant pressure at the solid-liquid interphase. The cause of this behavior was not probed further.

High molecular weight material produced very early in the course of the reaction indicates that propagation is rapid relative to initiation as is the case in a chain polymerization. A step mechanism would produce relatively low molecular weight species initially and give rise to

Figure 31. Product Molecular Weight of Bulk Polymerization
as a Function of Extent of Reaction.

Conditions: Polymerization: Samples polymerized under 3 mL
of n-octane at 75°C.

Analysis: The crude mixture dissolved in 1 mL Me₂SO-d₆ and
analyzed by ¹H NMR spectroscopy. The sample was then
diluted with 5 mL N,N-dimethylformamide and heated for two
hours prior to analysis by GPC chromatography.



high polymer only in the later stages of the reaction.

High molecular weight material is observed to appear at low conversion, the molecular weight of the product showing a maximum at approximately 50% conversion, the average molecular weight decreasing slightly in the later stages of the reaction.

This behavior is consistent with the expectation that linear dimer, formed from a slow reaction of monomer molecules, is much more reactive to monomer than the monomer from which it was formed.

4.9.2 Treatment of Kinetic Data. Both the loss of moisture from the solid hydroxyethoxy zwitterion and the conversion of monomer to polymer (Figure 32) are apparently linear with respect to time. This behavior indicates empirically, a polymerization rate showing no dependence of instantaneous monomer concentration on time or zeroeth order kinetics.

This scenario is illustrated by considering a simple rate law where the rate of change of monomer concentration in the sample with respect to time is constant.

$$-dM/dt = k \quad (38)$$

Evaluated between the limits of M_0 (initial monomer concentration) at time = 0 and M (instantaneous monomer concentration) at time = t , the integrated rate expression

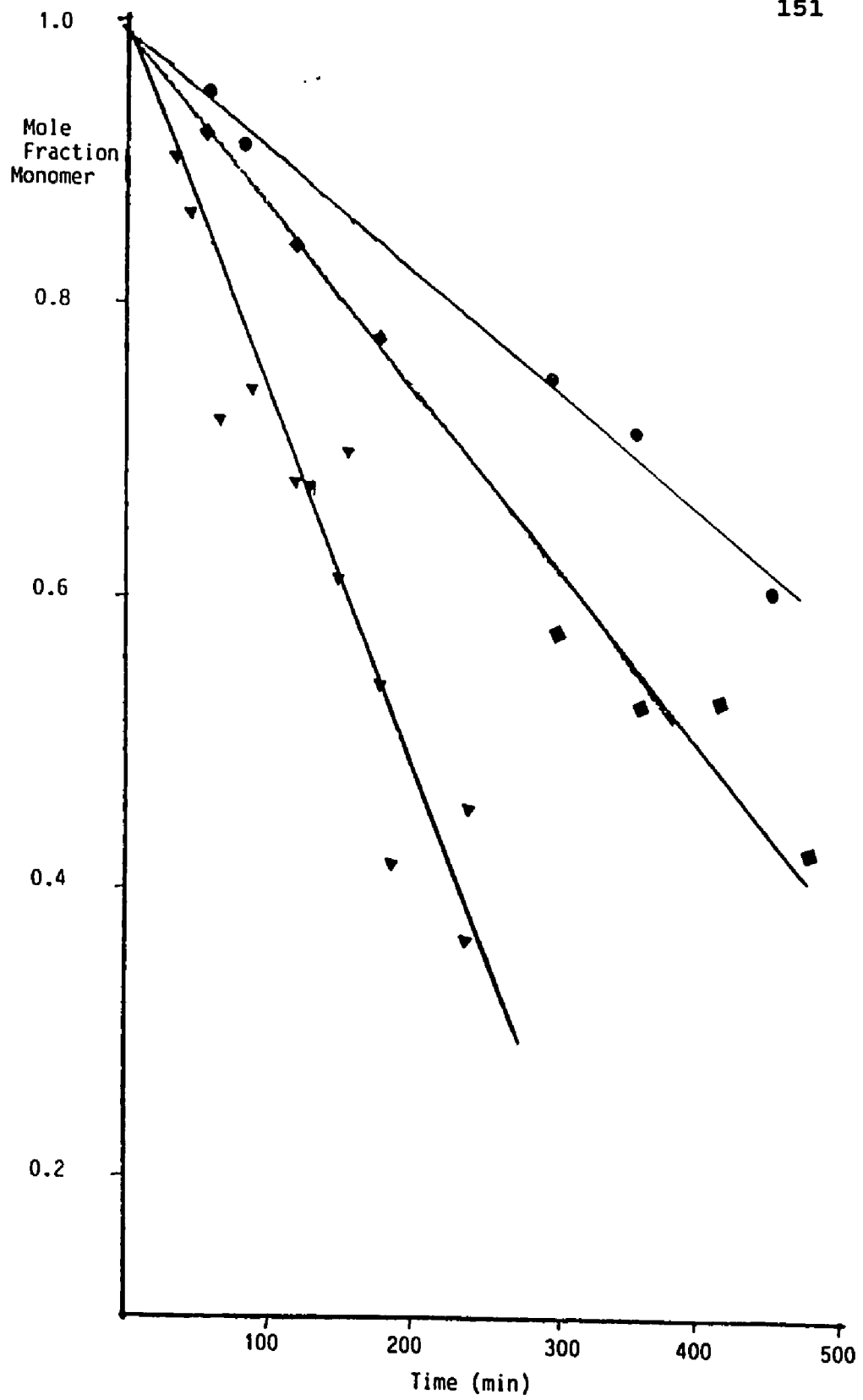
Figure 32. Conversion Versus Time Plots for the Bulk Polymerization of the Hydroxyethoxy Zwitterion

Conditions: Samples heated under a covering of n-octane

o ; Temperature = 70°C.

■ ; Temperature = 75°C.

> ; Temperature = 80°C.



follows as:

$$-dM = k dt \quad (39)$$

$$-(M-M_0) = k(t-0) \quad (40)$$

Dividing equation 40 by M_0 casts the equation in terms of mole fraction $M_f = M/M_0$, of monomer.

$$-(M-M_0)/M_0 = k/M_0 t \quad (41)$$

$$(1-M_f) = (k/M_0) t \quad (42)$$

In equation 42, $(1-M_f)$ is the extent of reaction and the apparent rate constant, $k'=k/M_0$, is obtained as the slope of linear extent of reaction versus time plots (Fig. 30). The treatment of monomer dehydration was carried out in the same manner with H_2O substituted for M .

Treatment of the kinetics as a zeroeth order process is useful to describe the polymerization but has no relevance to the elementary reaction steps of the mechanism. The polymerization is sensitive to the diffusion of moisture from the unreacted crystalline zone as well as the surface area of the substrate at which polymerization is occurring.

4.9.3 Kinetics of Monomer Dehydration. The loss of

moisture from the hydroxyethoxy zwitterion was monitored isothermally over a modest temperature range of 50-60°C. The profile of weight loss versus time was apparently linear to at least 80% dehydration. The rate data, presented in Table 15, indicates an activation energy of 36.9 Kcal/mol for the dehydration process. The observed rate of dehydration was influenced by the flow rate of purge gas. The rates reported were run at the flow rate of nitrogen at which the rate of reaction no longer increased as the flow rate of inert atmosphere was increased.

4.9.4 Kinetics of Polymerization. The activation energy of polymerization was the same as that determined for dehydration within the limits of experimental error, 34.5 Kcal for polymerization compared to 36.9 Kcal for dehydration. The experimentally observed reaction order was approximately zero. Table 16 shows the results of experiments monitoring the polymerization of solid monomer under a covering of n-octane over a temperature range of 70 to 80°C. Figure 33 shows Arrhenius plots for dehydration and polymerization.

4.9.5 Correlation between Rates of Dehydration and Polymerization. The conditions used to independently assess the dehydration and polymerization reactions of hydroxyethoxy zwitterion are sufficiently different to render any direct comparison of the data presented so far as questionable.

TABLE 15. EFFECT OF TEMPERATURE ON THE RATE OF MONOMER
DEHYDRATION

Temperature °C	Average rate constant ¹ f[H ₂ O]/s ² (X 10 ⁴)
49	1.52 (2, 15%)
56	4.66 (5, 6.2%)
59.3	9.47 (2, 5.4%)

¹ The numbers in parenthesis are the number of determinations and the relative standard deviation.

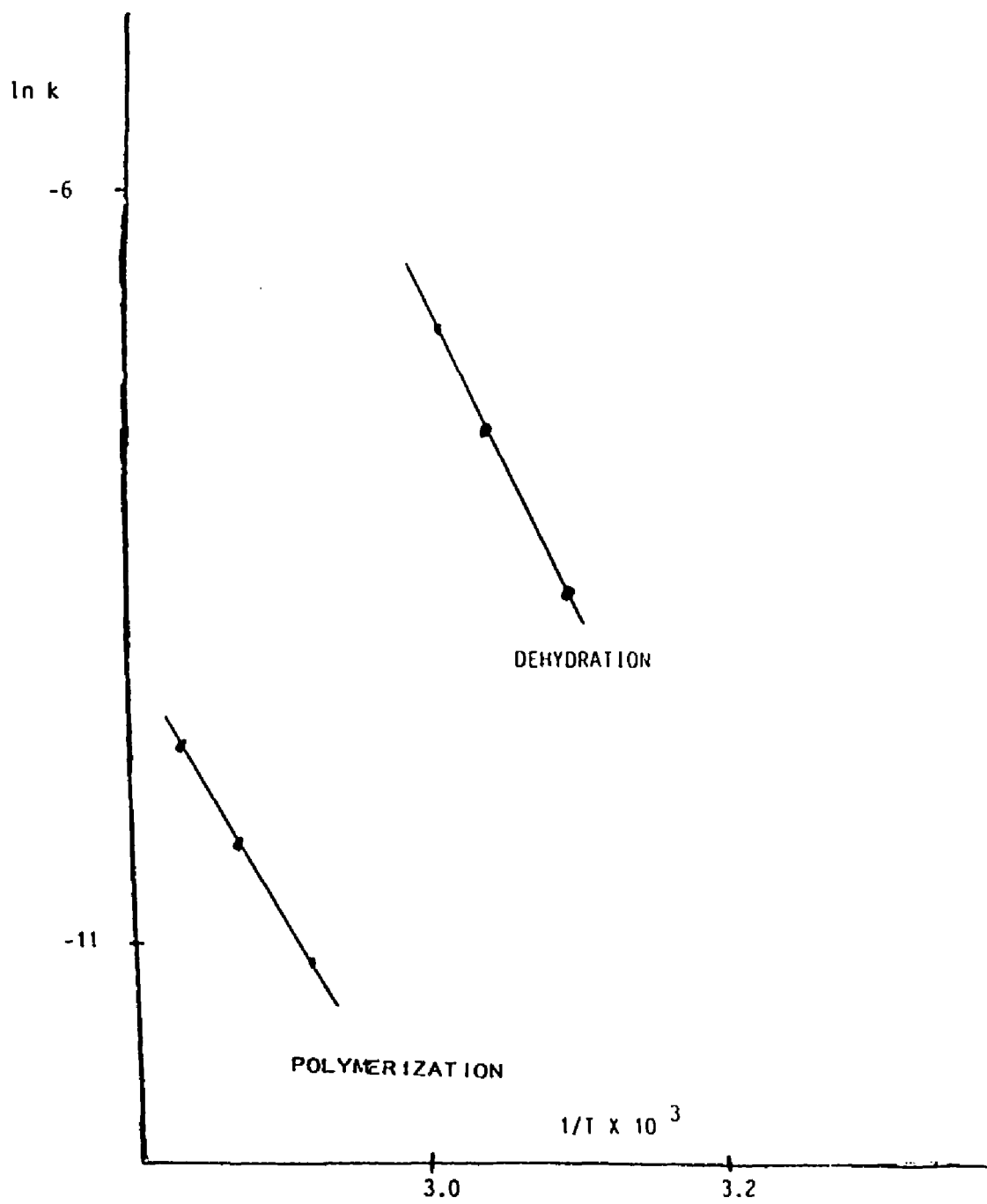
TABLE 16. EFFECT OF TEMPERATURE ON THE RATE OF BULK
POLYMERIZATION

Temperature °C	Average rate constant $f[\text{H}_2\text{O}]/\text{s}^2 \text{ (X } 10^5)$
70	1.32
75	1.99
80	5.38

TABLE 17. CORRELATION OF RATES OF POLYMERIZATION AND
DEHYDRATION OF THE HYDROXYETHOXY ZWITTERION

Fraction of Water Lost	Fraction of Polymer Formed
.308	.099
.385	.139
.615	.260
.788	.364

Figure 33. Arrhenius Plots for Bulk Polymerization and Dehydration.



Nonisothermal experiments were performed to correlate the two rates. Samples were heated in the TGA oven and allowed to cool, the fraction of moisture remaining being noted. The sample was then subjected to analysis using ^1H NMR spectroscopy. After heating the samples generally took 10 to 15 minutes to cool and were analyzed by ^1H NMR spectroscopy within 30 minutes. A listing of extent of dehydration compared to extent of polymerization for a series of samples is presented as Table 17.

These experiments indicate that although dehydration of the hydroxyethoxy zwitterion and polymerization occur simultaneously, dehydration occurs more rapidly than polymerization.

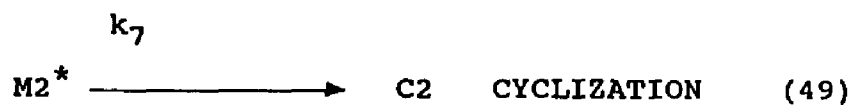
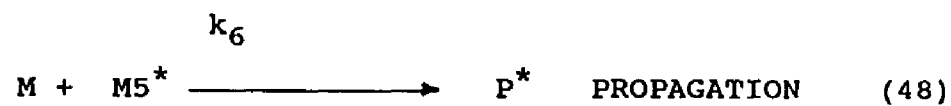
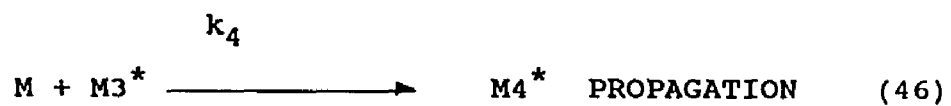
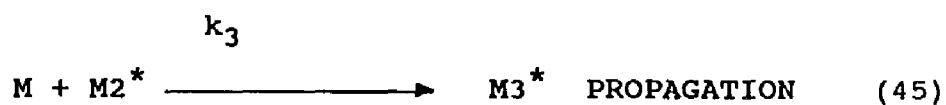
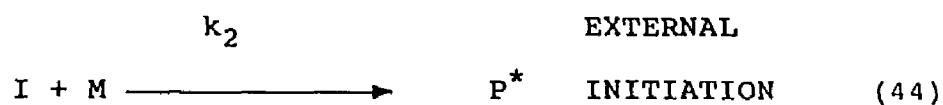
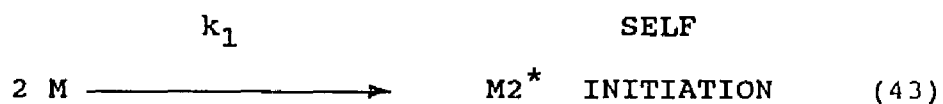
4.10 SOLUTION POLYMERIZATION KINETICS. The kinetics of the polymerization of the hydroxyethoxy zwitterion were observed in dilute solutions in $\text{Me}_2\text{SO-d}_6$. Solutions of the hydroxyethoxy zwitterion to which no added initiating specie was introduced are referred to as thermal polymerization samples. Experiments involving mixtures of monomer and the trifluoroacetate salt of the hydroxyethoxy zwitterion are referred to as initiated polymerization.

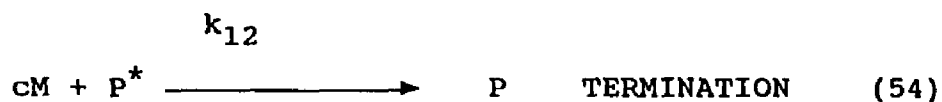
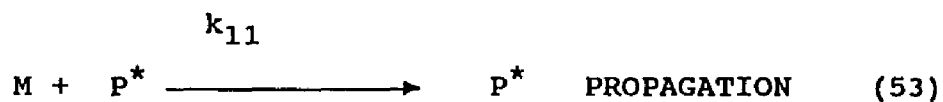
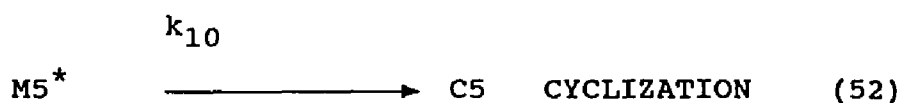
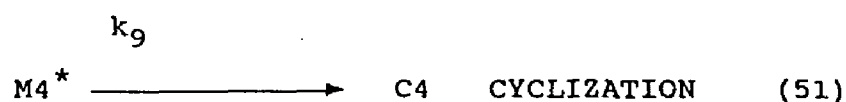
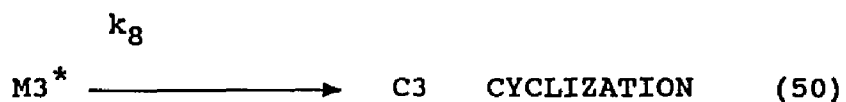
The analyses of solution polymerization reaction mixtures as a function of time were carried out using ^1H NMR spectroscopy. Using this analytical method, the instantaneous fractions of monomer and cyclic dimer were measured. The other components of the reaction mixture consisting of higher cyclics and linear polymer were not resolved from each other so only the sum of these fractions could be monitored.

The observed kinetics were consistent with the mechanism proposed in section 4.10.1; a chain polymerization, zwitterionic in the case of the thermal polymerization and cationic for the initiated polymerization in which trifluoroacetate anion is not consumed but behaves in a catalytic manner.

4.10.1 Mechanism. The thermal polymerization of the hydroxyethoxy zwitterion carried out in $\text{Me}_2\text{SO-d}_6$ with and

without added initiator was studied and shown to be consistent with the following kinetic scheme.

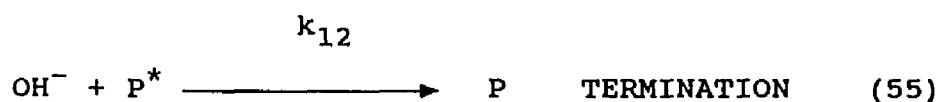




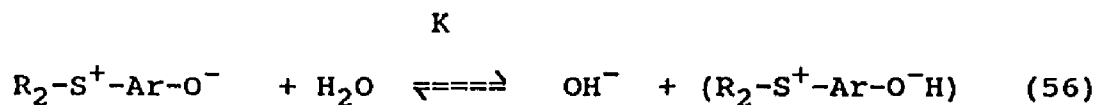
M represents the hydroxyethoxy zwitterion monomer; P^* , a propagating specie consisting of more than six monomer units with a low probability of undergoing cyclization. C2 through C5 are cyclic dimer through cyclic pentamer and P, the linear products of the reaction. I represents some initiating specie, for example the trifluoroacetate salt of the monomer, and $M2^*$ through $M5^*$ represent propagating species consisting of two through

five monomer units, those low molecular weight propagating species able to cyclize. The scheme presented above would describe both polymerizations run in the presence of some initiating specie as well as the self initiating thermal polymerization which occurs when no initiator is added.

The step represented in equation 54 may be better represented by:



Hydroxide ion is produced in small amounts however and the quantity of OH^- is proportional to the monomer concentration. In dilute solution, the production of hydroxide ion is described by the following equilibrium:



With moisture not present in great excess but only added to the system from the dihydrate monomer, an expression for K , if the amount of monomer which is dissociated at equilibrium is x is:

$$K = x^2 / (M-x)(2M_0-x) \quad (57)$$

If x is small, and the activity coefficients close to unity, the concentration of hydroxide ion then would be:

$$OH^- = (2KM_0M)^{.5} \quad (58)$$

4.10.2 Thermal Polymerization. The polymerization of the hydroxyethoxy zwitterion in solution without added initiator displays second order decay of monomer and more complicated behavior for cyclization and polymerization processes. The simple kinetic behavior of monomer loss is taken as evidence that initiation, the bimolecular self reaction of monomer, is rate determining for the process.

The derived rate equations give good agreement with experimental data. The energy of activation for monomer loss in solution is significantly lower than that observed for bulk polymerization, 24.8 Kcal/mol compared to 34.5 Kcal/mol when polymerized without solvent.

4.10.2.1 Determination of Reaction Orders. The empirical order of reaction for monomer loss and cyclic dimer formation of the uninitiated polymerization were determined using the methods outlined in appendix I. Concentration-time profiles for the three substances of inte-

rest, monomer, cyclics and polymer plus higher cyclics, were gathered in ^1H NMR experiments employing varying monomer loadings at 80°C . Concentrations of 0.208, 0.101 and 0.0404 mol/L were used. The concentration-time profiles for monomer loss and cyclic dimer formation are presented as Figures 34-36 and Figures 37-39 respectively.

The calculated values shown in Figures 34-39 were calculated according to a two parameter model described in Section 4.10.2.3 using values of $k_1 = 1.29 \times 10^{-3}$ L/mol-s and $k_3/k_7 = 10.2$ L/mol.

The monomer loss reaction order determined by fractional life and initial rates yield an integral number. This is an indication that a simple rate law is followed. The reaction order of cyclic dimer formation determined by the initial rate and fractional life methods are fractional and provide guidance in deducing the appropriate rate law expression.

Loss of Monomer. Figures 34-36 show concentration time profiles for monomer loss as a function of time for samples of varying initial monomer concentration. Inspection of the curves was used to determine the time required for 30% of the monomer to react for each of the runs. A log-log plot of $t_{30\%}$ versus M_0 , corresponding to the relationship of equation A1-9, is shown in Figure 40. The slope of the line of -1.0 indicates the order of reaction

Figure 34. Calculated and Experimental Values for
Monomer Loss.

Conditions: 80.7°C; Samples in Me₂SO-d₆ M₀=0.208 mole/L

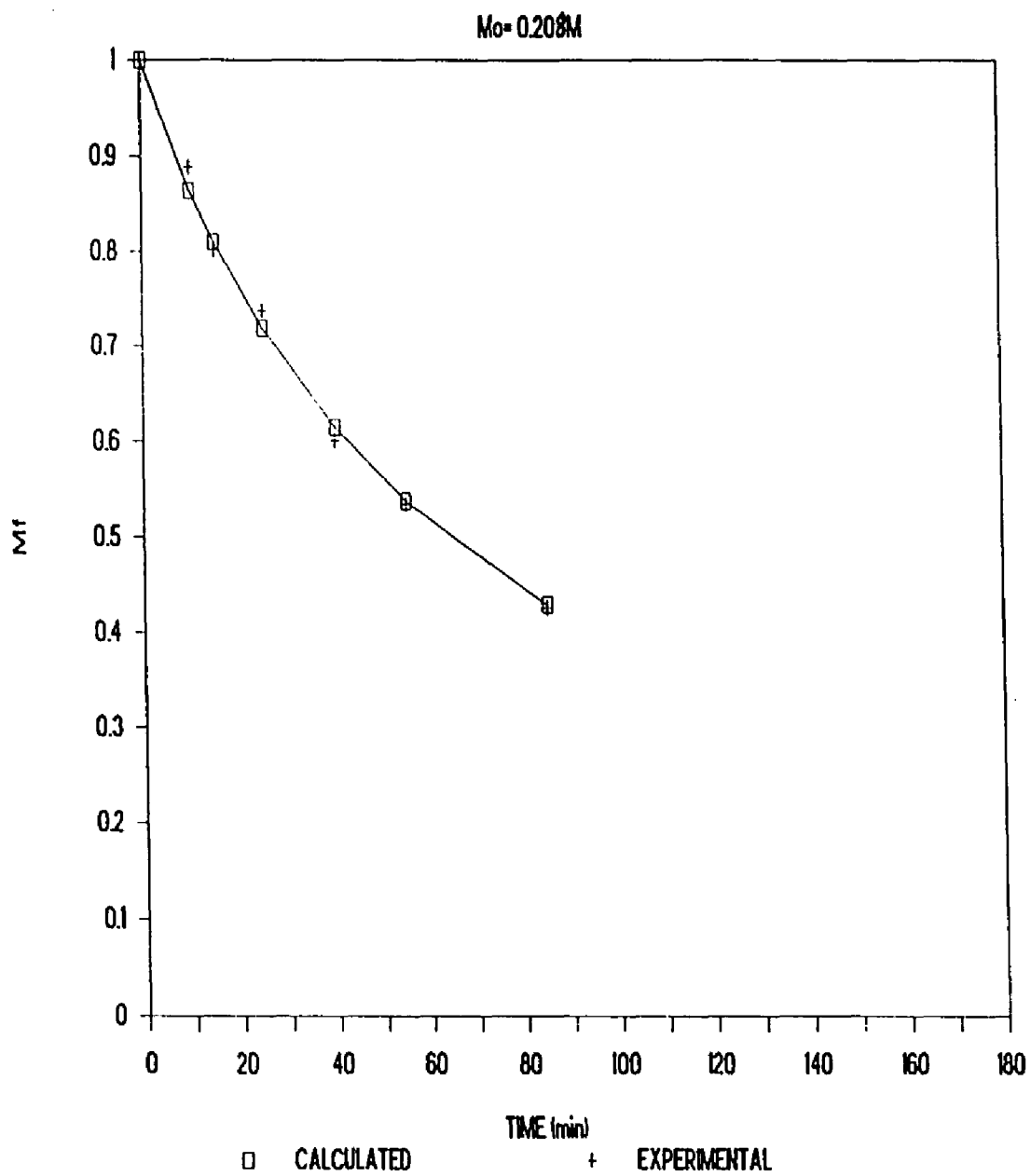


Figure 35. Calculated and Experimental Values for
Monomer Loss.

Conditions: 80.7°C; Samples in Me₂SO-d₆ M₀=0.101 mole/L.

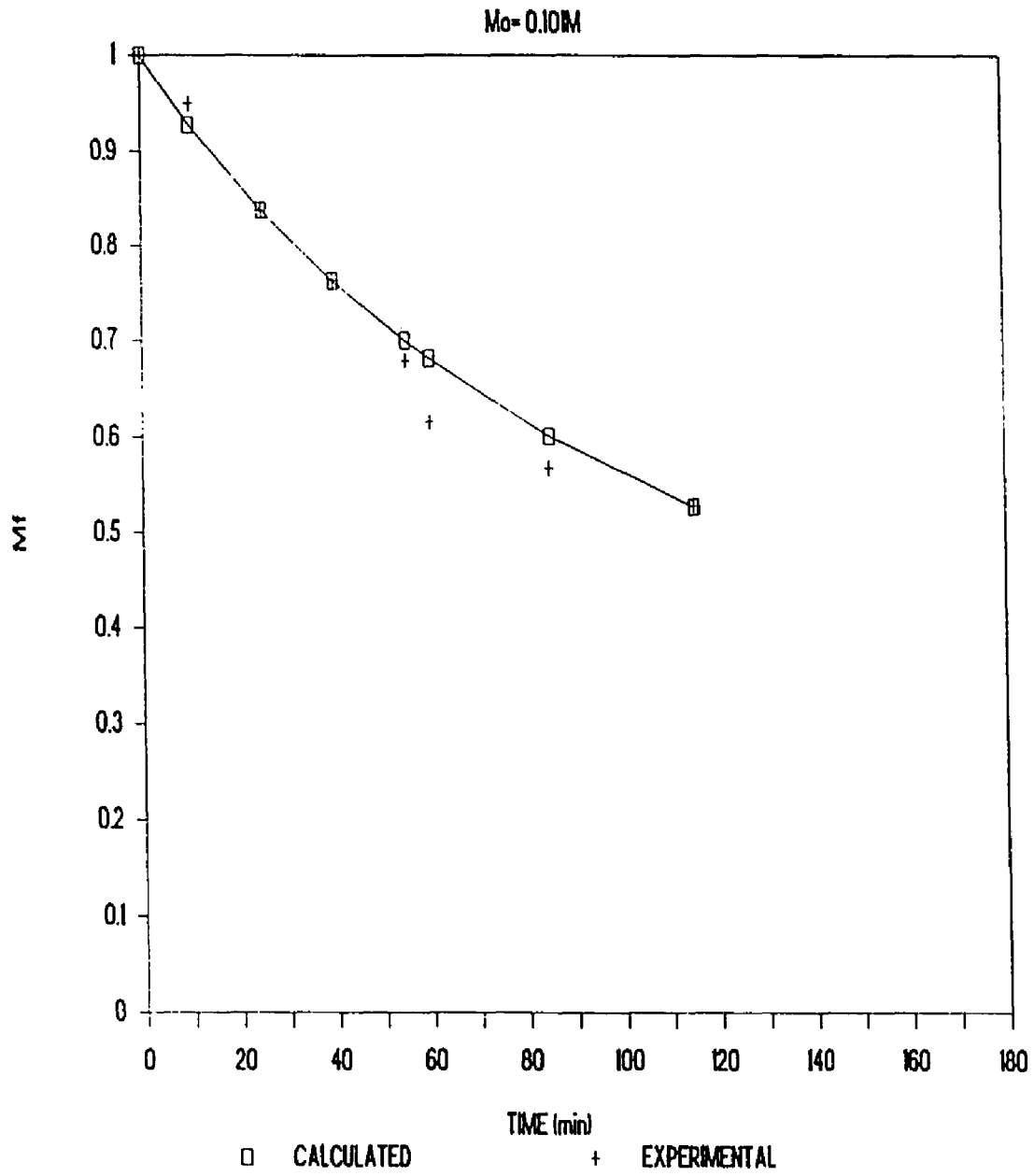


Figure 36. Calculated and Experimental Values for
Monomer Loss.

Conditions: 80.7°C; Samples in Me₂SO-d₆ M₀=0.0404 mole/L.

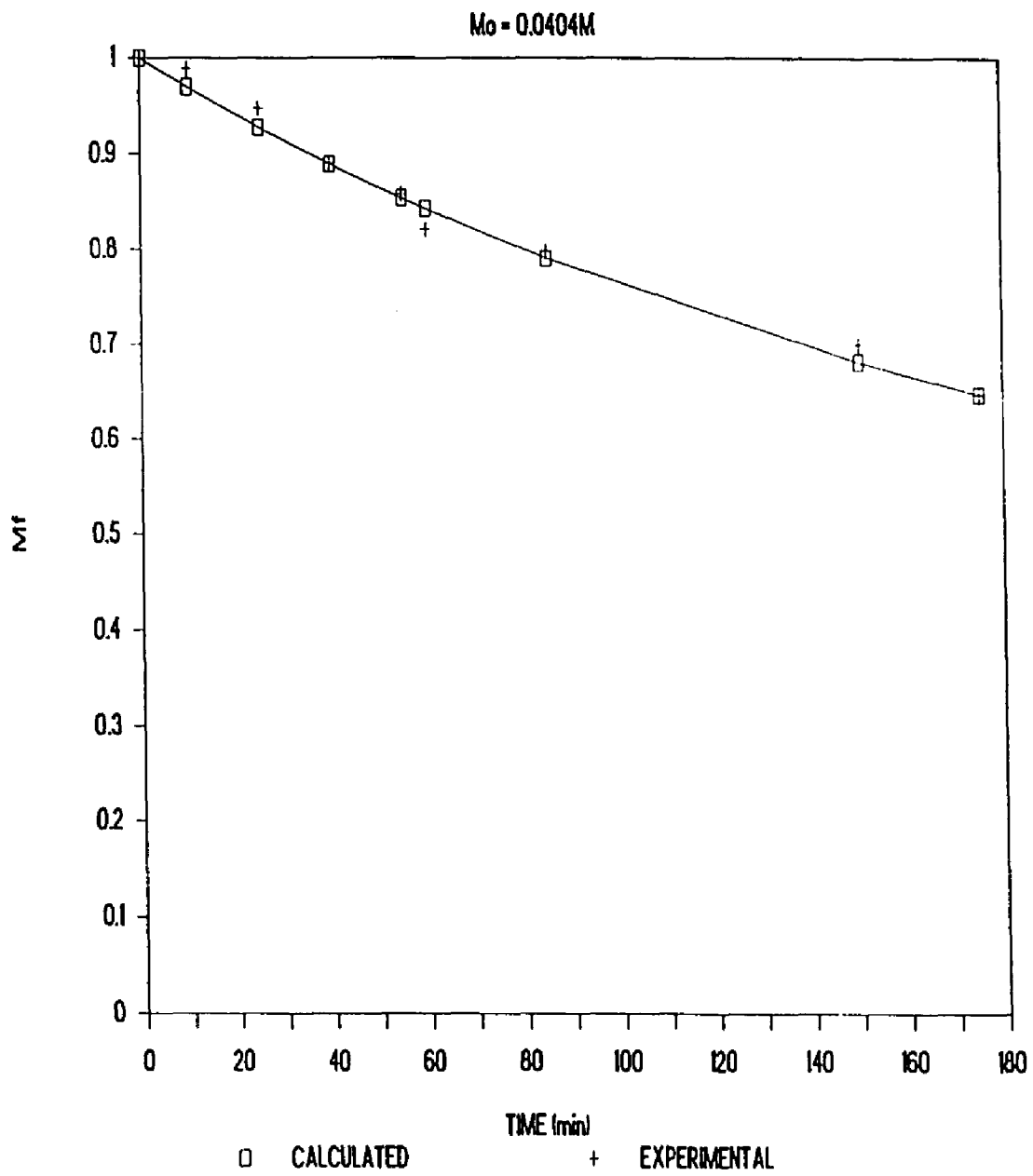


Figure 37. Calculated and Experimental Values for Cyclic
Dimer Formation.

Conditions: 80.7°C; Samples in Me₂SO-d₆ M₀=0.208 mole/L.

- ◄ ; Calculated
- ; Experimental

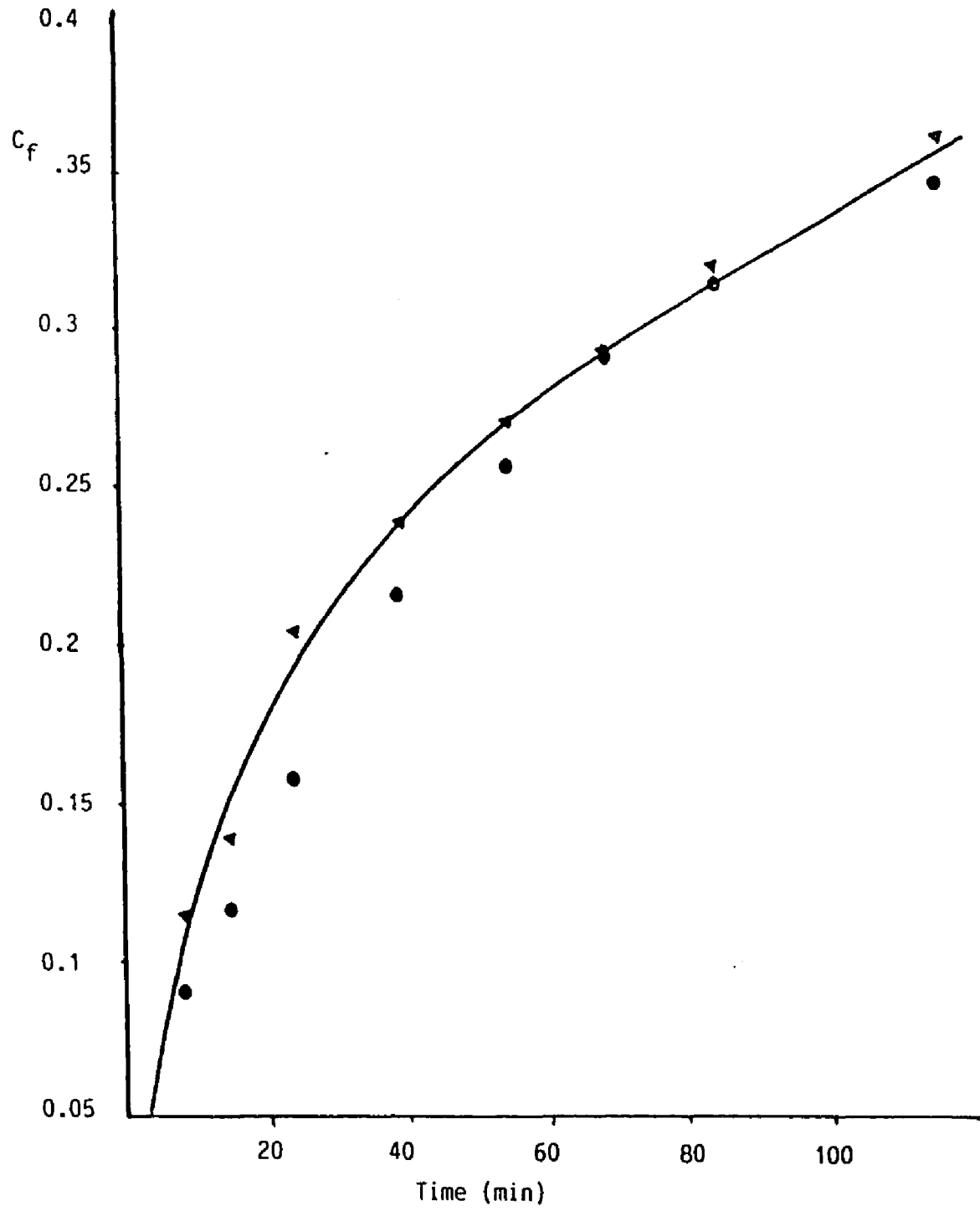


Figure 38. Calculated and Experimental Values for Cyclic
Dimer Formation.

Conditions: 80.7°C; Samples in Me₂SO-d₆ M₀=0.101 mole/L.

◄ ; Calculated

● ; Experimental

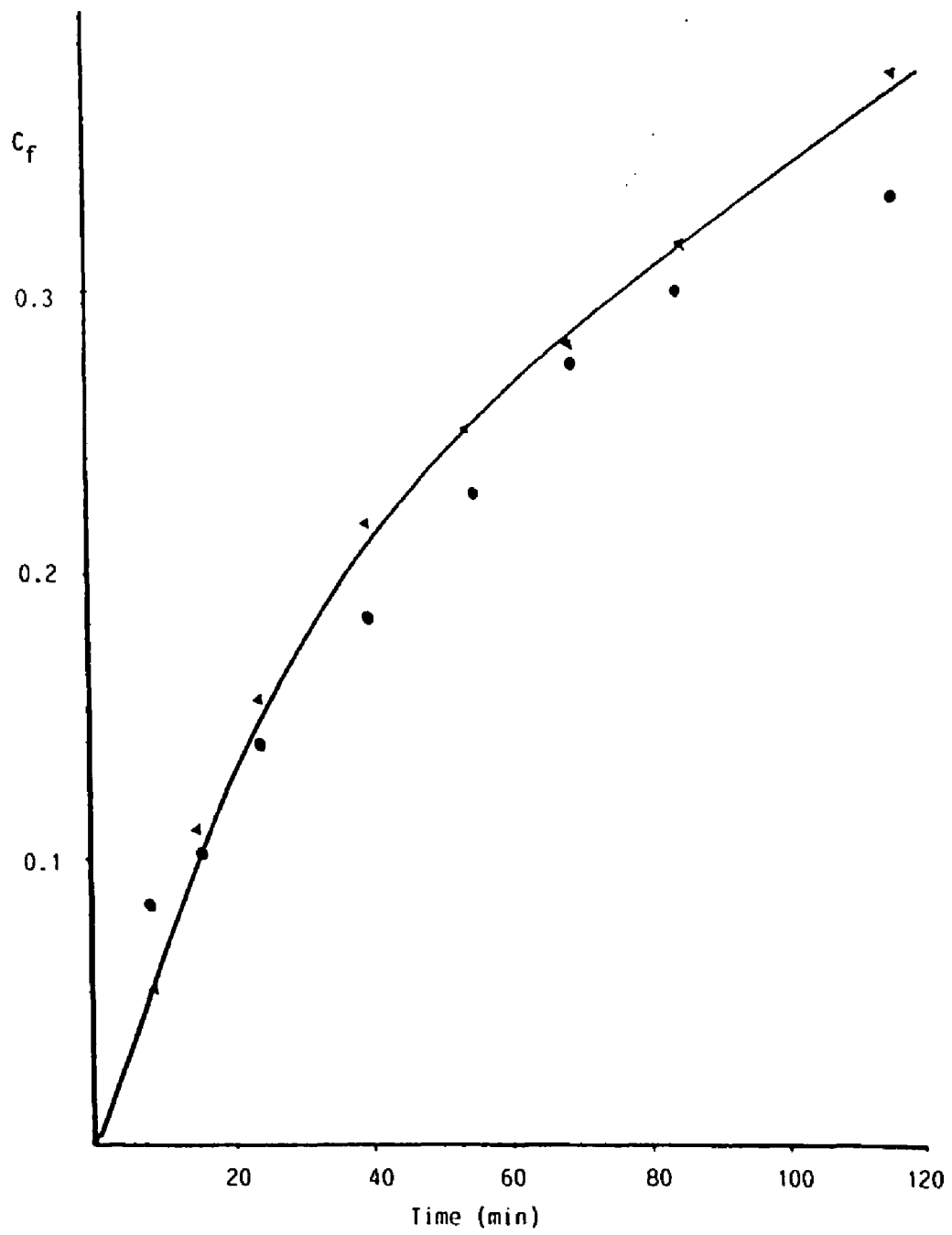


Figure 39. Calculated and Experimental Values for Cyclic
Dimer Formation.

Conditions: 80.7°C; Samples in Me₂SO-d₆ M₀=0.0404 mole/L.

◄ ; Calculated

● ; Experimental

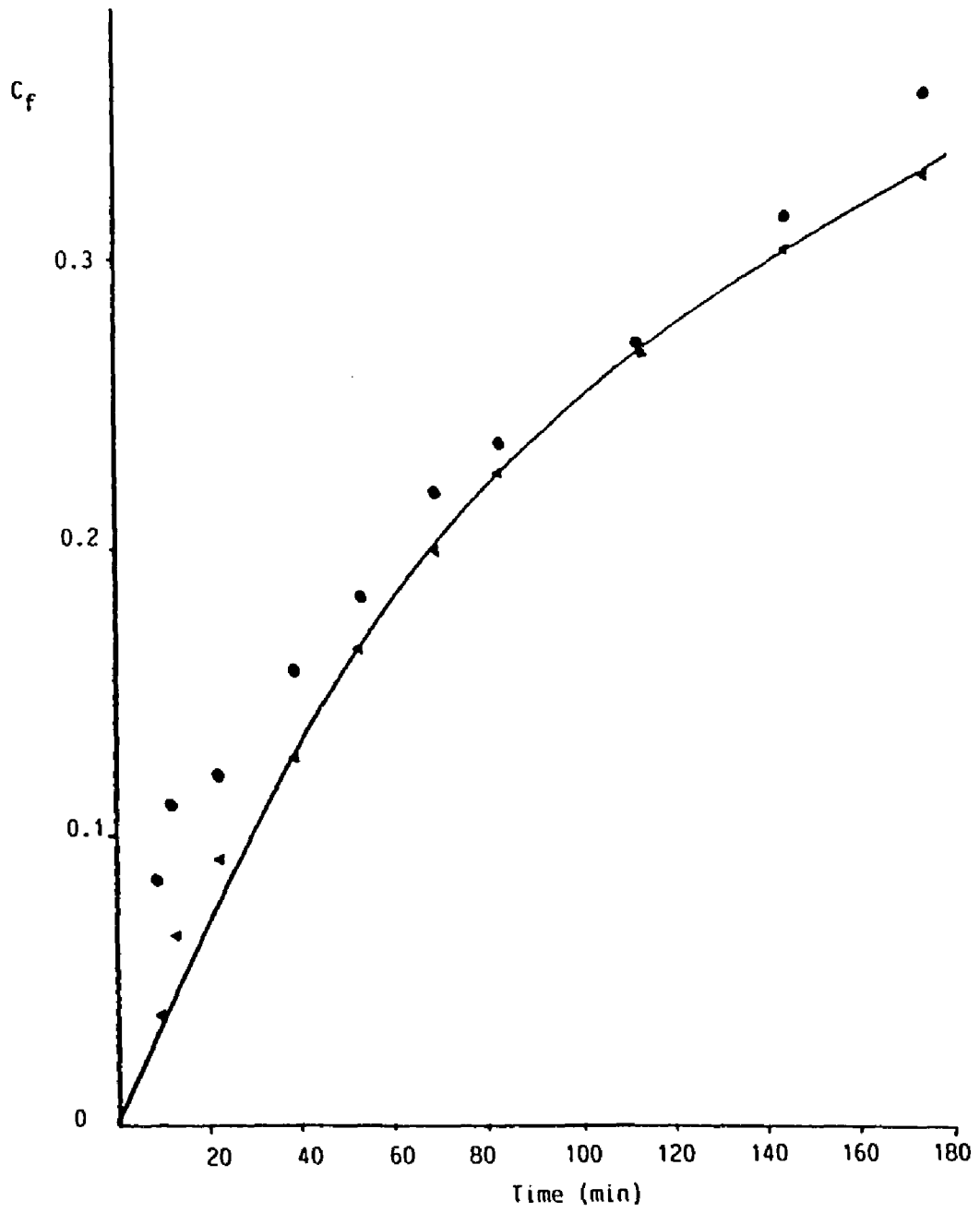
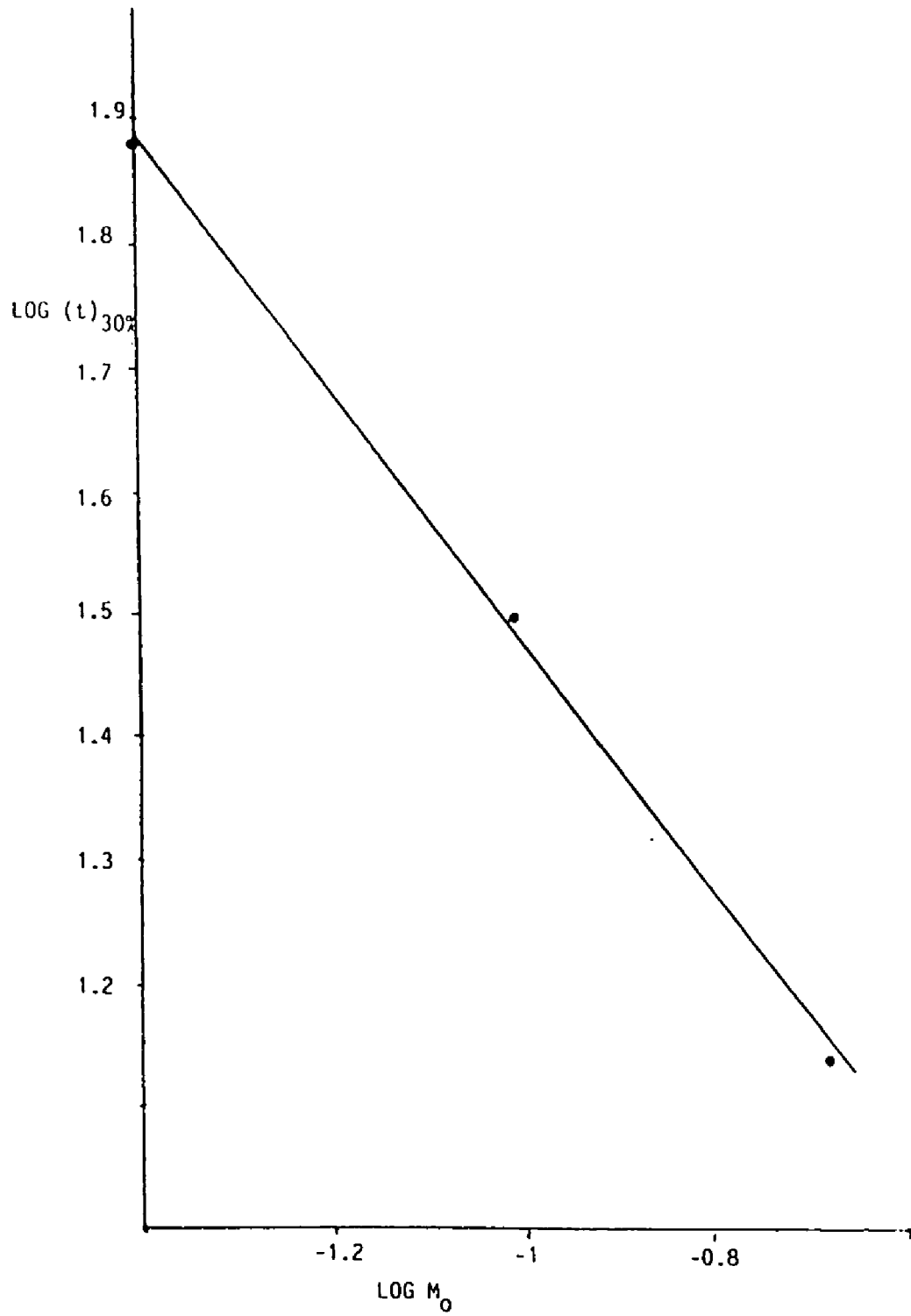


Figure 40. Order of Reaction of Monomer Loss ----
Fractional Life Method.

Conditions: 80.7°C; Samples in Me₂SO-d₆; Uninitiated
Polymerization



to be second order, or $dm/dt = kM^{2.0}$.

The integral value of n obtained as the order of reaction of monomer loss with respect to monomer concentration was checked by calculating the initial rate for each of the runs using only early data in the runs. Using values for rate of reaction up to 25 minutes, a log-log plot of initial rate of monomer loss versus initial monomer concentration, shown in Figure 41, shows an order of reaction of 1.95.

The simple rate expression for monomer loss indicates initiation is the rate determining step of the polymerization, occurring at a much slower rate than all subsequent steps.

Cyclic Dimer Formation. The order of reaction determined for cyclic dimer formation (Table 18) indicates an average order of reaction of 1.8 over the range of monomer concentrations studied. The order of reaction was determined in a manner analogous to that used for loss of monomer. A Log-Log plot of initial rate observed versus initial monomer concentration for cyclic dimer formation is shown in Figure 41. Figure 42 is a Log-Log plot of fractional-life versus initial monomer content, where fractional-life refers to the time required to produce a fixed fraction of cyclic dimer.

The observation of a non-integral order of reaction

Figure 41. Orders of Reaction; Uninitiated Polymerization
Initial Rate Method.

Conditions: 80.7°C; Samples in Me₂SO-d₆

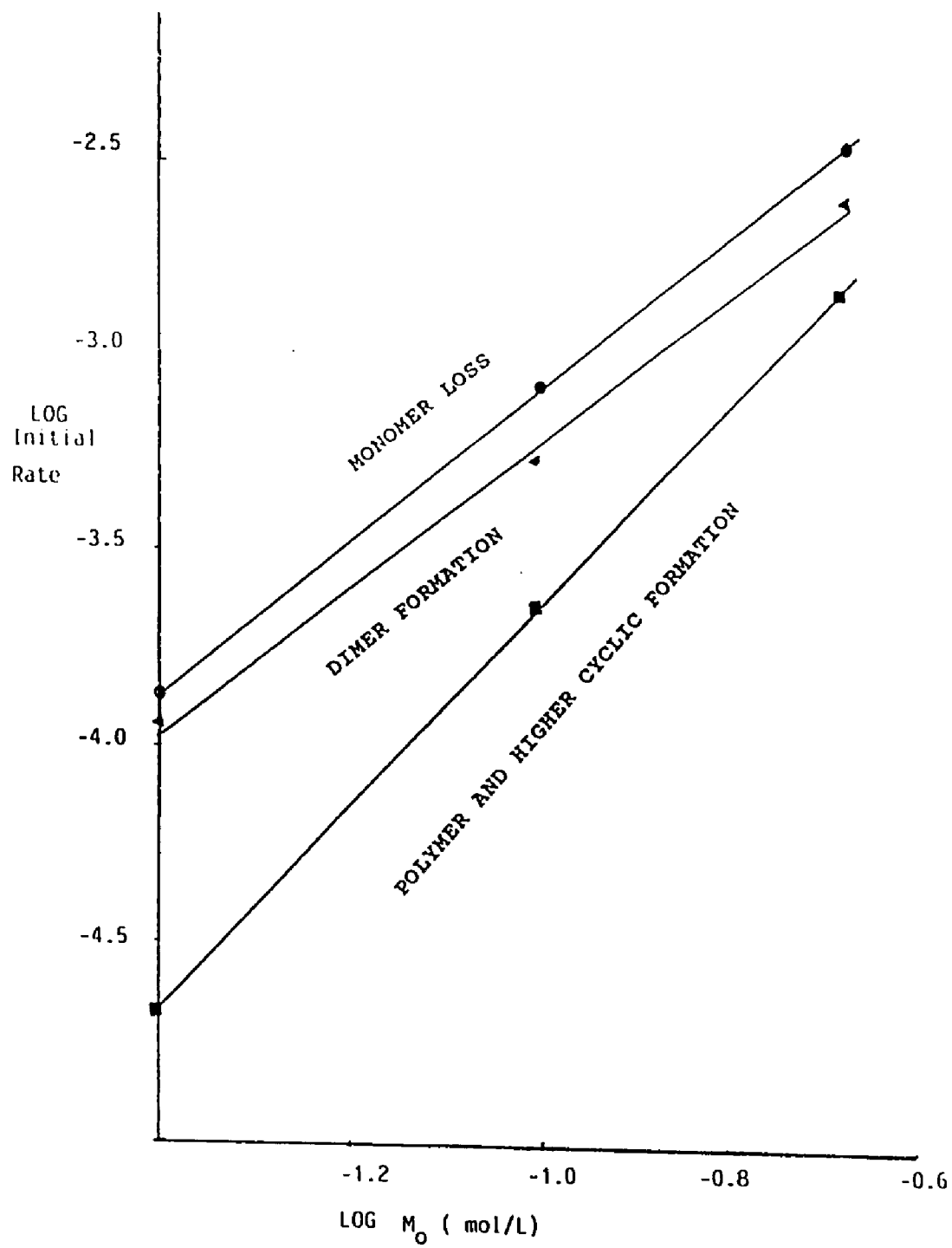


TABLE 18. SUMMARY OF ORDER OF REACTION EXPERIMENTS

Uncatalyzed Solution Polymerization

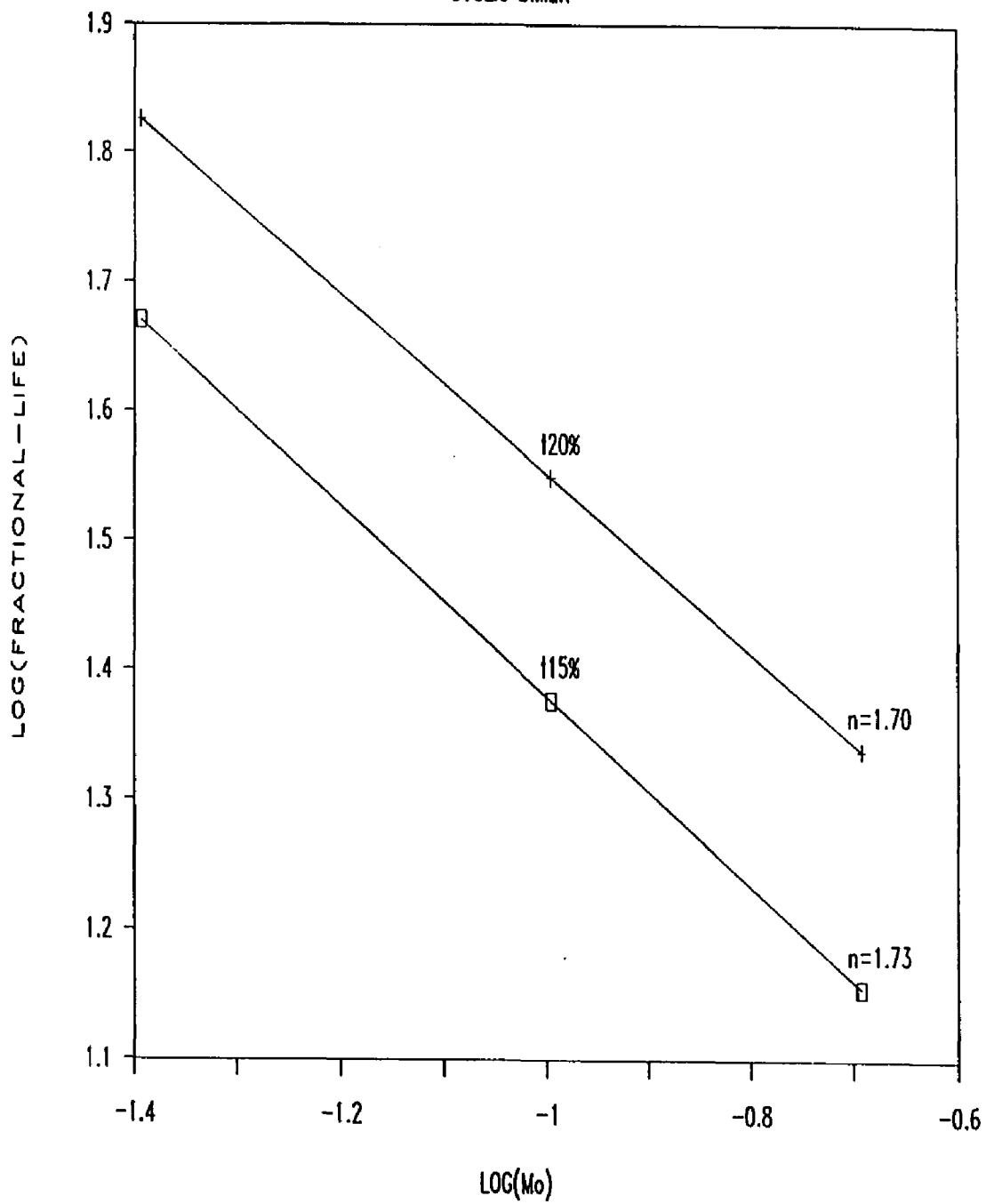
Substance	Method	
	Fractional Life	Initial rate
Monomer loss	2.0	1.95
Dimerization	1.71	1.86

Figure 42. Order of Reaction of Cyclic Dimer Formation
Fractional Life Method.

Conditions: 80.7°C; Samples in Me₂SO-d₆; Uninitiated
Polymerization

ORDER OF REACTION PLOT

CYCLIC DIMER



between 1 and 2 is consistent with the following type of rate expression:

$$dC/dt = k_a M^2 / (k_b + k_c M) \quad (59)$$

4.10.2.2 Derivation of Rate Equations.

Full

derivations of the rate equations operant for the thermal polymerization are presented in Appendix 2. The derivation is outlined here showing the results.

Consideration of the simple second order loss of monomer and the expected differences of reactivity between monomer and propagating species strengthens the assumption that initiation is the rate determining step and allows loss of monomer, dM/dt , to be formulated as:

$$dM/dt = k_1 M^2 \quad (A2-31)$$

Loss of monomer exhibiting simple second order behavior in a system in which a complex array of cyclic by products and linear polymer is formed is a strong indication that the self reaction of monomer is a slow step which limits the velocity at which subsequent faster reactions can occur.

Assuming that small steady state concentrations of dimeric and higher propagating species, M_2^* and P^* , are

formed allows the concentration of these intermediates to be calculated.

$$M2^* = k_1 M^2 / (k_7 + k_3 M) \quad (A2-18)$$

$$M3^* = k_1 k_3 M^3 / (k_7 + k_3 M) (k_8 + k_4 M) \quad (A2-22)$$

$$M4^* = k_1 k_3 k_4 M^4 / (k_7 + k_3 M) (k_8 + k_4 M) (k_9 + k_5 M) \quad (A2-26)$$

$$M5^* = k_1 k_3 k_4 k_5 M^4 / (k_7 + k_3 M) (k_8 + k_4 M) (k_9 + k_5 M) (k_{10} + k_6 M) \quad (A2-27)$$

$$P^* =$$

$$k_1 k_3 k_5 k_6 M^{5.5} / k^{12} (2KM_0)^{.5} (k_7 + k_3 M) (k_8 + k_4 M) (k_9 + k_5 M) (k_{10} + k_6 M) \quad (A2-30)$$

With the steady state value of $M2^*$ accessible, the rate of cyclic dimer formation is obtained from equations 49 and (A2-18).

$$dC/dt = k_7 M2^* = k_7 k_1 M^2 / (k_7 + k_3 M) \quad (A2-32)$$

Values for k_3 and k_7 are not directly accessible, but the ratio k_3/k_7 may be calculated by considering the change of monomer concentration with respect to cyclic

formation.

$$-dM/dC = (1+qM) \quad (A2-48)$$

where $q = k_3/k_7$.

Integrating (A2-48) and casting the variables in terms of $C_f = C/M_0$ and $M_f = M/M_0$ yields:

$$C_f M_0 = -(1/q) \ln((1 + q M_f M_0)/(1 + q M_0)) \quad (A2-51)$$

4.10.2.3 Modeling the Thermal Polymerization. k_1 was determined graphically using the data of Figure 34-36 and equation (A2-46).

$$(1-M_f)/M_f = M_0 k_1 t \quad (A2-46)$$

For each run experimental values of $(1-M_f)/M_f$ were plotted versus time and the best fit slope of the line calculated by least squares linear regression analysis. The average value of k_1 for the three runs was found as 1.29×10^{-3} L/mol-s.

The experimental data shown in Figures 34-36 was used to calculate values of q for data pairs of M and C and averaged to yield a value of $k_3/k_7 = 10.2$ L/mol. The calculation of values of q for individual M_f and C_f data

pairs was carried out on a microcomputer using commercially available software, TK SOLVER!, a program designed to solve equations by iteration. Given equation (A2-51) as the model to solve, the software chooses an arbitrary value for q and then calculates the numerical value of the left and right side of the equation. The numerical values of the two sides of the equation are compared and the value of q is incremented and the numerical values calculated again and compared. This iterative process is repeated until a value of q is converged upon that produces numerical values for the left and right hand of the equation (A2-51) of less than 10^{-8} .

The kinetics of thermal polymerization was modeled using these two parameters and the calculated values of monomer and cyclics compared to the experimental points.

A model of monomer decay was calculated for three initial monomer concentrations; 0.208M, 0.010M and 0.0404M using equation A2-46, the integrated expression for monomer loss. For given times corresponding to experimental points already acquired, the theoretical fraction of monomer expected was calculated. These calculated versus experimental time-conversion curves are shown in Figures 34-36 for initial monomer concentrations of 0.208M, 0.101M and 0.0404M respectively.

Calculated values of cyclic dimer content as a

function of time were obtained from equation A2-41. At each time used in Figures 34-36, the associated calculated fraction of monomer was used to calculate the theoretical fraction of cyclic dimer expected. The calculated and experimental cyclic dimer conversion-time relationships are compared in Figures 37-39 for reaction mixtures employing initial monomer concentrations of 0.208M, 0.101M and 0.0404M, respectively.

The calculated values are in good agreement with the experimental points for cyclic dimer formation and monomer loss over the range of concentrations studied using the two parameter model which results from the kinetic relationships derived from the proposed mechanism.

4.10.2.4 Effect of Temperature on Rate. The effect of temperature on the rate of the thermal polymerization was studied over the range of 59.5 to 81.2°C using 0.145M solutions of the hydroxyethoxy zwitterion dissolved in Me₂SO-d₆ (Table 19). The energy barrier to loss of monomer is lower for the solution polymerization of the hydroxyethoxy zwitterion than for the bulk polymerization carried out in the solid state (24.8 Kcal/mol compared to 34.5). The difference in activation energy may be ascribed to the necessity of removing moisture of hydration from the crystal lattice in the bulk polymerization. In the polymerization occurring in solution, hydroxyethoxy zwitt-

TABLE 19. EFFECT OF TEMPERATURE ON REACTION RATES OF
UNINITIATED SOLUTION POLYMERIZATION ¹

T (°C)	k ₁ (L/mole-sec X 10 ³)
59.5	0.198 ± 2.5% ²
65.6	0.401 ± 1.1%
70.6	0.684
81.2	2.10 ± 7.2%

¹ Temperature variation was approximately 1°C.

² relative standard deviations.

$$E_a = 24.8 \text{ Kcal/mole} \quad A = 4.1 \times 10^{12} \text{ L/mole-sec}$$

erion molecules are stabilized to some extent by solvent. The solvent is present in large excess over moisture which is present in amounts equivalent only to hydroxyethoxy zwitterion concentration.

4.10.3 Initiated Polymerization. Polymerization of the hydroxyethoxy zwitterion, initiated with trifluoroacetic acid, showed pronounced differences in the rate and order of reaction in comparison to uninitiated thermal polymerization. The rate of polymerization of a reaction mixture containing 5 mole percent trifluoroacetic acid in the form of the trifluoroacetate salt of the hydroxyethoxy zwitterion polymerized approximately 2.5 times faster than an uninitiated polymerization run under the same conditions. Besides the differences in product distribution and product molecular weight discussed in section 4.8, the kinetics of the reaction were observed to be different: first order with respect to monomer concentration and between zero and first order with respect to initiator concentration.

4.10.3.1 Determination of Reaction Orders. The empirical orders of reaction for monomer loss with respect to initiator and monomer concentrations were determined using the methods outlined in Appendix 1. Monomer concentration - time profiles were gathered at 65°C using ^1H NMR spectroscopy for sets of solutions of constant

monomer concentration and varying initiator contents to determine the order of reaction with respect to initiator concentration. Solutions of constant initiator loading and varying monomer concentration were reacted and examined kinetically to determine the reaction order with respect to monomer concentration. A summary of these experimental results are presented as Table 20.

a) Order of Reaction With Respect to Monomer. Reaction mixtures in which the initiator content was held constant at 6.2×10^{-3} mol/L and the initial monomer content varied at 0.203, 0.152 and 0.073 mol/L levels gave reaction half lives of 64, 68 and 69 minutes, respectively. The constancy of the half life time with varying initial monomer concentration indicates monomer loss to be a simple first order process with respect to instantaneous monomer concentration.

b) Order of Reaction With Respect to Initiator. Figure 43 shows a log-log plot of initial rate of monomer consumption versus initial initiator concentration for reaction mixtures of constant initial monomer loading and varying initiator contents. The order of reaction with respect to initiator indicated by the slope of the line is 0.64 order.

Possible rate equations indicated by the order of reaction are:

TABLE 20. SUMMARY OF ORDER OF REACTION EXPERIMENTS
INITIATED SOLUTION POLYMERIZATION

Order of Reaction With Respect to Monomer ¹

	Fractional Life	Initial Rate
	Method	Method
Monomer Loss	1.0	1.0
Polymer and Higher		
Cyclic formation	1.0	1.0

¹ Experiments run at constant Initiator loadings

$$I_0 = 0.0062M$$

Order of Reaction With Respect to Initiator ²

	Fractional Life	Initial Rate
	Method	Method
Monomer loss	1.75	0.64
Polymer and Higher		
Cyclic Formation	1.64	0.70

² Experiments run at constant monomer loadings

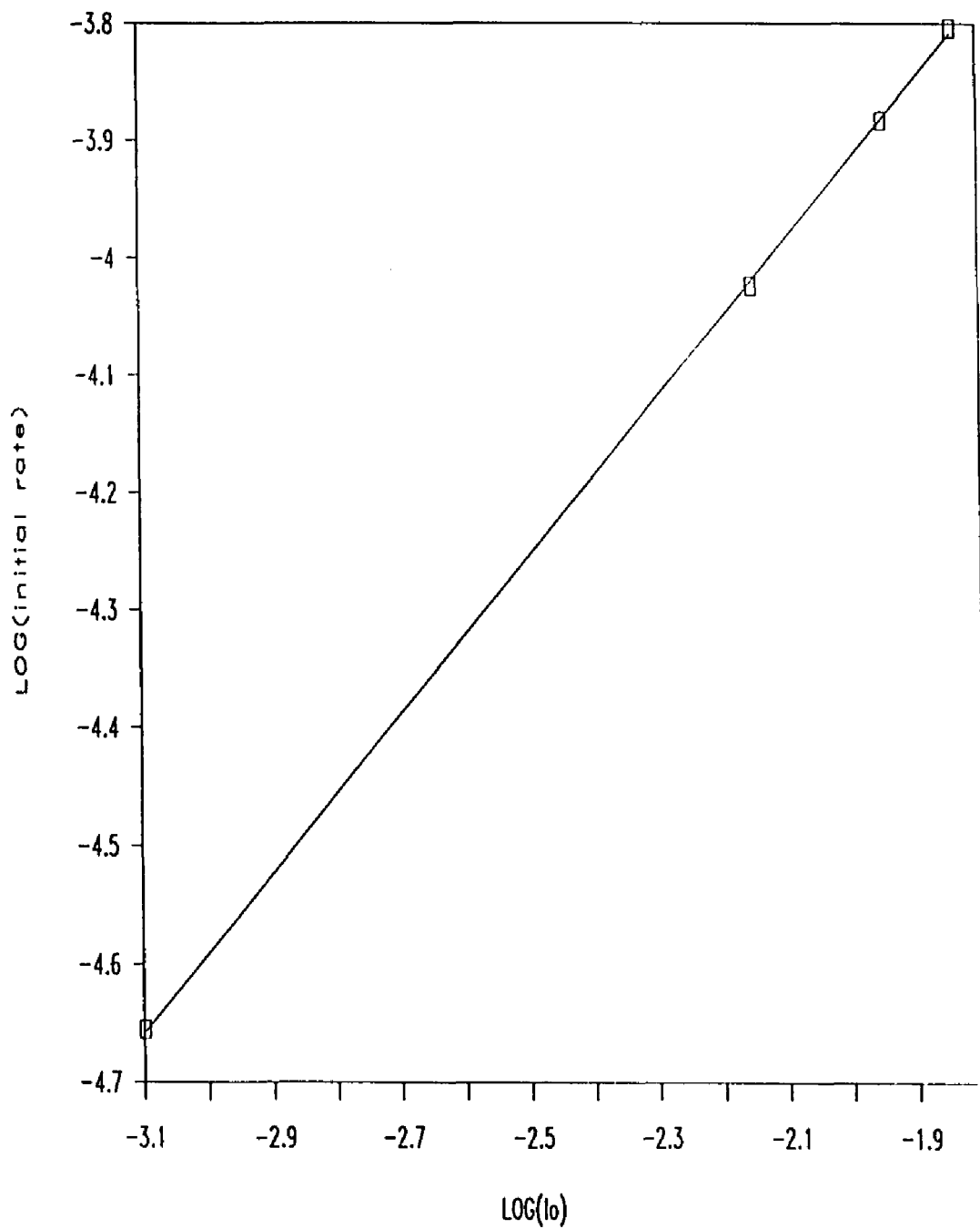
$$M_0 = 0.145M$$

Figure 43. Order of Reaction for Initiated Polymerization
With Respect to Initiator; Initial Rate Method.

Conditions: 65°C in Me₂SO-d₆; M₀=1.45 X 10⁻¹ M.

ORDER OF REACTION PLOT

INITIAL RATE METHOD



$$-dM/dt = kMI^{1/2} \quad (60)$$

or

$$-dM/dt = kM + k'MI \quad (61)$$

For these runs, the time required for 20% and 50% of the monomer employed to be consumed was observed and the apparent order of reaction determined by the fractional life method (Figure 44). This method indicated a reaction order of 1.75, which corresponds roughly to the overall order of reaction.

4.10.3.2 Derivation of Rate Expressions. For initiated polymerizations the rate expressions are simplified due to the polymerization conditions used and the simpler product distribution.

Conditions used for initiated polymerizations were such that $I_0 \ll M_0$; The initial initiator concentration was much lower than the monomer concentration initially present.

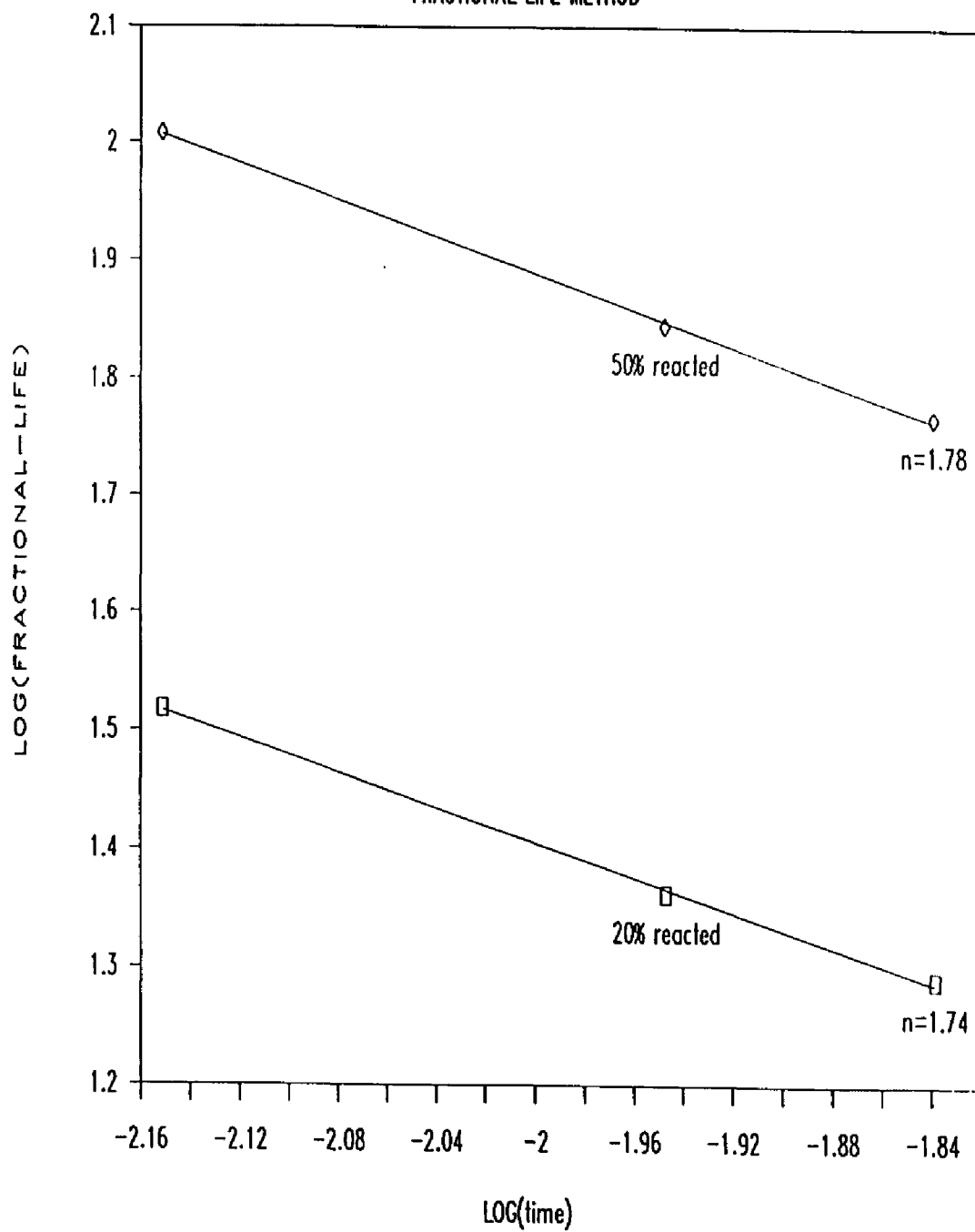
During the course of the initiated polymerizations, only small amounts of cyclic dimer formed and higher cyclic oligomer formation was limited to lower, almost constant levels. The consumption of monomer is assumed to be mostly due to reaction of monomer with P^* type propagating species formed by reaction of initiator with

Figure 44. Order of Reaction for Initiated Polymerization
With Respect to Initiator; Fractional Life Method.

Conditions: 65°C in Me₂SO-d₆; M₀=1.45 X 10⁻¹ M.

ORDER OF REACTION PLOT

FRACTIONAL LIFE METHOD



monomer. Very little M^* is formed which is capable of cyclizing.

If cyclization is neglected, it can be assumed that processes governed by the rate constant, k_1 , are slow enough to be ignored (equation 43). This simplifying assumption causes the rates of all of the other processes to approach zero except for those steps governed by k_2 , k_{11} and k_{12} .

Two assumptions concerning the initiator are also made. In $\text{Me}_2\text{SO-d}_6$, a good solvating solvent, it is assumed that the trifluoroacetate salt is completely ionized. It is also assumed that the concentration of initiator remains constant during the course of the reaction since the feebly nucleophilic trifluoroacetate anion only slowly opens the tetrahydrothiophenium ring. As termination of propagating specie to alcohol or vinyl terminated linear polymer occurs, trifluoroacetic acid is generated and reacts with monomer to form initiator in situ.

The main steps of the analysis of the proposed mechanism for the initiated solution polymerization are now outlined. The derivation of the cationic initiated solution polymerization of the hydroxyethoxy zwitterion is presented in greater detail in Appendix II.

Assuming a steady state for the propagating specie,

P^* :

$$dP^*/dt = - dP^*/dt \quad (\text{A2-52})$$

$$k_2IM = k_{11}MP^* + k_{12}(2KM_O)^{\cdot 5}M^{\cdot 5}P^* \quad (\text{A2-53})$$

$$P^* = k_2IM^{\cdot 5}/(k_{11}M^{\cdot 5} + k_{12}(2KM_O)^{\cdot 5}) \quad (\text{A2-54})$$

If the termination process is assumed to be slower than propagation:

$$P^* = k_2I/k_{11} \quad (\text{A2-55})$$

All of the initiator exists as added trifluoroacetate salt or the growing end of a propagating specie.

$$I_O = I + P^* \quad (\text{A2-56})$$

$$I_O = I + k_2I/k_{11} \quad (\text{A2-57})$$

$$I_O = (1 + k_2/k_{11})I \quad (\text{A2-58})$$

$$I = k_{11}I_O/(k_{11} + k_{12}) \quad (\text{A2-59})$$

Examination of the mechanism shows that the rate of

polymerization is equal to the rate of propagation.

$$dP/dt = k_{11}MP^* \quad (A2-60)$$

Since polymer is the only product considered:

$$dP/dt = -dM/dt = k_{11}MP^* \quad (A2-61)$$

Using equation A2-56:

$$dM/dt = k_{11}(I_0 - I)M \quad (A2-62)$$

Equation A2-62 predicts that the initiated polymerization will be first order with respect to monomer and between zero and first order with respect to initiator, between first and second order overall.

Substituting equation A2-59 into A2-62 produces:

$$dM/dt = k_{11}I_0(1 - k_{11}/(k_2 + k_{11}))M \quad (A2-63)$$

$$dM/dt = (k_2k_{11}/(k_2 + k_{11}))I_0M \quad (A2-64)$$

Equation A2-64 correctly predicts that a plot of apparent first order rate constant versus I_0 is linear.

(Fig 30).

4.10.3.3 Modeling the Initiated Polymerization. The rate constant of equation (A2-64) was determined graphically using the integrated form of a simple first order rate equation:

$$\ln(M/M_0) = -k'I_0t \quad (62)$$

where $k' = k_2k_{11}/(k_2 + k_{11}) = 0.0145 \text{ L/mol-sec.}$

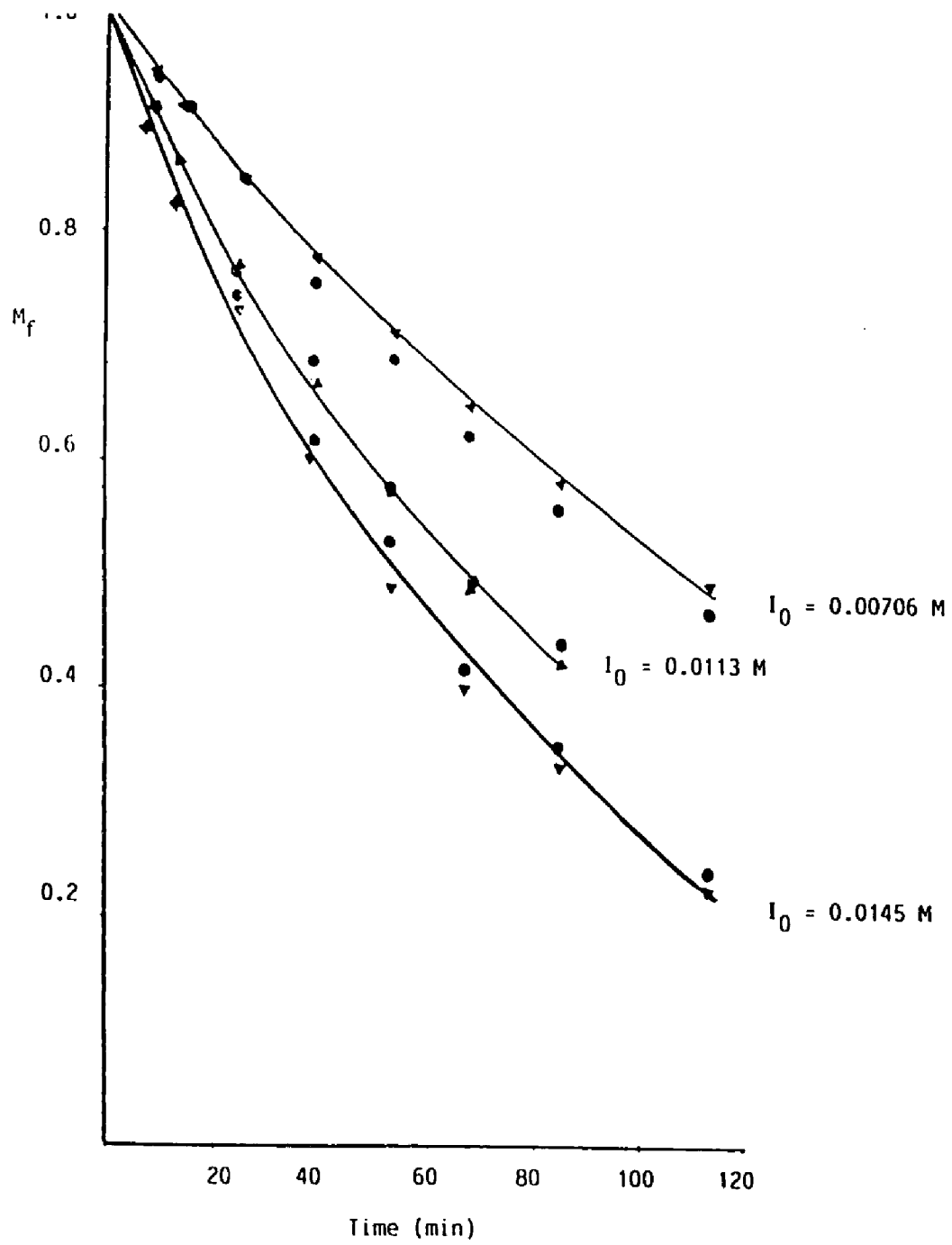
Figure 45 compares calculated and experimental data points for initiated solution polymerization mixtures prepared with 0.145M monomer and polymerized at 65°C with initiator loadings of $7.06 \times 10^{-3} \text{M}$, $1.13 \times 10^{-2} \text{M}$ and $1.45 \times 10^{-2} \text{M}$.

Figure 45. Calculated and Experimental Values for Monomer
Loss in Initiated Solution Polymerization.

Conditions: 1.45×10^{-1} M solutions of monomer in
 $\text{Me}_2\text{SO-d}_6$ at 65°C .

< ; Calculated

● ; Experimental



5.0 CONCLUSIONS

The hydroxyethoxy zwitterion polymerizes in bulk and solution without any added initiator to product of reasonable molecular weight. Gel permeation chromatography indicates the number average molecular weight, relative to monodisperse polystyrene standards, to range from 5,200 ($M_w=7,500$) to 94,000 ($M_w=290,500$) depending upon the reaction conditions. Determination of the product molecular weight as a function of extent of reaction in bulk polymerization experiments demonstrated that high molecular weight material is formed early in the course of the reaction, indicating a chain polymerization mechanism.

The monomer, polymeric and cyclic products were characterized spectroscopically. ^1H NMR spectroscopy revealed the monomer to be associated with water of hydration, TGA analysis indicating two moles of water per mole of monomer. ^{13}C NMR spectroscopy was consistent with the structure proposed for monomer. The structures proposed for polymer and cyclic dimer were also consistent with spectral data and elemental analysis.

The main by-product of the polymerization was found to be cyclic dimer, produced in large quantity in solution (41-77 mol%) and only in moderate quantities when the

hydroxyethoxy zwitterion was reacted in bulk (4-5 mol%) or in the presence of more than 1% added trifluoroacetic acid (2.9-7.7 mol%).

Significant quantities of cyclic products up to the pentamer were observed in solution polymerization. From 8.5 to 30% cyclic trimer, 2.2 to 10.4% cyclic tetramer and 1.9 to 6.8% cyclic pentamer were observed in solution polymerization experiments.

Other termination reactions observed included elimination and addition processes which opened the tetrahydrothiophenium ring to produce butenyl and hydroxy butyl end groups. Model compounds prepared with vinyl and alcohol groups exhibited ^1H NMR spectra that enabled end group signals of the polymer to be assigned.

Addition of trifluoroacetic acid to solutions of hydroxyethoxy zwitterion altered the polymerization, causing a cationic mechanism to be operant. The cationic polymerization was found to produce less cyclic by-product, a result of reactivity differences between the cationic and zwitterionic propagating species.

Kinetic evidence relating to the reaction mechanism was also gathered. The reaction of hydroxyethoxy zwitterion carried out in bulk proceeded with the loss of water as polymerization occurred. Zero order kinetics were observed for both polymerization and dehydration of the

hydroxyethoxy zwitterion polymerized in the solid state. The cause of the zero order bulk polymerization reaction is not understood although similar kinetics have been observed for the solid state oxidation of sodium metal which proceeds with contraction of volume and displays zero order kinetics.

Reactions carried out in solution with and without added initiator were easier to interpret. In uninitiated solution polymerizations it was found that loss of monomer was simple second order in nature. The formation of cyclic dimer was more complex, exhibiting an non-integral empirical order of reaction between 1 and 2.

These kinetic observations are in accord with the proposed mechanism. Hydroxyethoxy zwitterion molecules are much less reactive with themselves than with the zwitterionic propagating specie formed from self reaction. Thus, two molecules of monomer self reacting constitutes the rate determining step governing loss of monomer. Once formed, propagating specie reacts quickly with excess hydroxyethoxy zwitterion until termination occurs. The termination reactions are competitive; intramolecular reaction to form cyclic specie are unimolecular and termination to linear polymer by addition or elimination are bimolecular steps.

The kinetics of initiated solution polymerization is

also in accord with this scenario. With added initiator the bimolecular reaction of two hydroxyethoxy zwitterions is no longer rate determining, as the tetrahydrothiophenium trifluoroacetate initiator is more reactive with hydroxyethoxy zwitterion than a second hydroxyethoxy zwitterion molecule. The proton capped propagating specie is much less prone to intramolecular reaction to form cyclic species and the formation of these products is sharply reduced.

Taken with the work of Schmidt who polymerized the dichloro zwitterion using an anionic initiator, sodium methoxide, and observed a dramatic effect on product distribution, the proposed zwitterionic structure of the propagating specie in the spontaneous polymerization finds support. The zwitterionic propagating species responsible for the polymerization of the tetrahydrothiophenium arene oxide inner salts have now been shown to be susceptible to modification by both anionic and cationic reagents.

APPENDIX 1 TREATMENT OF KINETIC DATA

A1.1 Empirical Orders of Reaction. For the simplest kinetic expression, the rate of reaction is proportional to a single term involving species raised to respective powers. For example a reaction pathway in which reactants A and B form the product P:



The simplest kinetic expression could be expressed as:

$$dP/dT = k A^a B^b \quad (A1-2)$$

Where k is the rate constant governing the process and the exponents a and b are regarded as the orders of reaction with respect to A and B. The overall order of reaction is the sum of $a + b$. Methods used to estimate the order of reaction are only valid for simple expressions such as the above equation, but are instructive in deducing more complicated expressions. For example, a reaction process described by the following expression may be analyzed in

simplistic terms.

$$dP/dt = k_1 A^2 B + k_2 AB \quad (A1-3)$$

The empirical order of reaction with respect to A would be found to be between 1 and 2. For extreme limiting cases, if k_2 were very small compared to k_1 , the empirical order of reaction would be found to be 2. If the value k_2 was much larger than k_1 , the reaction would display first order behavior with respect to A.

The experimental data would be expected to show an empirical order of reaction of unity with respect to B and an overall order of reaction of between 2 and 3.

Two methods (25,27) were used to estimate the order of reaction for the experimental data obtained in these studies. Each method will be discussed.

a) Initial Rate Method. For a simple rate equation in the form of equation (A1-2), the initiated polymerization may be simply expressed as :

$$-dM/dT = k I^a M^n \quad (A1-4)$$

Several reaction mixtures were analyzed holding the initial concentration of monomer, M_0 , constant with small, varying amounts of initiator utilized in the reaction.

For the set of reactions described, the initial rate of monomer loss would be:

$$(-dM/dt)_0 = k I_0^a M_0^n \quad (A1-5)$$

The initial rate of monomer consumption, $-dM/dt$, was obtained by inspecting curves of M vs. time for the different reaction mixtures and estimating the initial rate from the initial portions of the curves. linear regression of the first 25 minute portion of the reaction was used to estimate the initial rate. Taking logarithms of both sides of equation (A1-5) yields:

$$\log(-dM/dt)_0 = a \log I_0 + \log k M_0^n \quad (A1-6)$$

Since k and M_0^n are constant, a log-log plot of $(dM/dt)_0$ vs. the initial initiator concentration, I_0 , should yield a straight line of slope, a , the order of reaction with respect to initiator.

The order of reaction with respect to monomer, n , could be determined in a second set of experiments in which The initial monomer concentration is varied while I_0 , the initial initiator concentration is kept constant. Method a can be applied to the uninitiated polymerization if it is assumed that $a=0$ in equation (A1-4).

b) Fractional Life Method. the fractional life method is not directly applicable to reactions involving more than one reactant. For this reason the uninitiated polymerization, equation (A1-4) for $a=0$ is used to derive the relationship between initial monomer concentration employed and the time for some fraction of monomer to disappear.

Integrating equation (A1-4) for the case, n not equal to 1 and $I^a=1$ produces:

$$1/M^{n-1} - 1/M_0^{n-1} = (n-1) kt \quad (\text{A1-7})$$

Expressing M as the fraction remaining, $f = M/M_0$, is accomplished by multiplying both sides by M_0^{n-1} :

$$(1/f-1) = M_0^{n-1} (n-1) kt \quad (\text{A1-8})$$

For different runs, the time, t_f , required to reach some constant conversion, f , was found for different initial monomer concentrations, M_0 . The logarithmic form of equation (A1-8), rearranged, is:

$$\log t_f = - (n-1) \log M_0 + \log C \quad (\text{A1-9})$$

$$\text{Where } C = (1/f-1)/((n-1)k) \quad (\text{A1-10})$$

Thus, a plot of $\log t_f$ vs. $\log M_0$ generates a straight line for simple kinetic expressions of slope = $-(n-1)$.

For cyclic dimer formation, the fractional life method for the determination of empirical order of reaction is also applicable if it is known or assumed that decay of monomer is a simple second order process. The simple rate expression is:

$$dC/dt = k M^n \quad (A1-11)$$

For uninitiated polymerizations the decay of monomer is found to be a simple second order process and monomer concentration can be expressed as a function of time (see Appendix 2):

$$M = M_0 (k_1 M_0 t + 1)^{-1} \quad (A2-42)$$

Substituting equation A2-42 into A1-11 yields:

$$dC/dt = k M_0^n (k_1 M_0 t + 1)^{-n} \quad (A1-12)$$

k is an n^{th} order rate constant and k_1 is the second

order rate constant governing the loss of monomer. Integrating over the limits of some constant quantity of cyclic dimer formed with the restriction that n is not equal to -1 produces:

$$CM_0^{-n}/k = [(1 + k_1M_0t)^{(1-n)} - 1]/(1-n)k_1M_0 \quad (A1-13)$$

The following approximation may be made if the binomial term is expanded to two terms:

$$(1 + k_1M_0t)^{(1-n)} = (1-n)k_1M_0t + 1 \quad (A1-14)$$

Equation (A1-13) then becomes:

$$(1-n)k_1CM_0^{(1-n)}/k = (1-n)k_1M_0t \quad (A1-15)$$

Simplifying equation (A1-15) and casting in logarithmic form yields:

$$\text{Log } t_f = (1-n) \text{ Log } M_0 + \text{Log } C_f/k \quad (A1-16)$$

t_f is the time required for the formation of some constant fraction of cyclic dimer, C_f . $C_f = C/M_0$.

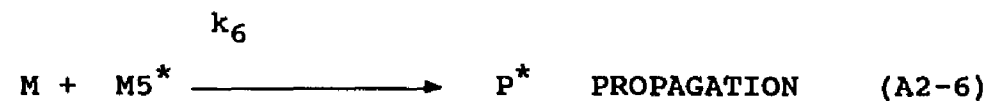
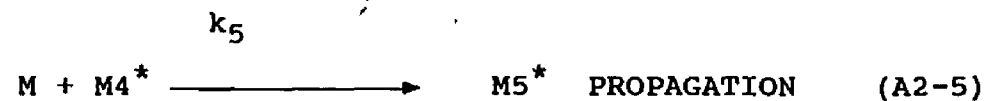
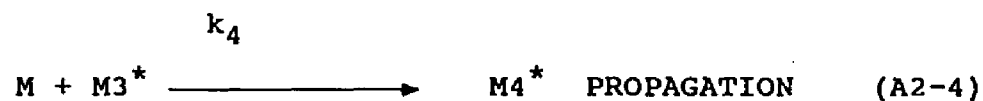
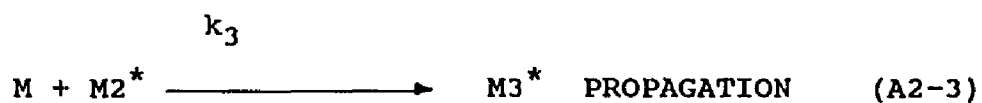
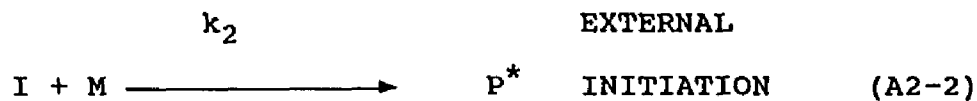
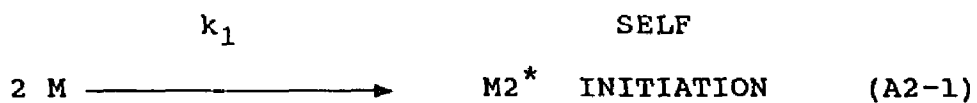
Equation (A1-16) shows that a logarithmic plot of the time required to reach some constant fraction of cyclic

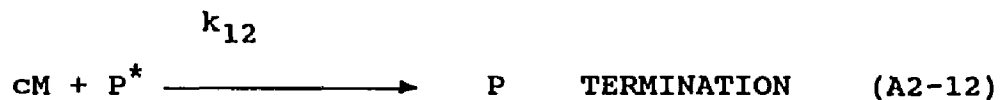
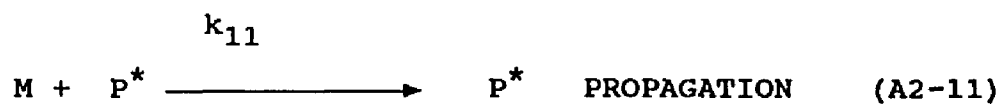
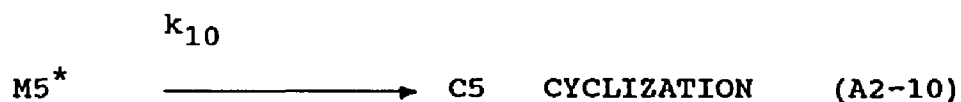
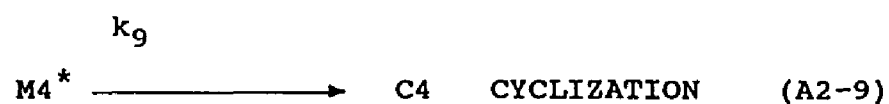
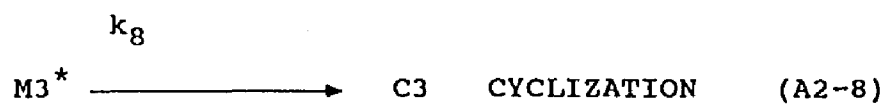
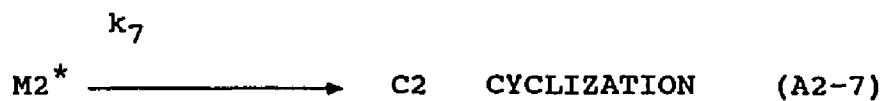
dimer versus the initial monomer concentrations used in the experiments will produce a straight line whose slope will reflect the average order of reaction with respect to monomer over the concentration range studied.

Bamford (27) suggests caution in using the fractional life method in reactions involving two different orders of reaction. In the present study, using a constant small amount of initiator, I_0 , relative to larger varying initial monomer concentrations, M_0 , yielded the order of reaction with respect to monomer. In experiments in which an excess of monomer was employed with varying smaller initiator charges, the fractional life method yielded an apparent overall order of reaction, $(a+n)$.

APPENDIX 2. DERIVATION OF KINETIC EXPRESSIONS

A2.1 Proposed Mechanism. The following mechanism is consistent with the observed kinetics:





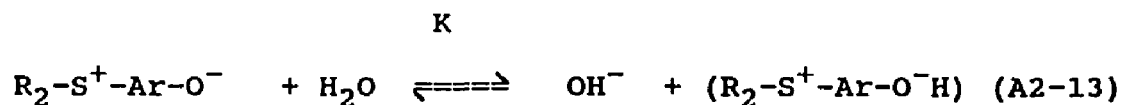
M represents the hydroxyethoxy zwitterion monomer; P^* , a propagating specie consisting of more than six monomer units. C2 through C5 are cyclic dimer through cyclic pentamer and P, the linear products of the

reaction. I represents some initiating specie, for example the trifluoroacetate salt of the monomer, and M_2^* through M_5^* represent propagating species consisting of two through five monomer units, those low molecular weight propagating species able to cyclize. The scheme presented above would describe both polymerizations run in the presence of some initiating specie as well as the self initiating thermal polymerization which occurs when no initiator is added.

The step represented in equation A2-12 may be better represented by:



Hydroxide ion is produced in small amounts however and the quantity of OH^- is proportional to the monomer concentration. In dilute solution, the production of hydroxide ion is described by the following equilibrium:



With moisture not present in great excess but only added

to the system from the dihydrate monomer, an expression for K , if the amount of monomer which is dissociated at equilibrium is x , is:

$$K = x^2 / (M-x)(2M_o-x) \quad (\text{A2-14})$$

If x is small, and the activity coefficients close to unity, the concentration of hydroxide ion then would be:

$$\text{OH}^- = (2KM_oM)^{.5} \quad (\text{A2-15})$$

Equation A2-12a is used to indicate the role of elimination and substitution processes which produce olefinic and hydroxyl end groups. k_{12} would be an average rate constant for the two processes.

A2.2 Uninitiated polymerization. The polymerization scheme for the self initiating thermal polymerization of hydroxyethoxy zwitterion in dilute solution holds when $k_2=0$. It is assumed that a small steady concentration of smaller sized propagating species, M_2^* through M_5^* , and larger propagating species, P^* , are attained early in the course of the polymerization and a valid steady state concentration of these materials can be calculated.

Assumption of a low steady state concentration of dimeric propagating specie, M_2^* , attained during the course of the reaction gives:

$$dM_2^*/dt = -dM_2^*/dt \quad (A2-16)$$

$$k_1 M^2 = k_3 M_2^* M + k_5 M_2^* \quad (A2-17)$$

$$M_2^* = k_1 M^2 / (k_7 + k_3 M) \quad (A2-18)$$

Calculating the steady state concentration of trimeric propagating specie, M_3^* , attained during the course of the reaction gives:

$$dM_3^*/dt = -dM_3^*/dt \quad (A2-19)$$

$$k_3 M M_2^* = k_4 M_3^* M + k_8 M_3^* \quad (A2-20)$$

$$M_3^* = k_3 M M_2^* / (k_8 + k_4 M) \quad (A2-21)$$

Substituting the expression for M_2^* yields:

$$M_3^* = k_1 k_3 M^3 / (k_7 + k_3 M) (k_8 + k_4 M) \quad (A2-22)$$

The tetrameric and pentameric propagating species are

calculated in the same manner. For the tetrameric propagating specie:

$$dM_4^*/dt = -dM_4^*/dt \quad (A2-23)$$

$$k_4 M M_2^* = k_5 M_4^* M + k_9 M_4^* \quad (A2-24)$$

$$M_4^* = k_4 M M_3^* / (k_9 + k_5 M) \quad (A2-25)$$

Substituting the expression for M_3^* yields:

$$M_4^* = k_1 k_3 k_4 M^4 / (k_7 + k_3 M) (k_8 + k_4 M) (k_9 + k_5 M) \quad (A2-26)$$

The expression for pentameric propagating specie is:

$$M_5^* = k_1 k_3 k_4 k_5 M^4 / (k_7 + k_3 M) (k_8 + k_4 M) (k_9 + k_5 M) (k_{10} + k_6 M) \quad (A2-27)$$

Assumption of a low steady state concentration of propagating specie, P^* , attained during the course of the reaction gives:

$$dP^*/dt = -dP^*/dt \quad (A2-28)$$

$$k_6 M_5^* M = k_{12} P^* (2KM_0)^{.5} M^{.5} \quad (A2-29)$$

$$P^* = \frac{k_1 k_3 k_5 k_6 M^{5.5}}{k_1^2 (2KM_0)^{.5} (k_7 + k_3 M) (k_8 + k_4 M) (k_9 + k_5 M) (k_{10} + k_6 M)}$$

(A2-30)

For uninitiated polymerizations, initiation is the rate determining step, as the zwitterionic monomer should be less reactive than linear species. The empirical determination of reaction order over the concentration range tested shows that the reaction order with respect to monomer is 2.0 and supports the assignment of equation (A2-1) as the rate determining step of monomer loss.

The rates of cyclic dimer formation and monomer loss are given as dC/dt and $-dM/dt$.

$$-dM/dt = k_1 M^2 \quad (A2-31)$$

$$dC/dt = k_7 M 2^* = k_7 k_1 M^2 / (k_7 + k_3 M) \quad (A2-32)$$

In solving equations A2-31 and A2-32, the differential expression describing the loss of monomer, equation (A2-31), is first solved to yield the instantaneous monomer concentration, M , as a function of time. In this manner, k_1 is determined graphically. The

ratio k_3/k_7 can be calculated from more complicated equations by iteration using a microcomputer.

The following terms are used:

M - Instantaneous monomer concentration.

C - Instantaneous cyclic dimer concentration.

M_f - Instantaneous fraction of monomer.

C_f - Instantaneous fraction of cyclics.

k_1 - simple second order rate constant for loss of monomer.

M_0 - initial monomer concentration, moles/liter.

Instantaneous concentrations and fractions of the substances are related as follows:

$$M = M_f M_0 \quad (A2-33)$$

$$C = C_f M_0 \quad (A2-34)$$

The concentration of monomer as a function of time is easily solved (equation A2-42).

$$-dM/dt = k_1 M^2 \quad (A2-35)$$

$$dM/M^2 = -k_1 t \quad (\text{A2-36})$$

$$[-1/M]_{M_0} = -k_1 t \quad (\text{A2-37})$$

$$-1/M + 1/M_0 = -k_1 t \quad (\text{A2-38})$$

$$1/M - 1/M_0 = k_1 t \quad (\text{A2-39})$$

$$1/M = k_1 t + 1/M_0 \quad (\text{A2-40})$$

$$1/M = (k_1 M_0 t + 1)/M_0 \quad (\text{A2-41})$$

$$M = M_0 (k_1 M_0 t + 1)^{-1} \quad (\text{A2-42})$$

An expression to solve for k_1 graphically can be derived (equation A2-46).

$$1/M - 1/M_0 = k_1 t \quad (\text{A2-43})$$

$$(M_0 - M)/MM_0 = k_1 t \quad (\text{A2-44})$$

Using equation A2-33:

$$(M_0 - M_f M_0)/M_f M_0^2 = k_1 t \quad (\text{A2-45})$$

$$(1-M_f)/M_f = M_0 k_1 t \quad (\text{A2-46})$$

An expression suitable for estimating the value of the ratio k_3/k_7 may be derived by removing time as a variable using equations (A2-31) and (A2-32).

$$-dM/dC = k_1 (M)^2 / (k_7 M^2 / (k_7 + k_3 M)) \quad (\text{A2-47})$$

Setting $k_3/k_7 = q$

$$-dM/dC = (k_7 + k_3 M) / k_7 = (1 + qM) \quad (\text{A2-48})$$

$$1/(1 + qm) dM = dC \quad (\text{A2-49})$$

Integrating both sides of equation (A2-49) over the limits of C_0 to C and M_0 to M yields:

$$C - C_0 = (1/q) \ln[(1 - qM_0)/(1 + qM)] \quad (\text{A2-50})$$

Using the relationships of equations (A2-33) and (A2-34):

$$C_f M_0 = -(1/q) \ln((1 + q M_f M_0) / (1 + q M_0)) \quad (\text{A2-51})$$

The relationship shown in equation (A2-51) is not

amenable to a graphical solution, but the value of the constant, q , may be estimated by iteration using a commercially available program such as TK SOLVER. The relationship is solved by iteration for individual experimental points which are then averaged to yield the best estimate of k_3/k_7 .

A2.3 Initiated Polymerization. For initiated polymerizations the rate expressions are simplified due to the polymerization conditions used and the simpler product distribution.

Conditions used for initiated polymerizations were such that $I_0 \ll M_0$; The initial initiator concentration was much lower than the monomer concentration initially present.

During the course of the initiated polymerizations, only small amounts of cyclic dimer formed. The amounts of higher cyclic species were correspondingly reduced to smaller almost constant values. If cyclization is neglected, it can be assumed that processes governed by the rate constant, k_1 , in equation (A2-1) are slow enough to be ignored. This simplifying assumption causes the rates of all the processes to approach zero except for equations (A2-2), (A2-11) and (A2-12).

Two assumptions concerning the initiator are also made. In $\text{Me}_2\text{SO } d-6$, a good solvating solvent, it is assumed that the trifluoroacetate salt is completely ionized. It is also assumed that the concentration of initiator remains constant during the course of the reaction since the feebly nucleophilic trifluoroacetate anion only slowly opens the tetrahydrothiophenium ring. As termination of propagating specie to alcohol or vinyl terminated linear polymer occurs, trifluoroacetic acid is generated and reacts with monomer to form initiator in situ.

Assuming a steady state for the propagating specie, P^* :

$$dP^*/dt = - dP^*/dt \quad (\text{A2-52})$$

$$k_2IM = k_{11}MP^* + k_{12}(2KM_O) \cdot^5M \cdot^5P^* \quad (\text{A2-53})$$

$$P^* = k_2IM \cdot^5 / (k_{11}M \cdot^5 + k_{12}(2KM_O) \cdot^5) \quad (\text{A2-54})$$

If the termination process is assumed to be slower than propagation:

$$P^* = k_2I/k_{11} \quad (\text{A2-55})$$

All of the initiator exists as added trifluoroacetate salt or the growing end of a propagating specie.

$$I_0 = I + P^* \quad (\text{A2-56})$$

$$I_0 = I + k_2 I / k_{11} \quad (\text{A2-57})$$

$$I_0 = (1 + k_2 / k_{11}) I \quad (\text{A2-58})$$

$$I = k_{11} I_0 / (k_{11} + k_{12}) \quad (\text{A2-59})$$

Examination of the mechanism shows that the rate of polymerization is equal to the rate of propagation.

$$dP/dt = k_{11} M P^* \quad (\text{A2-60})$$

Since polymer is the only product considered:

$$dP/dt = -dM/dt = k_{11} M P^* \quad (\text{A2-61})$$

Using equation A2-56:

$$dM/dt = k_{11} (I_0 - I) M \quad (\text{A2-62})$$

Equation A2-62 predicts that the initiated polymerization will be first order with respect to monomer and between zero and first order with respect to initiator, between first and second order overall.

Substituting equation A2-59 into A2-62 produces:

$$dM/dt = k_{11}I_0(1 - k_{11}/(k_2 + k_{11}))M \quad (A2-63)$$

$$dM/dt = (k_2k_{11}/(k_2 + k_{11}))I_0M \quad (A2-64)$$

Equation A2-64 correctly predicts that a plot of apparent first order rate constant versus I_0 is linear.

REFERENCES

1. Saegusa, T. Chem Technol. 1975, 5, 295.
2. Saegusa, T.; Ikeda, H.; Fuji H. Macromolecules 1972, 5, 354.
3. Saegusa, T.; Kimura, Y. Pure App. Chem. 1976, 48, 3071.
4. Saegusa, T. ; Kobayashi, S. Pure App. Chem. 1978, 50, 281.
5. Saegusa, T. Makromol. Chem. 1981, 4, 73.
6. Saegusa, T. ; Kobayashi, S. Macromol. Sci.Chem. 1979, A-13, 295.
7. Odian, G.; Gunatillake, P.A. Macromolecules 1984, 17, 1297.
8. Gunatillake, P.A.; Odian, G.; Macromolecules 1984, 17, 2236.
9. Hatch, M.J.; Yoshimine, M.; Schmidt, D.L.; Smith, H.B. J. Amer. Chem. Soc. 1971, 93, 4617.
10. Hatch, M.J.; Yoshimine, M.; Schmidt, D.L.; Smith, H.B. U.S. Pat. 3,636,052 1972.
11. Schmidt D.L.; Smith H.B.; Yoshimine M.; Hatch M.J. J. Polym. Sci. Polym. Chem. Ed. 1972, 10, 2951.
12. Schmidt, D.L., "Ring-Opening Pollymerization", Chap. 22, 1977, Saegusa, T.; Goethals, E. eds., Wash., D.C.
13. Schmidt, D.L. Polym. Preprints 1977, 18(1), 121.
14. Kobayashi, A.; Chow, T.Y.; Saegusa, T. Polym. Bull. 1983, 9, 588 and 10, 491.
15. Tomalia, D.A.; Dickert, Y.J. U.S. Pat. 3,746,691, 1973.
16. Tomalia, D.A. 1977, Paper Presented at Polymer Colloquium, Society of Polymer Science, Kyoto, Japan.
17. Gunatillake, P.A.; Odian, G.; Tomalia, D.A. Macromolecules 1987, 20, 2356.
18. Gunatillake, P.A.; Odian, G.; Tomalia, D.A. Macromolecules 1987, in Press.

19. Gunatillake, P.A.; Odian, G.; Schmidt, D.L. Macromolecules 1987, 19, 1779.
20. Odian, G.; Chien, C.; Periyasamy, M.; Schmidt, D.L. Polym. Preprints 1984, 25(1), 262.
21. Klingler, T.C.; Schmidt, D.L. U.S. Pat. 4,089,877 1978.
22. Odian, G. "Principles of Polymerization", 1981, 2nd Edition, Wiley-Interscience, New York.
23. Odian, G.; Chien, C. unpublished results.
24. Abraham, R.J.; Loftus, P. "Proton and Carbon-13 NMR Spectroscopy", 1979, Heyden and Son, Amsterdam.
25. Espenson, J.H. "Chemical Kinetics and Reaction Mechanisms", 1981, McGraw Hill, New York.
26. Galwey, A.K. "Chemistry of Solids", 1967, Chapman and Hall, London.
27. Bamford, C.H.; Tipper, C.F. "The Theory of Kinetics", Vol 2 in "Comprehensive Chemical Kinetics", 1969, Elsevier, Amsterdam.